Me 141

ACTA POLYTECHNICA SCANDINAVICA

MECHANICAL ENGINEERING SERIES No. 141

Effect of Nitrogen Content on Precipitation Behaviour and Properties of P/M High Nitrogen Austenitic Stainless Steels

JYRKI ROMU

Helsinki University of Technology
Department of Mechanical Engineering
Puumiehenkuja 3 A
P.O. Box 4200
FIN-02015 HUT
Finland

ESPOO 2000

ACTA POLYTECHNICA SCANDINAVICA

...a Scandinavian contribution to international engineering sciences

From 1958 to 1971 the monograph was published under the auspices of the Scandinavian Council for Applied Research. Since 1972 it has been published by the Finnish Academy of Technology. The Editor-in-Chief is Professor Mauri Luukkala.

Acta Polytechnica Scandinavica is divided into the following subseries:	**Subscription rates in 2000**
Chemical Technology Series, CH Editor Professor Seppo Palosaari	FIM 600
Civil Engineering and Building Construction Series, CI Editor Professor Jussi Hyyppä	FIM 600
Electrical Engineering Series, EL Editor Professor Seppo Halme	FIM 600
Industrial Management and Business Administration Series, IM Editor Professor Eero Eloranta	FIM 600
Mathematics and Computing Series, MA Editor Professor Reijo Sulonen	FIM 600
Mechanical Engineering Series, ME Editor Professor Markku Lampinen	FIM 600
Applied Physics Series, PH Editor Professor Mauri Luukkala	FIM 600
Complete series	FIM 2750

Subscriptions may be entered for the complete series or any number of subseries. Single copies may be purchased through booksellers or directly from the publisher:

The Finnish Academy of Technology
Tekniikantie 12
FIN-02150 ESPOO
FINLAND

Tel: +358 9 455 4565 Fax: +358 9 455 4626
Email: facte@facte.com

Me 141

ACTA POLYTECHNICA SCANDINAVICA

MECHANICAL ENGINEERING SERIES No. 141

Effect of Nitrogen Content on Precipitation Behaviour and Properties of P/M High Nitrogen Austenitic Stainless Steels

JYRKI ROMU

Helsinki University of Technology
Department of Mechanical Engineering
Puumiehenkuja 3 A
P.O. Box 4200
FIN-02015 HUT
Finland

Dissertation for the degree of Doctor of Technology to be presented with due permission for public examination and debate in Auditorium K216 at Helsinki University of Technology (Espoo, Finland) on the 21st of January 2000, at 12 o'clock noon.

ESPOO 2000

Romu, Jyrki. **Effect of nitrogen content on precipitation behaviour and properties of P/M high nitrogen austenitic stainless steels.** Acta Polytechnica Scandinavica, Mechanical Engineering Series No. 141, Espoo 2000, 140 pp. Published by the Finnish Academy of Technology. ISBN 951-666-524-1. ISSN 0001-687X.

Keywords: austenitic stainless steel, nitrogen, powder metallurgy, precipitation, dilatometry, transmission electron microscopy, mechanical properties, corrosion resistance, hardness.

ABSTRACT

The effect of nitrogen content on the precipitation behaviour and properties of solution annealed and further isothermally at elevated temperatures (450 °C or 750 °C) annealed powder metallurgically manufactured (P/M) austenitic stainless steels (24Cr-22Ni-7,3Mo-3,5Mn-0,3...1,15N) was studied. The studied steels were manufactured by hot isostatic pressing (HIP) from gas atomized powders. Nitrogen alloying was performed during atomizing, and by further solid state nitriding of the powders in a fluidized bed furnace. The steels were studied with optical microscopy, transmission electron microscopy, dilatometric analyses, tensile testing, Charpy-V impact testing, hardness measurements and localized corrosion testing (6 % $FeCl_3$ solution; modified ASTM G48 and G76).

The solution annealed steels were observed to be fully austenitic, and to have a unique combination of high strength, good ductility and toughness, as well as excellent localized corrosion resistance, when the nitrogen content of the steel was 0,5 - 0,9 wt-%N. At lower nitrogen contents, intermetallic phases were precipitated, and at higher nitrogen contents, Cr_2N was precipitated. In both cases ductility, toughness and localized corrosion resistance of the steels was deteriorated.

Isothermal annealing at elevated temperatures (450 °C or 750 °C) resulted in either intermetallic phase (σ and Laves), or both chromium nitride (Cr_2N) and intermetallic phase precipitation, depending on the nitrogen content of the steel and on the annealing temperature and time. Intermetallic phases precipitated in the steels with ≤0,5 wt-%N when isothermally annealed at 450 °C for up to 500 h, and ductility, toughness, and localized corrosion resistance of the steels were deteriorated. The hardness and strength properties of the steels increased due to intermetallic phase precipitation. In steels with >0,5 wt-%N, intermetallic phases were not precipitated at 450 °C and the properties of the steels remained unaffected.

Annealing at 750 °C resulted in intermetallic phases precipitation in steels with ≤0,5 wt-%N, whereas in steels with >0,5 wt-%N, both intermetallic phases and Cr_2N were precipitated. The amount of intermetallic phase precipitation decreased with increasing nitrogen content of the steel. Precipitation of σ phase was retarded and Laves phase was stabilized in steels with >0,5 wt-%N. The tensile strength of the studied steels isothermally annealed at 750 °C either increased, remained unaffected, or decreased as their nitrogen content increased. The tensile ductility, impact toughness and localized corrosion resistance of the steels annealed at 750 °C decreased with increasing annealing time. The decrease in tensile ductility was the smaller the higher the nitrogen content of the steel was. The effect of nitrogen content on the decrease of impact toughness and localized corrosion resistance was not as clear as in the case of tensile ductility. Precipitation of intermetallic phases was more detrimental to tensile ductility and localized corrosion resistance than Cr_2N, whereas Cr_2N precipitation was more detrimental to impact toughness than intermetallic phases. The hardness of the studied steels annealed at 750 °C increased with increasing annealing time, due to precipitation of intermetallic phases and Cr_2N.

PREFACE

This thesis is based on the results of the projects ´´Properties of Powder Metallurgically Manufactured Corrosion Resistant and High Strength Steels´´, ´´Corrosion and Wear Resistant P/M Steels´´ and ´´Advanced P/M High Nitrogen Austenitic and Duplex Stainless Steels´´. All the projects were carried out in co-operation with Rauma Materials Technology Oy and were funded by the Technology Development Center of Finland (TEKES), which is gratefully acknowledged. The financial support of Jenny and Antti Wihuri Foundation is also gratefully acknowledged.

I would like to thank the supervisor of the thesis Professor Hannu Hänninen for his guidance and advices. Dr. Jari Liimatainen from Rauma Materials Technology Oy is acknowledged for his advices and for supplying the powders and hot isostatic pressing for the studies. Dr. Jyrki Tervo is especially acknowledged for his co-operation and numerous discussions during the projects. M.Sc. Jussi Laurila from Tampere University of Technology I would like to thank for the TEM analyses. M.Sc. Pertti Koskinen and Ms. Hannele Virtasalo from VTT Manufacturing Technology are acknowledged for the dilatometric analyses. M. Sc. Jouko Virta from VTT Manufacturing Technology I would like to thank for the help in performing the fluidised bed nitriding of the powders. M.Sc. Antero Jokinen from VTT Manufacturing Technology is acknowledged for the hot isostatic pressing of the powders. M.Sc. Laura Taivalaho is acknowledged for helping in performing the localized corrosion testing. M. Sc. Päivi Moisanen is acknowledged for the help in optical microscopy. Ph.D. Yuri Yagodzinskyy and Lic. Tech. Sergiy Smuk are acknowledged for useful comments and the help in preparing part of the figures. Ph.D. Wade Karlsen is acknowledged with gratitude for checking the grammar. The personnel of the Laboratory of Engineering Materials is gratefully acknowledged. My dear wife Marja I would like to thank for her patience and support throughout the work.

In Otaniemi, November, 1999

Jyrki Romu

CONTENTS

LIST OF SYMBOLS

A	Elongation to fracture
a_N	Activity of nitrogen dissolved in steel
C_N	Atomic concentration of nitrogen in solid solution
D	Grain size
e_N^j	Interaction parameter
$e_{N,2073K}^j$	Interaction parameter at 2073 K
f_N	Activity coefficient of nitrogen
HV	Vickers hardness
%j	Alloying element content in at-%
%k	Alloying element content in at-%
K_N	Equilibrium constant of nitriding reaction
k_y	Constant for the Hall-Petch relationship
K_1	Strength factor (MPa)
K_2	Strength factor (MPa)
M	Metallic element
n_1	Strain hardening exponent in Hollomon equation
n_2	Strain hardening exponent in Hollomon equation
p_{N_2}	Partial pressure of nitrogen
P	Pressure
PRE	Pitting resistance equivalent
p_{H_2}	Partial pressure of hydrogen
p_{H_2O}	Partial pressure of water vapour
$q_{N,2073K}^j$	Interaction parameter at 2073 K
r_N^j	Interaction parameter
r_N^{jk}	Interaction parameter
$r_{N,2073K}^j$	Interaction parameter at 2073 K
σ_r	0,2 % flow stress for grain interior
R	R phase
R^2	Correlation coefficient in linear regression analysis
$R_{p0,2}$	Yield strength (MPa)
R_m	Ultimate tensile strength (MPa)

t	Time
T	Temperature
T	T phase
wt-%	Weight percent
Z	Reduction of area
σ	Sigma phase
λ	Laves phase
χ	Chi phase
γ	Austenite phase
ε	True strain
π	Pi-nitride

ORIGINAL FEATURES

The experimental data and analyses of this thesis report are directed firstly toward evaluation of the effect of nitrogen content on the microstructure and properties of solution annealed powder metallurgically manufactured (P/M) high-nitrogen austenitic stainless steels. Secondly, they are directed to the evaluation of the effect of nitrogen content on the development of microstructure and properties of the studied steels when isothermally annealed at elevated temperatures. The following features are believed to be original:

1 Powder metallurgical manufacturing of steels with nominal composition of 24Cr-22Ni-7,3Mo-3,5Mn-0,3...1,15N and with fine-grained homogeneous microstructure as well as with unique combination of strength, ductility, toughness and localized corrosion resistance has been developed.

2 Nitrogen alloying increases strength without deteriorating ductility and toughness of the studied P/M steels as long as nitrogen remains in solid solution. The best combination of strength and ductility as well as toughness is achieved, when the nitrogen content of the steel is 0,5 - 0,9 wt-%N.

3 Nitrogen alloying improves the localized corrosion resistance of the studied steels in 6 % $FeCl_3$ solution as long as nitrogen remains in solid solution. The best localized corrosion resistance is achieved, when the nitrogen content of the steel is 0,5 - 0,9 wt-%N.

4 Powder metallurgical manufacturing method including solid state nitriding made it possible to study the effect of nitrogen content on precipitation behaviour of austenitic stainless steels on a wide scale of the nitrogen content (0,34 - 1,15 wt-%N), while the rest of the chemical composition of the steels being similar to each other. Nitrogen alloying retards the onset of precipitation of intermetallic phases during solution annealing and during exposure to elevated temperatures.

5 Despite Cr_2N precipitation the nitrogen content of the austenite matrix in steels with 0,7 - 0,9 wt-%N remains high enough to retard the precipitation of intermetallic phases during exposure at elevated temperatures.

1 INTRODUCTION

1.1 Background

The main reason for the interest towards nitrogen as an alloying element in austenitic stainless steels, is to save other expensive alloying elements such as nickel, and at the same time to introduce good property combinations to steels. Austenitic stainless steels are considered to be high nitrogen austenitic stainless steels if they contain more than 0,4 wt-% nitrogen in solid solution (Speidel, 1989). High nitrogen austenitic steels have a unique combination of high yield and ultimate tensile strength as well as high toughness and ductility, which is not typical for other steels. Strength properties, especially yield strength, of high nitrogen steels can be effectively further increased by cold working (Rayaprolu and Hendry, 1988; Uggowitzer et al., 1990; Soussan et al., 1991). High nitrogen austenitic stainless steels also have excellent corrosion properties, such as resistance to stress corrosion cracking, crevice corrosion, and pitting corrosion (Janik-Czachor et al., 1975; Eckenrod and Kovach, 1977; Jargelius and Wallin, 1986; Levey and van Bennekom, 1995; Grabke, 1996; Jargelius-Petterson, 1998). In addition to good mechanical and corrosion properties, high nitrogen austenitic stainless steels have low magnetic permeability, good wear resistance, and good creep resistance at high temperatures.

Powder metallurgy as a manufacturing method makes it possible to obtain steels with combinations of attractive properties, and offers a possibility for near-net-shape manufacturing, savings in machining and waste material costs, and the possibility to avoid all kinds of casting defects typical of conventional ingot metallurgy. Because of the homogeneous microstructures obtained, powder metallurgy manufacturing route is the only way to obtain combinations of certain properties and microstructures (Rhodes and Conway, 1996; Rhodes et al., 1997; Tervo et al., 1997; Tervo, 1998). Another reason for powder metallurgy to become a potential manufacturing route, is the possibility to effectively introduce high nitrogen contents to the steels either by solid state nitriding of powder, or during atomizing utilizing elevated nitrogen pressures. Powder metallurgy manufacturing of high nitrogen steels has high technical potential, since nitrogen alloying of powder in a nitrogen atmosphere is very promising due to kinetic aspects (Wilson, 1989; Zheng et al., 1990; Zheng, 1991, Feichtinger, 1991; Johansson et al., 1991; Simmons, 1996A; Simmons et al., 1996C).

When austenitic stainless steels with good strength and toughness properties, as well as with good corrosion resistance are required, it generally means that the steels are alloyed with high amounts of chromium, molybdenum and nickel. As a result, the risk for intermetallic phase

precipitation during manufacturing is increased due to the especially high amounts of chromium and molybdenum (Thier et al., 1969; Brandis et al., 1976A; Kearns and Deverell, 1987; Heubner et al., 1989; Rechsteiner, 1994; Gagnepain et al., 1996). The precise control of the solution annealing temperatures and cooling times are, thus, of uttermost importance. Prolonged exposure of the steels to elevated temperatures results in an increased tendency for intermetallic phase precipitation when their chromium and molybdenum contents increase. In both cases, the toughness and ductility as well as corrosion resistance of austenitic stainless steels are decreased. Nitrogen alloying of austenitic stainless steels has been observed to have a positive effect when the risk for intermetallic phase precipitation is considered (Thier, 1969; Brandis et al., 1976A; Heubner et al., 1989; Jargelius-Petterson, 1994; 1996; 1998). Nitrogen contents up to 0,4 - 0,5 wt-%N can retard or even prevent intermetallic phase precipitation in austenitic stainless steels. In austenitic stainless steels with higher nitrogen contents (> 0,5 wt-%N), chromium nitride (Cr_2N) precipitation during manufacturing and prolonged exposure to elevated temperatures can take place (Rayaprolu and Hendry, 1988; 1989; Simmons et al., 1994; Simmons, 1995A; 1995B, Taillard et al., 1999). Precipitation of intermetallic phases has also been observed in austenitic stainless steels with high nitrogen contents (> 0,5 wt-%N), but in clearly smaller amounts as compared with that of chromium nitrides. The onset of precipitation of intermetallic phases is delayed to considerably longer times than that of chromium nitrides in high nitrogen austenitic stainless steels during exposure to elevated temperatures.

1.2 Nitrogen solubility in steels

In order to produce high nitrogen steels, it is important to know as exactly as possible the nitrogen solubility in steels. In casting, interest is in nitrogen solubility in the liquid state and during solidification of the melt, since the solubility of nitrogen determines the capability of the process technology and the soundness of the castings. In powder metallurgical manufacturing of austenitic stainless steels, nitrogen solubility in solid austenite phase is of interest in addition to nitrogen solubility in the liquid state. Nitrogen solubility in alloyed steels is usually determined by thermodynamic analysis. Comprehensive investigations in the field of thermodynamic analysis of iron-base alloys have been done by many researchers (e.g., Zheng, 1991; Feichtinger et al., 1989; Frisk and Hillert, 1989; Frisk, 1990; Jarl, 1978; Hertzman and Jarl, 1987; Kikuchi et al., 1989; Hillert and Qiu, 1992). The influence of alloy composition, temperature, and pressure on nitrogen solubility in iron-base alloys both in liquid and solid state are included in the calculations.

1.2.1 Nitrogen solubility in pure iron

Thermodynamic investigations of nitrogen solubility in alloyed steels are mostly based on equilibrium with nitrogen containing gas phase. This is referred to as Sievert´s law, i.e., the quantity of nitrogen dissolved in the metal is proportional to the square root of nitrogen partial pressure. Nitrogen solubility in pure iron in all three phases follows Sievert´s law at least up to 200 MPa nitrogen pressure (Zheng, 1991; Feichtinger and Zheng, 1990; Feichtinger, 1991; Rawers et al., 1990; 1992; 1994B). Three different phases can exist in pure iron: liquid, ferrite (delta and alpha ferrite) and austenite phases. In the liquid phase, nitrogen solubility increases slightly with temperature. Nitrogen solubility in ferrite increases with temperature as in the liquid phase, but the temperature dependence is slightly stronger. Nitrogen solubility in the austenite phase is different from that of the liquid and ferrite phases. Nitrogen solubility in austenite is higher than that in the ferrite phases, and the solubility increases with decreasing temperature. In order to predict nitrogen solubilities in iron-base alloys, it is necessary to use thermodynamic analysis, as described in Appendix A.

1.2.2 Nitrogen solubility in multicomponent alloys

Alloying elements have an effect on nitrogen solubility in iron-base alloys. C, B, Si, Co, Ni, Al, etc. decrease nitrogen solubility and V, Cr, Mn, Mo, W, etc. increase nitrogen solubility, as can be seen in Figure 1. Although some elements, such as V, strongly increase nitrogen solubility, their effect is usually not noticeable, since their concentration is limited, especially in stainless steels. The most important alloying elements affecting nitrogen solubility in austenitic stainless steels are Cr, Ni, Mn and Mo.

Steels usually contain several alloying elements and impurities. In order to be able to determine the theoretical nitrogen solubilities in multicomponent alloys in liquid and austenite phases, it is necessary to evaluate the combined effects of all of the alloying elements for which there is information available. Nitrogen solubility in multicomponent alloys in the liquid and solid (austenite) phase can be calculated with the interaction parameter method described in Appendix A, where the influence of different alloying elements is expressed by using the interaction parameters, which depend on the temperature.

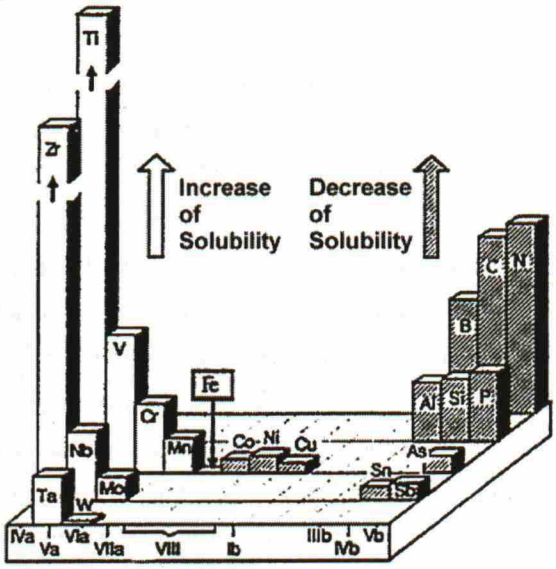

Figure 1. Effect of different elements on nitrogen solubility in iron-base alloys (Feichtinger and Zheng, 1990).

1.3 Solid state nitriding of powders

The high solubility of nitrogen in the solid phase of austenitic stainless steels combined with the lower temperatures and pressures (atmospheric pressure) utilized as compared to the molten route manufacturing of high nitrogen stainless steels, makes powder metallurgy a potential manufacturing method. The short diffusion distance of nitrogen in the austenitic stainless steel powder due to small powder particle size, makes solid state nitriding of austenitic stainless steels an effective method for introducing high nitrogen contents to austenitic stainless steels. The powder nitriding process has to ensure the desired average nitrogen content of the entire manufactured component, and also as homogeneous a distribution of nitrogen as is possible (Zheng et al., 1990; Zheng, 1991; Feichtinger and Zheng, 1990; Feichtinger, 1991; Simmons et al., 1996B). In the powder metallurgy route, the nitriding can be done at different stages: in the melting of the alloy before atomizing, during atomizing utilizing high pressure nitrogen as atomizing gas, powder nitriding with nitrogen gas or nitrogen gas mixtures, or by mixing the metal powders with additive powders having high nitrogen contents. In the first two methods, the highest nitrogen contents were earlier limited to the equilibrium solubility and to short reaction time, since the nitriding process takes place in the liquid phase. However, pressurized atomizing facilities have been developed lately, which allow nitrogen contents above the solubility limit of nitrogen in the melt at atmospheric pressure to be achieved in the powders already during atomizing (Rhodes et al., 1997;

Rhodes and Eisen, 1999; Biancaniello et al., 1997). In this method, both the melt chamber and the collection chamber of the atomizing equipment are pressurized to levels higher than atmospheric pressure. Solid state nitriding of the powder with nitrogen gas or nitrogen gas mixtures is also a suitable method, and mechanical alloying of powders is an attractive method to achieve powders with high nitrogen contents.

The basic principle of solid state nitriding of powder is the same in all methods, whether using nitrogen gas or nitrogen gas mixtures. The nitriding process is divided into two phases: a) the nitriding gas flows through the powder bed, which is controlled by the bed´s gas permeability, and b) absorption of nitrogen by the powder particles, which is controlled by several reactions on the surfaces of the powder particles, and by diffusion of nitrogen atoms in the metal lattice (Ferriss, 1983; Zheng, 1991). The nitriding behaviour of different powders depends on several factors: 1) powder characteristics (chemical composition, particle size and shape, and surface state of the powder particles), 2) process parameters (pressure, time and temperature), 3) geometry of the powder bed, and 4) nitriding route.

1.3.1 Diffusion of nitrogen in austenitic stainless steel powders

The diffusivity of nitrogen in solid iron-base alloys seems to be generally inversely proportional to its equilibrium solubility, as is generally known for gases in metals in both liquid and solid state (Kunze, 1973; Hales and Hill, 1977). On the other hand, the diffusivity of nitrogen in f.c.c.-iron alloys decreases exponentially with temperature. Diffusivity of nitrogen at atmospheric pressure is higher in pure iron than in austenitic iron-base alloys, Figure 2. Therefore, achieving high nitrogen contents in the austenite phase of austenitic stainless steels is restricted by the slow diffusion rate of nitrogen in the solid phase (at appr. 600 - 1200 °C), as compared to the diffusion rate of nitrogen in the liquid state.

The kinetics of nitrogen absorption in the powder particles is important, since it makes it possible to determine the suitable temperature and time range for nitriding, and to control the nitrogen content during nitriding. The nitrogen diffusivity in the powder particles, and the nitrogen content of the powder particles, can be controlled by adjusting the temperature and nitrogen partial pressure of the nitriding equipment (Zheng, 1991; Simmons et al., 1996C). The most suitable nitriding temperature ranges for austenitic stainless steels have been observed to be 600 - 700 °C for steels with high manganese contents, and 700 - 800 °C for steels with high nickel contents. For the high manganese austenitic stainless steels, nitriding can be performed already at 600 °C, but since the nitriding rate is so slow, the nitriding should be performed at temperatures close to 700 °C, depending on the steel composition. Nitriding of powders can also be performed in the temperature range of 1100 - 1200 °C, where the diffusion of nitrogen in the powder particles is fast and the

saturation nitrogen content is reached in a short time. The saturation nitrogen content is smaller, however, at the high temperatures due to the temperature dependence of nitrogen solubility in the austenite phase.

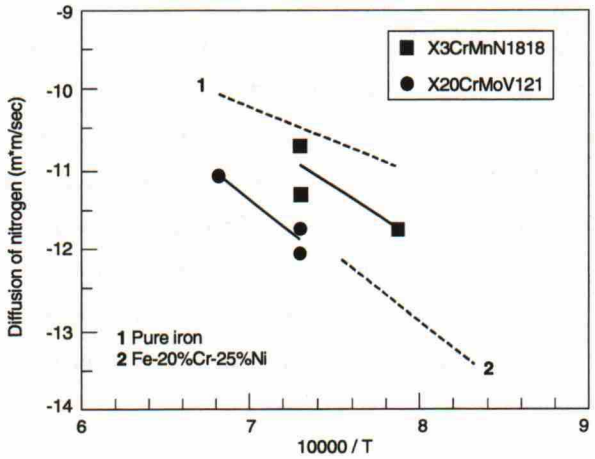

Figure 2. Diffusivity of nitrogen in austenitic and ferritic iron-base alloys (Zheng, 1991).

Nitrogen partial pressure also affects the nitriding kinetics and diffusion of nitrogen in the powder particles, as well as the resulting nitrogen content of the powder at elevated temperatures. As the nitrogen partial pressure increases, the nitrogen content of a stationary powder bed increases (Zheng, 1991). According to Rawers et al. (1994B), diffusion of nitrogen and the kinetics of nitriding of austenitic stainless steel powder increases with increasing pressure of the nitriding gas. It is also known that, in general, independent of the pressure of the nitriding gas, the diffusion rate of nitrogen decreases exponentially with temperature in f.c.c.-iron alloys.

1.3.2 Interaction of oxide films on powder particle surfaces with nitriding gases

The surface of a powder particle is always covered with oxide layers, which decrease the diffusion rate of nitrogen into the powder particles. The thickness of the oxide layers depends on the manufacturing methods of the powder. Austenitic stainless steel powders are generally manufactured by water or by inert gas atomizing. Powders manufactured by water atomizing generally have clearly thicker oxide layers on their surfaces, and consequently, higher oxygen content, as compared with inert gas atomized powders. According to the research work made by Nyborg et al. (1990), and Ferriss (1983) the surfaces of water atomized AISI 304 L austenitic stainless steel powder is covered with Fe-, Cr-, Mn- and Si-oxides. In the studies by Bracconi et al. (1994), the surface of nitrogen gas atomized AISI 304 L powder was covered mainly with Mn-, Cr,-

and Fe-oxides and Si-oxides were observed only in very small amounts. The outermost layers of AISI 304 L powder particles in all of the studies were observed to consist of Fe-oxides. The surface oxide layers of gas atomized ferritic and martensitic stainless steel powders have also been observed to consist of Fe-, Cr-, Mn- and Si-oxides (Nyborg and Olefjord, 1988; Olefjord and Nyborg, 1985).

Nitriding gases often contain hydrogen in addition to nitrogen in order to prevent the powder from being oxidised during nitriding, or even to reduce the oxide layers on the surface of powder particles. Therefore, the stability of different oxides on the surfaces of powder particles is of great importance. The relative stability of oxides can be determined from the thermodynamic point of view, but not from the kinetic standpoint. The reactants and products are considered to be in their standard states, i.e., as the pure metal and oxide. However, in reality, they do not exist in their standard states in steels. Therefore, the reduction of oxides in steels takes place at lower temperatures or at higher dew points than in the case of pure oxides and metals. On the other hand, even for the relatively unstable oxide, the residual oxygen level of the reducing atmosphere has to generally be impractically low in order to initiate the reduction of the oxide. However, it is possible to calculate equilibrium conditions at which different oxides are either formed or reduced in hydrogen containing atmospheres at any temperature. If hydrogen in the nitriding gas reacts with the oxides on the surface of the powder particles, water vapour is formed. Therefore, the ratio of partial pressures p_{H_2} / p_{H_2O} of the atmosphere has to be considered and converted to the water vapor content of the atmosphere, i.e., to the dew point of the atmosphere. The lower the dew point of an atmosphere at a certain temperature is, the more likely the reduction of the oxide is to take place. Also, the higher the temperature is at a certain dew point, the more likely the reduction of the oxide is to take place. In both cases, the magnitude of the change of either variable, i.e., dew point or temperature, depends on the equilibrium conditions for the different oxides (Lall, 1991). The equilibrium temperature for reduction of different metal oxides as a function of dew point is shown in Figure 3. According to Bracconi et al. (1994), the only oxides, which can possibly be reduced by hydrogen during a reduction treatment of austenitic AISI 304 L powder prior to hot extrusion, are Fe-oxides. Reduction of Fe-oxides is possible only around 400 °C, because at higher temperatures the residual oxygen and moisture in the reducing atmosphere result in reoxidation of the powders. It is also important that the dew point of the cooling atmosphere is low enough that reoxidization will not occur.

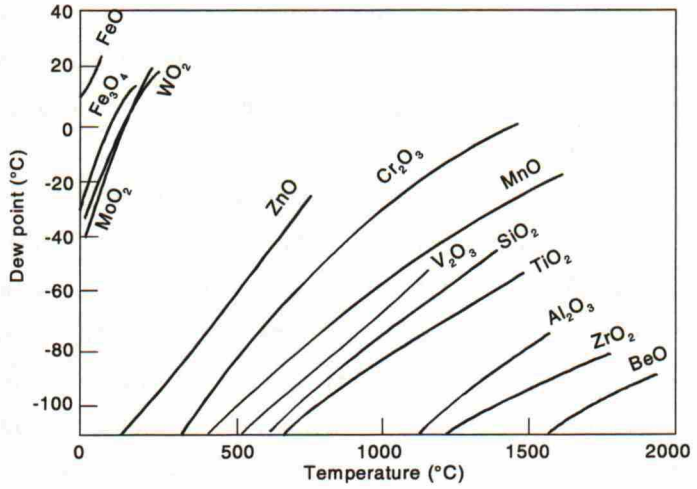

Figure 3. The equilibrium temperature for reduction of metal oxides as a function of dew point (Lall, 1991).

1.3.3 Fluidized bed nitriding

When a dry, finely-divided particle bed (typically aluminum oxide) is fluidized, it behaves like a liquid. The individual particles become microscopically separated from each other by a moving gas fed through the bed. Generally, the gas stream is fed through the bed so that the bed is ´´bubbling´´(Reynoldson, 1993; Kunii and Levenspiel, 1969; Werther, 1974). Fluidized bed furnaces are used in heat treatments because of their close control and uniformity of the atmosphere and temperature in the furnace, with reduced costs and acceptable environmental effects. The inherent advantages of fluidized beds in heat treatment are high heat transfer, and freedom from contamination of either the workpiece or the atmosphere (Reynoldson, 1993). The high heat transfer is due to the turbulent motion and rapid circulation rate of the particles in the bed, as well as the extremely high solid-gas interfacial area. In order to achieve as high heat transfer as possible, the particle diameter of the bed should be as small as possible. However, below a certain diameter, electrostatic effects can cause problems, and therefore, the optimum particle diameter is 100 μm. The density of the bed material also affects the heat transfer. Materials with high density produce lower heat transfer, and also require more power for fluidization, whereas materials with lower density suffer from electrostatic effects. Maximum heat transfer for a particular particle density and diameter requires an optimum gas flow rate, which is generally between two to three times the minimum fluidization velocity. The gas flow for minimum fluidisation, on the other hand, depends on temperature, i.e., the minimum necessary gas flow decreases with increasing temperature (Reynoldson, 1993). In order to achieve a bed which is well and evenly fluidized, the height/width ratio of the bed is also important, and should be less than 2 - 3. Tall and narrow beds should thus be

avoided, since the surface of the bed tends to be unstable due to the coalescence of gas bubbles (Werther, 1974).

The permeability of nitrogen gas through a gas fluidized powder bed is faster than through a stationary powder bed, and thus, nitrogen can be more readily absorbed into the powder particles. This is because the permeability of nitrogen gas through a powder bed and the kinetics of nitrogen gas flow through a powder bed do not restrict the nitriding process and the homogeneity of the nitrogen gas within the powder bed during nitriding, as in the case of nitriding in stationary powder beds. Nitriding of austenitic stainless steel powders in a fluidized bed furnace has been reported by Wilson (1989) and Virta and Hannula (1999). Wilson (1989) performed nitriding of gas atomized austenitic 20Cr - 25Ni - 1,8Ti-powder in a fluidized bed in order to introduce a fine dispersion of TiN into the powders, and to the material extruded from the nitrided powder. The goal to achieve an austenitic stainless steel with good high temperature strength. The fluidized bed furnace used in the tests is shown in Figure 4. Nitriding treatments were made at 1100 - 1150 °C in order to prevent chromium nitride precipitation from occurring instead of TiN precipitation. In the studies it was observed that the mean particle size of the powder bed cannot be < 50 μm, since defluidization of the powder bed occurs due to the high interparticle cohesive forces of the powder particles. The defluidization causes channeling and slugging of the nitriding gas, which can be reduced by using a stirrer. The high temperatures used in the nitriding treatments resulted in problems which, however, were not fully reported (Wilson, 1990).

Virta and Hannula (1999) nitrided gas atomized AISI 316-powder with a particle size range of 45 - 250 μm in a fluidized bed in ammonia gas at 570 °C, followed by a diffusion annealing treatment in nitrogen gas. The equipment consisted of a retort for the powder to be fluidized and nitrided in, as well as of a heating and cooling unit. The possibility to lower the nitriding temperature to below 600 °C, and thus, to eliminate the risk of sintering during nitriding, was considered to be the main advantages of ammonia gas. Also, the nitriding times to achieve reasonable nitrogen contents were observed to be short due to the high nitriding potential of ammonia gas. However, the powder particles were observed to have a nitride layer on their surfaces. According to Virta and Hannula (1999), an increase in the processing temperature results in a lower nitriding potential of the atmosphere and a higher diffusion rate of nitrogen into the powder particles. As a result, the nitride layer formation on the surface of the powder particles is retarded and a more uniform distribution of nitrogen in the powder particles can be achieved. However, as a disadvantage, the oxygen content of the powder increased approximately 100 - 200 ppm, depending on the nitriding and diffusion annealing time during the nitriding treatment, due to minor air leaks in the equipment.

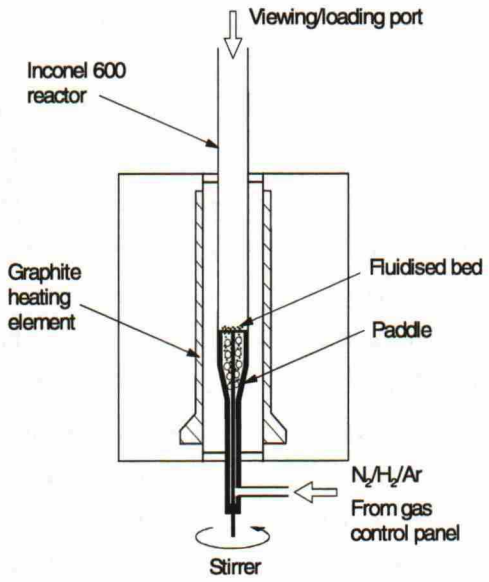

Figure 4. A fluidised bed reactor for nitriding of austenitic 20Cr - 25Ni - 1,8Ti-powder (Wilson, 1989).

1.3.4 Other nitriding methods

Rotary furnace nitriding

In order to avoid agglomeration of the powder bed during nitriding at high temperatures nitriding can be done in a rotary furnace before encapsulation and consolidation. As described above, permeability of nitrogen gas through a nonstationary powder bed is faster than through a stationary powder bed and nitrogen can be more readily absorbed into the powder particles. Simmons et al. (1996B; 1996C) have developed a mechanical fluidised bed nitriding furnace for powder nitriding. In this method, powders are nitrided in a sealed, heated, and rotable horizontal retort containing nitrogen atmosphere. Powder agglomeration typical for nitriding of stationary powder beds at high temperatures is prevented, and chemical uniformity of nitrogen in the powder bed is reported to be excellent due to the constant fluid-like movement of the powder. Simmons et al. (1996B; 1996C) studied nitriding of water atomized AISI 304 L stainless steel powder with the particle size range of 50 - 100 µm, and they were able to achieve nitrogen contents up to 3,5 wt-%N with practically no oxygen pick-up during the nitriding treatment. The highest nitriding temperature without agglomeration of the powder was 970 °C (Simmons et al., 1996C).

Container nitriding

Nitriding of stationary powder beds can be done at a high temperature range (1000 - 1200 °C) or low temperature range (600 - 800 °C), depending on the powder material. However, stationary powder beds have been observed to agglomerate when nitrided in the high temperature range. When nitriding of austenitic stainless steel powders is made in the lower temperature range, agglomeration of the stationary powder bed is not a problem (Zheng et al., 1990).

The nitriding gas must flow through the stationary powder bed before it can be absorbed into the powder particles producing a homogeneous nitrogen distribution in the powder bed. Therefore, the nitriding rate depends on the gas flow rate through the powder bed, which, on the other hand, is controlled by its gas permeability. Permeability of a powder bed depends on its microstructural characteristics, such as porosity, specific surface area, and the surface state of the powder particles. The permeability of the powder bed has been observed to be constant up to 1000 - 1100 °C, and at higher temperatures the bed starts to densify. Gas permeation increases with decreasing temperature, which is contrary to the nitrogen diffusivity behaviour described earlier. During nitriding of a stationary powder bed, an inhomogeneous distribution of nitrogen may result due to the poor permeability of nitriding gas through the powder bed and also due to temperature differences in the powder bed. The temperature differences are caused by poor thermal conductivity, which in turn is caused by the small contact areas of the powder particles (Zheng et al., 1990; Zheng, 1991).

Nitriding of a stationary powder bed is usually performed in a container either by introducing a certain volume of the nitriding gas in a container in the temperature range of 1000 - 1200 °C, or by setting the pressure of the nitriding gas to a certain level during nitriding at 600 - 800 °C. Nitriding of Ti-modified AISI 316L-powder with pure nitrogen gas at 900 - 1000 °C in a container has also been performed by controlling the nitrogen activity of the nitriding gas in order to achieve a fine dispersion of TiN particles into the powder particles (Johansson et al., 1991). Johansson et al. (1991) observed that, in general, if a certain nitrogen content of the powder is aimed for, the required equilibrium nitrogen activity increases with increasing temperature.

HIP-N process

The nitriding of powder can also be performed during the HIP cycle (Hot Isostatic Pressing), i.e., in connection with consolidation of the powder. The nitriding gas is nitrogen and it is supplied to the powder bed from a source outside the HIPing equipment. The nitrogen gas is stored in the interparticle space in the powder bed. Nitrogen is then absorbed at lower temperatures due to the high pressure associated with heating during the HIP cycle. The nitrogen distribution in the powder bed is reported to be homogeneous. Nitriding by this so called HIP-N process does not affect the

normal HIP cycle, which means that the manufacturing time for a high nitrogen steel component is not affected by the nitriding process (Feichtinger and Zheng, 1990; Feichtinger, 1991).

Powder nitriding by mechanical alloying

In the mechanical alloying process, a high-energy ball-mill deforms the powder particles plastically, bringing the matrix interior to the surface. This newly exposed surface then reacts with the atmosphere of the ball mill. When the atmosphere is nitrogen, nitrogen molecules adhere to the newly formed surface, dissociate, and are entrapped into the matrix during subsequent cold welding of the colliding milled particles (Rawers and Doan, 1994A; Dunning et al., 1994).

High nitrogen wear resistant hard alloys with nitrogen containing martensite matrix have been manufactured by mechanical alloying of steel powders with additive powders having high nitrogen contents (Berns and Wang, 1990). The powders are mixed in a ball mill under a nitrogen atmosphere from a few hours up to 100 hours, depending on the composition of the powders. AISI 316 stainless steel powder has been mixed with Fe_4N powder (Foct et al., 1990). Nitrogen redistribution during milling led to the formation of dispersed nitride particles when the steel powder was aged briefly at 200 °C. However, a slight nitrogen loss will occur during the milling, which has to be taken into account when nitrogen alloyed steel powders are manufactured with this method.

Nitriding of gas atomized Fe-, Fe-2Al- and Fe-18Cr-8Ni-powders in a nitrogen atmosphere by mechanical milling has been observed to increase the nitrogen content up to 20 times higher than what the as-cast nitrogen solubility of Fe-powder is (Rawers and Doan, 1994A; Dunning et al., 1994). Nitrogen concentration was observed to increase linearly with processing time. The metal matrix had a nanocrystalline structure, and nitrogen was distributed interstitially as well as at grain boundaries and dislocations. Nitrogen concentration was observed to increase with decreasing particle size.

High pressure powder nitriding

Powder nitriding tests have been performed for different gas atomized powders at pressures up to 150 MPa (Rawers et al., 1994B; Dunning et al., 1994). Nitriding was performed in a HIP chamber under a nitrogen atmosphere at 1000 °C for 15 min. The particle size range of the powders was < 100 μm, with an average particle size between 30 to 50 μm. In Figure 5, the nitrogen content as a function of nitrogen pressure for the studied powders is shown. The nitrogen content of the powders increased with increasing pressure. Nitrogen concentrations up to 6 wt-% N were achieved, and nitrogen was observed to be uniformly distributed in the powder particles. In the nitriding tests for Fe-10Cr-5Mn and Fe-18Cr-8Ni-powders, chromium nitrides of the type CrN (Cr_2N was not observed) were formed immediately even at 0,1 MPa nitrogen pressure, and the

amount of CrN increased with increasing nitrogen content. After the nitrides (CrN, Fe_4N, $(Fe, Al)_4N$) in the different alloys were formed, the interstitial nitrogen content increased according to the nitrogen solubility in pure iron (Rawers et al., 1994B; Dunning et al., 1994).

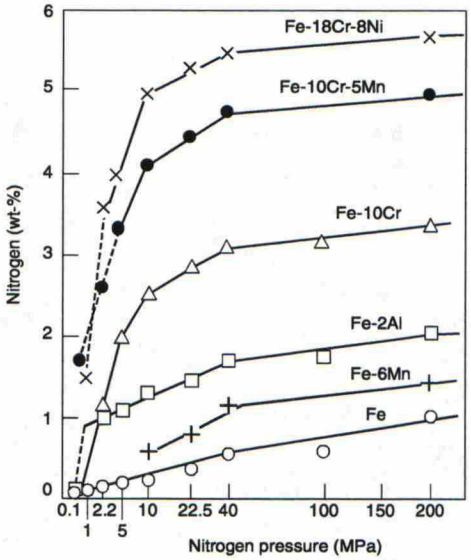

Figure 5. Nitrogen contents as a function of nitrogen pressure for different powders (< 100 µm) nitrided for 15 min at 1000 °C in a HIP chamber (Dunning et al., 1994).

1.4 Mechanical properties of nitrogen alloyed austenitic stainless steels

Nitrogen in solid solution is the most beneficial alloying element in promoting high strength in austenitic stainless steels without affecting their good ductility and toughness properties. Additionally, nitrogen so strongly stabilizes the austenite phase, that nitrogen alloyed austenitic stainless steels can be work hardened to very high strength levels without fear of strain-induced martensite formation.

1.4.1 Tensile properties of nitrogen alloyed austenitic stainless steels

Tensile strength

Yield and ultimate tensile strengths of austenitic stainless steels increase with increasing interstitial nitrogen content of the steel. The influence of nitrogen on the tensile properties does not depend on the manufacturing method of the steels, i.e., whether they are manufactured

conventionally, via pressurized metallurgy processes, or by powder metallurgical manufacturing method (Speidel, 1989; Simmons, 1996A; Rawers and Grujicic, 1996; Rhodes and Conway, 1996; Rhodes et al., 1997; Rhodes and Eisen, 1999; Romu et al., 1996; Tervo, 1994; Tervo et al., 1997; Tervo, 1998). The effect of nitrogen content on the tensile properties of austenitic stainless steels is shown in Figure 6.

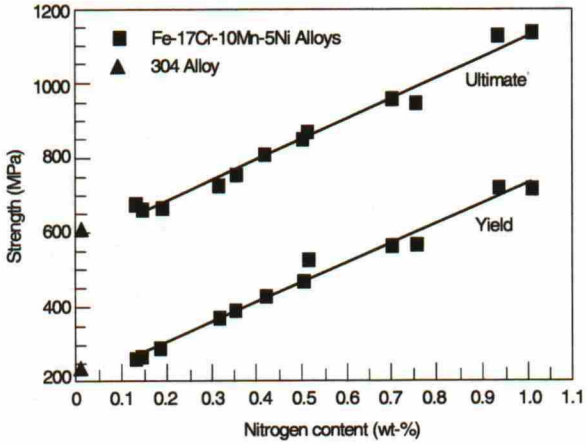

Figure 6. The effect of nitrogen content on yield and ultimate tensile strength for a series of Fe-17Cr-10Mn-5Ni-N steels. The typical values of yield and ultimate tensile strength for AISI 304 austenitic stainless steel at room temperature are shown for comparison (Simmons, 1996A).

The yield strength of nitrogen alloyed austenitic stainless steels at room temperature is due to solid solution hardening and grain boundary hardening when nitrogen is in interstitial solid solution (Norström, 1977; Byrnes et al., 1987; Werner, 1988; Harzenmoser et al., 1990; Uggowitzer and Harzenmoser, 1990; Simmons, 1996A). The matrix strength of the steels also has an effect on their yield strength, but its effect is small as compared with the two above mentioned factors. Matrix strength is the strength attained due to the frictional stress of dislocations in the interstitial-free austenitic crystal lattice containing substitutional alloying elements such as Cr, Ni, Mn, Mo, etc.

Solid solution hardening is generally based on the atomic size misfit of the solute atoms with the austenitic crystal lattice. Localized, predominantly modulus interactions between lattice disturbances in the immediate vicinity of nitrogen atoms and slip dislocations, have also been explained to cause solid solution hardening (Byrnes et al., 1987; Uggowitzer and Harzenmoser, 1990; Rawers and Grujicic, 1996). Solid solution hardening of austenitic steels by dissolved nitrogen is proportional to the change in the lattice parameter of the austenitic matrix caused by nitrogen atoms (Werner, 1988). Solid solution hardening by substitutional alloying elements is

small, whereas interstitial alloying elements such as nitrogen, carbon and boron have a far more stronger hardening effect (Irvine, 1961; Norström, 1977; Sandström and Bergqvist, 1977; Werner, 1988). Nitrogen has the greatest effect on yield strength among interstitial alloying elements, and this effect is approximately ten times higher than that of the substitutional alloying elements. The effect of nitrogen content on yield strength due to solid solution hardening is proportional to $C_N^{1/2}$. The main contribution of substitutional alloying elements to the strengthening of nitrogen alloyed stainless steels, is through their ability to increase nitrogen solubility in stainless steels and ability to ensure that nitrogen remains in interstital solid solution instead of precipitating as nitrides (Rawers and Grujicic, 1996).

The grain size hardening in nitrogen alloyed austenitic stainless steels is based on the grain size dependence of the yield strength. This dependence can be described by the Hall-Petch equation (Herzberg, 1989):

$$R_{p0,2} = \sigma_r + k_y/\sqrt{D} \qquad (1)$$

where σ_r is the 0,2 % flow stress for very large grain size material and is thus considered as a measure of the yield strength of the grain interior, k_y is a measure for the grain size hardening effect and D is the grain size. According to this equation, the smaller the grain size the higher the yield strength of the steel. Nitrogen has a very strong effect on k_y. According to Uggowitzer and Harzenmoser (1990) and Werner (1988) this can be interpreted as a measure for the efficiency of grain boundaries in impeding dislocation motion. The effect of nitrogen content on grain boundary hardening increases proportionally as the nitrogen content of the steel increases (Norström, 1977; Sandström and Bergqvist, 1977; Byrnes et al., 1987; Werner, 1988). It has also been suggested that the effect of nitrogen on grain boundary hardening can be explained by the planar dislocation structures observed in nitrogen alloyed austenitic steels, and thus, by the decreasing effect of nitrogen on the stacking fault energy (SFE) in austenitic stainless steels. However, nitrogen alloying of austenitic stainless steels has also been reported to increase the stacking fault energy, and thus, any conclusions on the effect of stacking fault energy on the grain boundary hardening or on any other phenomena related to mechanical properties cannot be made (Swann, 1963; Latanision and Ruff, 1971; Schramm and Reed, 1975; Stoltz and Vander Sande, 1980; Müllner et al., 1993).

Short range ordering has also been considered as a possible explanation for the planar dislocation arrangement in nitrogen alloyed austenitic stainless steels, and for the resulting grain boundary hardening. Grain boundary hardening increases therefore with increasing nitrogen content of the steel, and is related to the strong affinity between chromium and nitrogen atoms. As a result, local increase in the elastic shear modulus and some anisotropic elastic strain in the immediate

vicinity of nitrogen atoms takes place (Byrnes et al., 1987; Grujicic et al., 1989; Rawers and Grujicic, 1996).

Temperature affects the yield strength of nitrogen alloyed austenitic stainless steels. The yield strength of nitrogen alloyed austenitic stainless steels depends very little on temperature in the temperature range of 250 - 600 °C, i.e., yield strength decreases very little with increasing temperature (Norström, 1977; Uggowitzer and Harzenmoser, 1990; Rawers and Grujicic, 1996). On the other hand, the yield strength of nitrogen alloyed austenitic stainless steels increases markedly with decreasing temperature below room temperature. The increase in yield strength is more pronounced as the nitrogen content of the steel increases. The pronounced increase in yield strength with decreasing temperature is typical for materials with a b.c.c. crystal structure but not for materials with an f.c.c. crystal structure including austenitic stainless steels (Sandström, 1977; Byrnes et al., 1987; Reed and Simon, 1989; Uggowitzer and Harzenmoser, 1990; Harzenmoser et al., 1990).

The tensile properties of nitrogen alloyed austenitic stainless steels can be effectively increased with strain hardening by cold working. The yield and ultimate tensile strength values of the steel increase with increasing degree of cold work and nitrogen content. The pronounced increase in tensile properties is due to the high strain hardening rate, which increases with increasing nitrogen content of the steel. Planar dislocation structures with high dislocation density, slip-band formation, and extensive twin formation have been observed in cold worked nitrogen alloyed austenitic stainless steels. These phenomena have been explained to be due to the low stacking fault energy of the steels (Defilippi et al., 1968; Schramm and Reed, 1975; Norström, 1977; Uggowitzer and Harzenmoser, 1990; Paulus et al., 1993; Simmons, 1996A; Tervo, 1998). It has also been noticed that nitrogen alloying of austenitic stainless steels increases the strength coefficient K_1, which means that the ability of the steel to be strengthened by strain is increased (Soussan et al., 1991; Tervo, 1998).

Tensile ductility

Tensile ductility, i.e., elongation to fracture and reduction of area, of solution annealed nitrogen alloyed austenitic stainless steels is practically unaffected by nitrogen content at room temperature as long as the nitrogen is interstitially dissolved.

The ductility of nitrogen alloyed steels decreases markedly with decreasing temperature, and the effect is more pronounced as the nitrogen content of the steel increases. This phenomenon is due to the ductile-to-brittle transition, which nitrogen alloyed austenitic stainless steels undergo at low temperatures. The ductile-to-brittle transition at cryogenic temperatures has been observed to be

more pronounced in Fe-Cr-Mn-N steels as compared with Fe-Cr-Ni-N alloyed steels (Harzenmoser et al., 1990; Uggowitzer et al., 1992; Ilola et al., 1996).

The tensile ductility of cold-worked nitrogen alloyed austenitic stainless steels decreases rapidly with increasing amount of cold work, and is not significantly influenced by the nitrogen content of the steel. In order to keep the ductility of the steel as high as possible after cold working, the interstitially dissolved nitrogen content of the steel has to be as high as possible, since then the amount of cold work necessary to obtain the desired yield strength is reduced (Paulus et al., 1993).

1.4.2 Impact toughness properties of nitrogen alloyed austenitic stainless steels

Nitrogen alloyed austenitic stainless steels have high impact toughness as long as the nitrogen is interstitially dissolved. The impact toughness of nitrogen alloyed austenitic stainless steels depends upon temperature and alloying elements. The impact energy of nickel alloyed nitrogen containing austenitic stainless steels has been generally observed to decrease only slightly with decreasing temperature down to cryogenic temperatures. On the other hand, the impact energy of manganese alloyed nitrogen containing austenitic stainless steels decreases sharply with decreasing temperature in a narrow temperature range, i.e., they exhibit a ductile-to-brittle transition which is not usual for steels with an f.c.c. crystal structure (Defilippi et al., 1969; Harzenmoser et al., 1990; Uggowitzer et al., 1992). However, according to Ilola et al. (1996), a ductile-to-brittle transition also takes place in Ni alloyed high nitrogen steels, but the phenomenon is not as pronounced as in Mn alloyed high nitrogen steels. The effect of temperature on the impact energy of Cr-Ni and Cr-Mn nitrogen containing austenitic stainless steels is shown in Figure 7a. The ductile-to-brittle transition temperature increases with increasing nitrogen content of the Cr-Mn steel, Figure 7b. Similar behaviour has been observed in the case of tensile ductility. However, the phenomenon is more pronounced in impact testing than in tensile testing. According to Uggowitzer et al. (1992), the fact that nickel alloyed nitrogen containing austenitic stainless steels do not have a clear ductile-to-brittle transition can be explained by their higher stacking fault energy as compared to that of Mn alloyed high nitrogen austenitic stainless steels. The ductile-to-brittle transition temperature has also been observed to depend on the grain size of the steel. As the grain size of the steel decreases, the ductile-to-brittle transition temperature increases slightly, according to Tomota and Endo (1990) and Uggowitzer et al. (1992).

Powder metallurgically manufactured nitrogen alloyed austenitic stainless steels have lower impact toughness values than conventionally or pressurized metallurgy manufactured materials. That is explained to be a result of the oxide films on powder particle surfaces resulting in fracture in the consolidated steels taking place more easily along the weak prior particle boundaries (Romu et

al., 1993; 1996; Tervo, 1994; Rhodes and and Conway, 1996; Rhodes et al.,1997; Rhodes and Eisen, 1999).

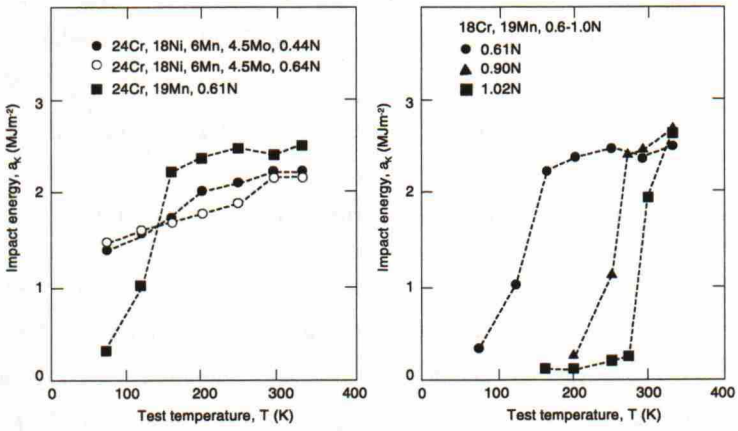

a) b)

Figure 7. Effect of a) temperature on impact energy of Cr-Ni and Cr-Mn nitrogen containing austenitic stainless steels and b) nitrogen content on impact energy for Cr-Mn nitrogen containing austenitic stainless steels (Uggowitzer et al., 1992).

1.4.3 Ductile-to-brittle transition mechanisms

As described previously, nitrogen alloyed austenitic stainless steels undergo ductile-to-brittle transition during tensile and impact toughness testing at low temperatures. Also, as the nitrogen content of the steel increases, the phenomenon becomes more pronounced, and the ductile-to-brittle transition temperature increases. The proposed mechanisms related to this phenomenon are described in the following.

Plastic deformation in nitrogen alloyed austenitic stainless steels at low temperatures has been observed to be highly locally concentrated to slip bands and/or deformation twins. The fracture stress of nitrogen alloyed austenitic stainless steels at low temperatures has been observed to decrease with increasing nitrogen content of the steel, due to heterogeneous plastic flow and grain boundary hardening. The fracture stress is higher for Ni alloyed nitrogen containing austenitic stainless steels than that for Mn alloyed steels, due to the higher stacking fault energy of Ni alloyed steels. The flow stress of nitrogen alloyed austenitic stainless steels increases with increasing nitrogen content, and is high as a result of solid solution and grain boundary hardening, especially at low temperatures. Thus, a cleavage-like fracture without extensive plastic deformation at low temperatures is possible in nitrogen alloyed austenitic stainless steels (Uggowitzer et al., 1992).

The dislocation arrangement in nitrogen alloyed austenitic stainless steels becomes planar during deformation with increasing nitrogen content of the steel. Thus, even after small amounts of plastic deformation, slip bands with high dislocation density and deformation twins are formed, and the cracking mode is considered to be slip band and twin boundary cracking, especially at low temperatures. Also, during deformation at low temperatures, extensive finely spaced stacking faults are formed. Slip band fracture is considered to be a result of strong slip concentration in suitably oriented grains with respect to the direction of deformation. Strong slip concentration is explained to be caused by low stacking fault energy, ordering or by coarse precipitates (Tobler and Meyn, 1988; Harzenmoser et al., 1990). Accumulation of dislocation-induced defects and formation of local stress fields in the slip bands weaken them, until finally fracture takes place along them. The brittle transgranular cleavage-like fracture of Mn alloyed (and Ni alloyed) nitrogen containing austenitic stainless steels has been observed to take place along slip bands consisting of {111} planes. Increasing the nitrogen content of austenitic stainless steels is explained to increase the slip concentration in the slip bands. As a result, the fracture stress of the slip bands decreases and the ductile-to-brittle transition temperature increases (Defilippi et al., 1969; Tobler and Meyn, 1988; Harzenmoser et al., 1990; Tomota and Endo, 1990; Ilola et al., 1996).

1.5 Resistance of nitrogen alloyed austenitic stainless steels to localized corrosion

A number of apparently contradictory results have been presented on the effects of nitrogen alloying on the corrosion resistance of stainless steels. There are several theories developed to describe the actual mechanisms of how nitrogen affects the corrosion resistance of stainless steels, and these theories are sometimes contradictory. However, it is well known that nitrogen alloying of stainless steels improves their resistance to localized corrosion, and in some environments, also resistance to general corrosion (Janik-Czachor et al., 1975; Eckenrod and Kovach; 1977; Kearns and Deverell, 1987; Tervo, 1994; Levey and van Bennekom, 1995; Uggowitzer et al., 1993, Jargelius-Petterson, 1998).

Nitrogen alloying is beneficial in improving the pitting and crevice corrosion resistance of all kinds of stainless steels. The beneficial effect of nitrogen on the corrosion resistance of stainless steels can be utilized as long as the solubility limit of nitrogen in the steel is not exceeded, i.e., as long as nitrogen is in interstitial solid solution. In order to characterize the effect of different alloying elements on pitting corrosion resistance, and to rank different alloys, a pitting resistance equivalent (PRE) is used:

$$PRE = \% Cr + 3{,}3\% Mo + x\% N \quad (2)$$

The values 10 and 30 have been used for tthe coefficient for nitrogen (x), which means that nitrogen has the greatest beneficial effect on pitting corrosion resistance. Nitrogen and molybdenum as well as nitrogen and chromium have synergistic effects in increasing the pitting corrosion resistance of stainless steels. By increasing the chromium, molybdenum, and especially nitrogen contents of an austenitic stainless steel, it is possible to achieve crevice corrosion resistance comparable to that of some nickel-base alloys, Figure 8. Partial replacement of molybdenum with tungsten has also been observed to improve the localized corrosion resistance of austenitic stainless steels (Jonsson et al., 1999). The beneficial effect of chromium, molybdenum, and nitrogen can be utilized even better in powder metallurgically manufactured austenitic stainless steels, due to their more homogeneous microstructures as compared to those of steels manufactured conventionally or via pressurized metallurgy (Tervo, 1994; Rhodes and Conway, 1996; Rhodes et al., 1997; Rhodes and Eisen, 1999; Romu et al., 1996).

Even though nickel is a beneficial alloying element in enhancing the localized corrosion resistance of austenitic stainless steels, nickel-free austenitic stainless steels have been developed with good resistance to localized corrosion. Their good localized corrosion resistance is due to nitrogen alloying. Nitrogen is an austenite stabilizing element like nickel, and can thus be used instead of nickel to ensure a fully austenitic microstructure (Uggowitzer et al., 1993). Manganese has been observed to be detrimental to the pitting corrosion resistance of nitrogen alloyed austenitic stainless steels (Sedriks, 1986; Jargelius-Petterson, 1996; Biancaniello et al., 1997). However, the detrimental effect of manganese can be compensated for by nitrogen alloying, especially since the nitrogen contents attainable in the steels increase with increasing manganese content of the steel. This is due to the fact that manganese increases nitrogen solubility in austenitic stainless steels. Alloying molybdenum together with nitrogen has been observed to be beneficial in overriding the detrimental effects of manganese sulfides on localized corrosion resistance (Sedriks, 1986). According to Jargelius-Petterson (1996, 1998), nitrogen alloying markedly improved the pitting corrosion resistance of an austenitic stainless steel (20Cr-18Ni-4,5Mo, with the amounts of manganese and nitrogen varying between 0,2 - 10 wt-%Mn and 0,01 - 0,5 wt-%N, respectively). The positive effect of nitrogen on crevice corrosion resistance is, however, according Jargelius - Petterson (1998), smaller than that on pitting corrosion resistance. The positive effect of nitrogen was observed to be largest in the range of 0 - 0,2 wt-% N. However, nitrogen alloying was observed to improve the pitting and crevice corrosion resistance of the steels also in the range of 0,2-0,5 wt-% N, although the effect was less pronounced. Similar results have been observed by Janik-Czachor et al. (1975) for a steel with a nominal composition of Fe-18Cr-5Ni-10Mn-N, with the nitrogen contents varying between 0,07 - 0,35 wt-%N.

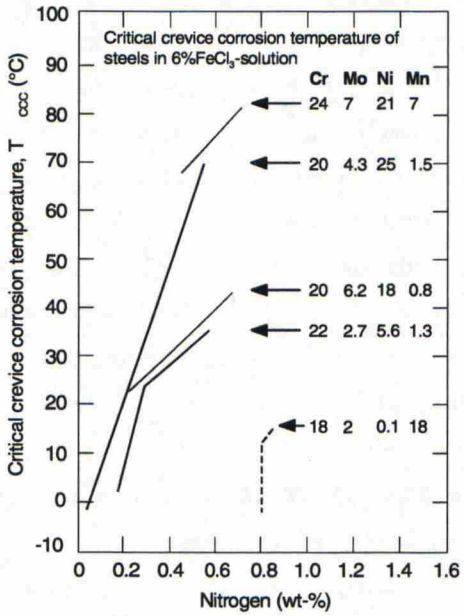

Figure 8. The effect of major alloying elements on critical crevice corrosion temperature of austenitic stainless steels (Uggowitzer et al., 1993).

In addition to the direct effects, nitrogen also affects the localized corrosion resistance of stainless steels indirectly, via the retarding effect of nitrogen on the precipitation of intermetallic phases such as sigma, chi, etc. These phases can act as initiation sites for corrosion pits, since they may cause a discontinuous passive film, and because their formation consumes chromium resulting in chromium depletion around them. Nitrogen is an austenite stabilizing element, and thus, suppresses martensite formation. Martensite formed in austenitic stainless steels can act as an initiation site for corrosion pits.

Effect of nitrogen content on initation and propagation of localized corrosion

Nitrogen alloying of austenitic stainless steels results in increased resistance to localized corrosion, since nitrogen influences the initiation and propagation of both pitting and crevice corrosion.

Pitting corrosion

Nitrogen alloying has been observed to retard pitting initiation to some extent by increasing the incubation time, which results in a decreased extent of attack in potentiostatic corrosion measurements for Fe-N alloys as compared with pure Fe (Grabke, 1996). It seems that the stable pit growth is suppressed effectively by an immediate repassivation enhanced by nitrogen alloying, i.e.,

nitrogen has a strong effect on the repassivation kinetics. This is partly explained by the reduced anodic dissolution rate of metals in acids with increasing nitrogen content of the steel, which, in turn, helps in the repassivation of the pits (Newman and Sharabi, 1987; Lu et al., 1991). The anodic dissolution rate of metals has been explained to be impeded by increased cathodic dissolution of nitrogen leading to an enrichment of nitrogen, NH_4^+ -ions or as nitrides on the steel surface. On the other hand, it has been observed that anodic dissolution of metals in acids is increased with increasing nitrogen content of the steel (Truman, 1989; Grabke, 1996). Nitrogen has also been observed to enhance the surface enrichment of chromium, and hence, to inhibit anodic dissolution at the pit site. However, despite the discrepancies in the observations, it is generally accepted that nitrogen suppresses stable pit growth by repassivation.

In potentiodynamic corrosion measurements of nitrogen containing austenitic stainless steels, it has been observed that pitting potentials are increased as a result of nitrogen alloying (Jargelius and Wallin, 1986; Levey and van Bennekom, 1995). Repassivation of the pits is promoted by the increase in the nitrogen content of the steel in potentiodynamic corrosion tests. The potential range, where repassivation takes place, has been observed to broaden as the nitrogen content of the steel increases (Newman and Sharabi, 1987; Jargelius and Wallin, 1986). Nitrogen decreases the growth rate of a pit by increasing the pH of the solution inside the pit (Grabke, 1996). Nitrogen has also been observed to suppress the stable growth of the pit, which is repassivated immediately, and thus, the pits remain very small (Jargelius and Wallin, 1986).

Crevice corrosion

Pitting and crevice corrosion take place by the same mechanism, but the probability of crevice corrosion is increased by the presence of a stagnant corrodent of limited quantity within the crevice. As a result, the corrosive solution in the crevice becomes more aggressive, since its pH decreases (Truman, 1989). Also, the breakdown of the passive layer, i.e., depassivation of the steel within the crevice, is more laterally widespread than in case of pitting corrosion (Jargelius-Petterson, 1998). The active dissolution rate of metals in crevice corrosion has been observed to decrease with increasing nitrogen content of the steel. Resistance to initiation of crevice corrosion has been explained to be improved, i.e., the incubation time for crevice corrosion initation is lengthened, with increasing nitrogen content of the steel, which is anticipated to be due to suppression of acidification (decrease of pH) of the crevice solution by ammonium formation in the vicinity of the alloy/solution interface (Truman, 1989; Azuma et al., 1996). However, the probability for crevice corrosion attack is not affected by nitrogen alloying, because nitrogen has not been observed to have an effect on depassivation, i.e., break down of the passive layer (Azuma et al., 1996; Jargelius - Petterson, 1998).

Once corrosion in the crevice site takes place, its propagation is suppressed and the penetration depth of the corrosion attack is decreased, with increasing nitrogen content of the steel. This is because repassivation takes place faster, and the anodic dissolution rate of metals is decreased with increasing nitrogen content of the steel in acidic solutions (Truman, 1989; Azuma et al., 1996; Jargelius-Petterson, 1998). The positive effect of nitrogen alloying on repassivation during crevice corrosion has been explained to be less than in pitting corrosion, because depassivation is more laterally widespread in the crevice geometry, and the anodic dissolution rates of metals are restricted (Jargelius - Petterson, 1998).

1.6 Precipitation processes in nitrogen alloyed austenitic stainless steels

Precipitation may take place in nitrogen alloyed austenitic stainless steels during manufacturing, or during exposure to elevated temperatures. The microstructure of a solution annealed steel is not the equilibrium structure either at room temperature or at elevated temperatures. Therefore, when the exposure temperature is high enough for diffusion of alloying elements to take place, the microstructure of the steel begins to change towards the equilibrium structure. The equilibrium structure depends on the exposure temperature and is different at all the temperatures. The higher the exposure temperature the sooner the equilibrium structure is reached, since diffusion of alloying elements becomes faster with increasing temperature.

The precipitated phases are nitrides (mainly chromium nitrides) and/or intermetallic phases. Carbides ($M_{23}C_6$ and M_6C) have also been reported to precipitate in nitrogen alloyed austenitic stainless steels during exposure to elevated temperatures. This has been observed to take place mainly in steels with chemical compositions similar to AISI 304 steel. Nitrogen alloying of the steels up to 0,16 wt-%N retarded carbide precipitation and sensitization, but higher nitrogen contents of up to 0,25 wt-%N, however, enhanced sensitization (Thier et al., 1969; Briant et al., 1982; Mozhi et al., 1985; Sedriks, 1986; Betrabet et al., 1987). As the nitrogen content of the steel increases from ~ 0,15 wt-%N to ~ 0,25 wt-%N, precipitation of M_6C type carbide becomes more favourable than the precipitation of $M_{23}C_6$ type carbide during exposure to elevated temperatures, according to Thier et al. (1969). Additionally, Cr_2N was observed to precipitate as the nitrogen content of the steel increased. However, carbon contents of the steels in the above mentioned studies were higher than those in high nitrogen austenitic stainless steels. Therefore, carbides in these steels precipitate in such low amounts that they are not considered to have any marked effect on the properties of high nitrogen austenitic stainless steels.

1.6.1 Nitride precipitation

Nitride precipitation in high nitrogen austenitic stainless steels may take place during solution annealing or during exposure to elevated temperatures, and it may be either beneficial or detrimental, depending on the composition of the nitrides and on the application of the steel. Nitride precipitation can be divided into two categories: chromium nitride precipitation, and precipitation of nitrides with strong nitride forming additives such as V, Ti and Nb, which can be alloyed in small quantities in high nitrogen steels. The mechanism of nitride precipitation in these iron-base alloys does not differ much from those in other ferrous and non-ferrous systems (Jack, 1989).

Chromium nitrides

Cr_2N is often referred to as ε-nitride, and it is an extremely brittle hexagonal phase. Therefore, toughness and ductility of nitrogen alloyed austenitic stainless steels are decisively affected by Cr_2N. Composition of Cr_2N is not fixed in a stoichiometrical way, and it has been observed to vary in a relatively broad range. In addition to nitrogen, carbon can be found in it. Also, in addition to chromium, small amounts of Fe, Ni or Mn can replace part of Cr (Thier et al., 1969; Uggowitzer et al., 1993).

In high nitrogen austenitic stainless steels it is important to prevent chromium nitride precipitation. Precipitation of chromium nitrides has adverse effects on mechanical properties, especially on ductility and toughness. It also has adverse effects on corrosion resistance when the precipitation is localized at the austenite grain boundaries. It is due to the fact that the regions adjacent to the grain boundaries are depleted in chromium, and as a result, intergranular corrosion may occur. The most commonly observed chromium nitride is Cr_2N, which is formed at elevated temperatures depending on the composition of the steel. Chromium nitride of the type CrN has been reported to form in austenitic stainless steel powders when they are solid state nitrided at high pressures (Rawers, 1994). However, CrN has not been reported to have precipitated in consolidated nitrogen alloyed austenitic stainless steels. According to thermodynamic calculations by Frisk (1990) CrN may appear in steels with low Cr content. Cr contents of austenitic stainless steels are high, and thus, CrN is not believed to precipitate in them.

It is possible to calculate the maximum temperature of Cr_2N precipitation by thermodynamic analysis based on the nitrogen activity data (Feichtinger, 1991; Zheng, 1991). The data and formulas needed for these calculations are shown in Appendix C. The maximum nitrogen solubility in certain temperature ranges for different austenitic stainless steels can be determined from the calculated nitrogen solubilities. The minimum temperature for complete dissolution of Cr_2N during solution annealing of the different alloys with various nitrogen contents can also be evaluated by the

calculations. Utilizing the interaction parameters, it is possible to evaluate the phase equilibrium of Cr_2N in multicomponent iron-base alloys with relatively good precision.

The maximum nitrogen solubility depends on the chemical composition of an alloy. The effect of different alloying elements on maximum nitrogen solubility is shown in Figure 9. Elements decreasing the nitrogen activity in solid solution, such as Mn, Mo, V, Nb, Ta and Ti, increase nitrogen solubility and the nitrogen content for Cr_2N formation, whereas elements decreasing the nitrogen solubility, such as Ni, Si, C, Cu, P and B, promote Cr_2N precipitation.

It has been observed that Cr_2N precipitation is 10 times faster in nickel alloyed austenitic stainless steels as compared to that in manganese alloyed austenitic stainless steels, when the steels contain equal nitrogen concentrations. The formation of chromium nitrides is controlled by diffusion of chromium, as in the case of chromium carbides (Stawström and Hillert, 1969; Brandis et al., 1976A; Bruemmer, 1990; Uggowitzer and Speidel, 1990; Simmons, 1995A). Chromium decreases the nitrogen activity in the austenite phase, and therefore, it should retard Cr_2N precipitation. However, the activity of chromium is directly proportional to the chromium content and, therefore, the precipitation of Cr_2N is promoted by chromium. Thus, the influence of chromium depends on the total effect of these two factors. In Fe-Cr alloys at 1200 °C, nitrogen solubility reaches a minimum value at approximately 10 wt-% chromium. At lower chromium contents, the higher nitrogen solubility is due to the low chromium activity, whereas at higher chromium contents the action of chromium to decrease the nitrogen activity is stronger than the increase of chromium activity (Zheng, 1991).

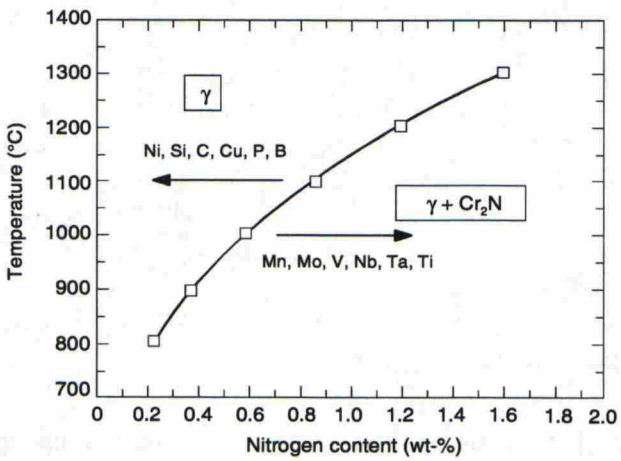

Figure 9. Influence of alloying elements on maximum nitrogen solubility curve in stainless steels (Zheng, 1991).

Precipitation of Cr_2N can take place during the manufacturing of nitrogen alloyed austenitic stainless steels, or during exposure to elevated temperatures. During manufacturing, Cr_2N can

precipitate mainly due to too low solution annealing temperature, and/or too slow cooling rate from the solution annealing temperature. The time for Cr_2N precipitation to start, is reduced with increasing nitrogen content of the steel at all temperatures (Brandis et al., 1976A; Uggowitzer and Speidel, 1990). The precipitation behaviour of Cr_2N in solution annealed manganese alloyed austenitic stainless steels is shown in Figure 10. In Figure 10, temperatures for minimum recrystallization as a function of nitrogen content of the steel are also shown. These temperatures represent minimum recrystallization annealing temperatures leading to Cr_2N free microstructure in cold-worked steels. The higher the nitrogen content of the steel, the higher the minimum recrystallization temperature. The effect of prior cold work on Cr_2N precipitation will be described later in this chapter.

As high nitrogen austenitic stainless steels are isothermally exposed to elevated temperatures, they become thermally unstable, and Cr_2N begins to precipitate. Cr_2N precipitation has been observed to be heterogeneous, and to take place sequentially at the grain boundaries, by cellular precipitation (discontinuous precipitation), and inside the grains depending on annealing temperature, exposure time, and microstructure of the steel, i.e., whether the steel is solution annealed or cold worked (Brandis et al., 1976A; Mielityinen-Tiitto, 1979; Rayaprolu and Hendry, 1989; Simmons et al., 1994; 1996B; Simmons, 1995A; Taillard et al., 1999).

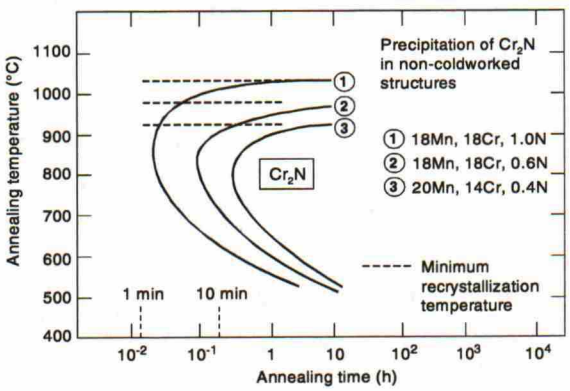

Figure 10. Precipitation behaviour of different nitrogen alloyed austenitic stainless steels in the solution annealed condition (Uggowitzer and Speidel, 1990).

The amount and the kinetics of all forms of Cr_2N precipitation in nitrogen alloyed austenitic stainless steels have been observed to increase with increasing annealing temperature and time. As the annealing temperature of solution annealed steel is increased, Cr_2N precipitation is first observed to occur intergranularly. Intragranular as well as cellular precipitation of Cr_2N is observed as the annealing time is increased in the temperature range of Cr_2N precipitation, i.e., from 600 °C

up to the solution annealing temperature. The temperature range for Cr_2N precipitation depends on the chemical composition of the steel, and especially on the nitrogen content. At temperatures below 600 °C, Cr_2N precipitation has not been observed in the solution annealed steels even after long aging times. Cr_2N has been observed to begin to precipitate at 600 - 650 °C after relatively long times (after 100 h of annealing). Precipitation begins discontinuously at the grain boundaries and grain boundary coverage of Cr_2N increases as the aging time increases. As the annealing temperature is further increased up to 700 °C, Cr_2N precipitation occurs by intergranular precipitation. Cellular precipitation takes place at annealing temperatures above 900 °C after intergranular precipitation, and is followed by intragranular precipitation. The size of Cr_2N precipitates at the grain boundaries has been observed to increase with increasing annealing temperature (Mielityinen-Tiitto, 1979; Simmons et al., 1994; 1996B; Simmons, 1995A; Rayaprolu and Hendry, 1989).

As described earlier, Cr_2N precipitation during isothermal annealing takes place sequentially in three ways: by intergranular, cellular and intragranular mode. Cr_2N precipitation has not been observed to take place simultaneously at all grain boundaries, which is assumed to be due to the differences between the characteristics of the grain boundaries, such as differences in the grain boundary structure, misorientation, and energy (Simmons et al., 1994; 1996B; Simmons, 1995A). Cellular precipitation of Cr_2N takes place by a decomposition process, in which austenite supersaturated with nitrogen decomposes to a lamellar structure consisting of Cr_2N and austenite, which has a lower nitrogen and chromium content than the supersaturated austenite. The cellular Cr_2N has a morphology very similar to that of pearlite forming in carbon steels, and it is a result of a discontinuous, non-steady-state growth process. In this growth process, the migration rate of cell boundaries decreases with increasing annealing time, and finally stops. Long-range diffusion of nitrogen from the untransformed supersaturated austenite into the growing cell is assumed to take place. Long-range diffusion is considered to be the chemical driving force for the precipitation process, since the nitrogen concentration averaged over the cell becomes higher than that of the initial austenite matrix from which the cell is transformed (Presser, 1983; Rayaprolu and Hendry, 1988; 1989; Kikuchi et al., 1991; Simmons et al., 1994; 1996B; Simmons, 1995A; Taillard et al., 1999). As the cellular precipitation proceeds, the nitrogen content of the untransformed austenite decreases, and the chemical driving force for Cr_2N precipitation decreases until it becomes so low that further precipitation stops. Intragranular precipitation of Cr_2N in the solution annealed steel has been observed to be limited, and isolated precipitates with a platelet morphology have been observed to form. The limited intragranular precipitation has been explained to be due to the small amount of defects in the solution annealed steel, and thus, it is not favoured over intergranular or, especially, cellular precipitation (Brandis et al., 1976A; Mielityinen-Tiitto, 1979; Rayaprolu and

Hendry, 1989; Simmons et al., 1994; 1996B; Simmons, 1995A). However, the solution annealed steels contain to some extent annealing twins. These twins are initiation sites for Cr_2N precipitation, which occurs primarily at the incoherent portions of the twin boundaries. Sporadic precipitation of Cr_2N has also been observed at annealing twin boundaries in the solution annealed steel, in addition to the other forms of Cr_2N precipitation.

Prior cold-working of nitrogen alloyed austenitic stainless steels markedly accelerates Cr_2N precipitation, especially intragranular Cr_2N precipitation. A similar effect of prior cold-working on the precipitation of Cr carbides has been observed in steels with low nitrogen contents (Advani et al., 1991). The effect of cold-working on the acceleration of Cr_2N precipitation in high nitrogen austenitic stainless steels is more pronounced as the annealing temperature increases. At the same time, cellular precipitation is retarded. Cr_2N has also been observed to nucleate at deformation twin/matrix interfaces. In the cold-worked condition, high-nitrogen steels have a high dislocation density, and the dislocations are arranged in planar arrays. Thus, slip bands are observed in the steels and they act as high diffusivity paths resulting in enhancement of chromium diffusion and precipitation of chromium nitrides. Thus, Cr_2N precipitation takes place much faster than in the solution annealed steels. Cr_2N precipitation is also enhanced due to an increased amount of cold-work induced defects, which can act as nucleation sites. Recovery has been observed to take place in the cold-worked steels annealed at elevated temperatures, becoming faster as the annealing temperature increases (Uggowitzer and Speidel, 1990; Simmons, 1995A; Simmons et al., 1996B).

Other nitrides

In addition to chromium nitrides, other transition metal nitrides (NbN, VN, ...) can precipitate in nitrogen alloyed austenitic stainless steels during manufacturing or during exposure to elevated temperatures, if these transition metal alloying elements are added to them. The relative amount of chromium nitrides and other transition metal nitrides depends on the nitrogen content of the steel, annealing temperature, and cooling conditions. Precipitation of these nitrides can be desireable in nitrogen alloyed austenitic stainless steels, since they stabilize the steels and reduce sensitization. They also improve mechanical properties, such as high temperature yield and tensile strength, and prevent grain size coarsening (Wada and Ohta, 1989; Rayaprolu and Hendry, 1988; 1989; Perrot and Foct, 1990; Wilson, 1990, Liska et al., 1990). A disadvantage of transition metal nitrides is that, even in small amounts, they decrease the ductility and work hardenability of the steel (Wada and Ohta, 1989).

Nitride precipitation is preceded in the austenite phase, like in other phases, by clustering of nitrogen atoms, which means that there exists (Guinier-Preston) GP zone formation (Jack, 1989). The precipitation sequence begins with the formation of GP zones which are coherent with the matrix, followed by formation of a metastable intermediate phase, which is partly or entirely incoherent, and finally by the precipitation of the stable equilibrium phase. The clusters are mixed clusters, i.e., nitrogen is combined with a transition metal atom (V, Ti, Nb, ...), which decreases the nitrogen activity coefficient f_N, and increases the nitrogen solubility before precipitation. The nitrogen solubility is higher also because the GP zones are metastable with respect to the equilibrium precipitate. The nitride precipitation is usually almost perfectly periodic in the <100> direction (Jack, 1989), which means that the precipitation results in a homogeneous structure. This almost perfect periodicity of nitrides in the austenite phase is due to the fact that the clustering takes place by spinodal decomposition and is not due, as it is in the ferrite phase, to strain minimisation. Nitride precipitation can also happen, for instance in strain aging processes, depending on the temperature and aging time. Strain-aging occurs by the diffusion of Cr, Mo, W, Si and V to N segregated at the dislocations, and by the coherency between the nitrides and matrix during the nitride formation process. In the initial stage, the nitride precipitates are coherent with the austenite matrix and the austenite matrix experiences high strain, resulting in an increase in strength. However, this strengthening effect is lost when the nitride precipitates become incoherent with the austenite matrix, and the strain experienced by the austenite matrix then decreases (Wada and Ohta, 1989).

Transition metal nitrides are introduced to the alloys by the addition of small amounts of strong nitride forming alloying elements such as V, Ti, Nb, etc. The compositions of the nitrides can vary from a simple metal-nitrogen structure (TiN, VN), to complex structures where two or more metallic elements are combined with nitrogen atoms (e.g., CrNbN). As mentioned before, these alloying elements decrease the nitrogen activity coefficient, and therefore, increase the nitrogen solubility. However, they also have a strong interaction with nitrogen, and easily form nitrides (Wilson, 1990). The stronger the affinity between nitrogen and the metallic element, the higher the nitrogen solubility is at first, and nitride precipitation occurs rapidly. It has also been determined, that a strong affinity between nitrogen and metallic elements implies a very negative Gibbs free energy of formation of the nitride, and hence, easy nitride precipitation. Mn and Cr are exceptions from this behaviour, since their nitrides are unstable although nitrogen solubility is high. Some elements, such as B and Si, tend to precipitate as nitrides when their concentrations are high enough (Perrot and Foct, 1990).

In nitrogen alloyed austenitic stainless steels, π nitride containing large amounts of chromium, molybdenum and nickel, as well as eta phase, which also has a high nitrogen content

with a nominal composition of M_5SiN, can precipitate in addition to chromium nitrides at elevated temperatures (> 700 °C) (Jargelius-Petterson, 1993A; 1994). π nitride is a transient nitride, which is replaced by intermetallic phases after a longer period exposure to elevated temperatures.

1.6.2 Precipitation of intermetallic phases

Intermetallic phases with noncubic symmetry may form in austenitic stainless steels containing the transition metal alloying elements Fe, Ni, Mn, Co, Cr, Ti, V, etc. Precipitation of intermetallic phases leads to deterioration in tensile ductility and impact toughness, as well as in the corrosion resistance of austenitic stainless steels. Nitrogen alloying increases the resistance of austenitic stainless steels to intermetallic phase precipitation. However, when nitrogen alloyed austenitic stainless steels are exposed to elevated temperatures from ~ 600 °C up to the solution annealing temperature, intermetallic phases are precipitated at the same time as nitrides (mainly Cr_2N). They can also precipitate during cooling from the solution annealing temperature, or they can precipitate due to too low of a solution annealing temperature. Improper selection of alloying elements increases the risk for intermetallic phase precipitation. The main intermetallic phase of interest is sigma (σ) phase, since it is mainly observed to precipitate in high-nitrogen austenitic stainless steels. Other intermetallic phases, such as Laves (λ) phase, chi (χ) phase, etc., have also been observed, especially during exposure to elevated temperatures.

Sigma phase (σ)

σ phase is a brittle intermetallic phase with a tetragonal structure, and its chemical composition varies over a wide range of transition metal alloying (Marshall, 1984; Uggowitzer et al., 1993). A typical composition is $(Cr, Mo)_x(Fe, Ni, Mn)_y$, where x and y may be of the same magnitude or they may vary between 1 and 7. Composition of σ phase has been found to vary with temperature and time.

Stability regions for σ phase differ greatly, and depend on the chemical composition of the steel. The possibility of σ phase formation in Fe-Cr-Ni-alloys can be evaluated with many models, such as Cr- and Ni- equivalents, d-electron concept, etc. (Morinaga et al., 1985; Ezaki et al., 1986; Orita et al., 1990; Uggowitzer et al. 1993; Rechsteiner, 1994). In general, it has been observed that some alloying elements, such as Cr, Mo, Mn, Ti, V and Nb promote σ phase formation. Silicon has been observed to increase markedly the rate of σ phase formation and to be the most effective σ phase stabilizer. Chromium and molybdenum, which are common alloying elements of austenitic stainless steels, are effective σ phase stabilizers. Therefore, as the trend nowadays is to increase the amount of alloying elements beneficial to corrosion resistance of austenitic stainless steels, such as

Cr and Mo, the danger for σ phase precipitation is increased. Molybdenum has a clearly higher promoting effect on σ phase precipitation than chromium. According to Uggowitzer et al. (1993) 1 wt-% molybdenum increases the stability region of σ phase 70 °C, whereas 1 wt-% chromium increases it only 45 °C. The adverse effect of increasing molybdenum content has been explained to be offset by replacing part of molybdenum with tungsten and, thus, a steel with a more stable austenitic microstructure and good corrosion resistance as well as good mechanical properties can be obtained (Gagnepain et al., 1996). However, according to Jonsson et al. (1999), although the partial replacement of molybdenum with tungsten decreases the tendency for σ phase precipitation, it promotes the precipitation of Laves phase. Manganese has been observed to accelerate the precipitation of σ phase, as well as other intermetallic phases, and to promote their intragranular precipitation (Jargelius-Petterson, 1996).

Alloying elements decreasing the precipitation rate of σ phase are Ni, Co, Cu, C and N. Nitrogen is especially effective in retarding the precipitation of σ phase in austenitic stainless steels during solution annealing heat treatments or during exposure to elevated temperatures. Therefore, it is one of the main reasons for the manufacture of nitrogen alloyed austenitic stainless steels (Brandis et al., 1976A; Kearns and Deverell, 1987; Uggowitzer et al., 1993; Jargelius-Petterson, 1994). 1 wt-% nitrogen has been observed to lower the $\gamma / (\gamma + \sigma)$ phase boundary temperature approximately 300 °C making it, thus, possible to lower the solution annealing temperature with regard to σ phase precipitation (Uggowitzer et al., 1993). On the other hand, as the nitrogen content of the steel is increased, the danger for Cr_2N precipitation is increased. Therefore, in order to achieve a fully austenitic microstructure, the solution annealing temperature has to be chosen carefully in order to avoid both σ phase and Cr_2N precipitation. In Figure 11, the suitable solution annealing temperature range with regard to σ phase and Cr_2N precipitation as a function of nitrogen content of the steel is shown. In order to ensure a precipitation-free austenitic microstructure for a steel, it is important to make a compromise in the contents of alloying elements enhancing σ phase precipitation and those enhancing Cr_2N precipitation.

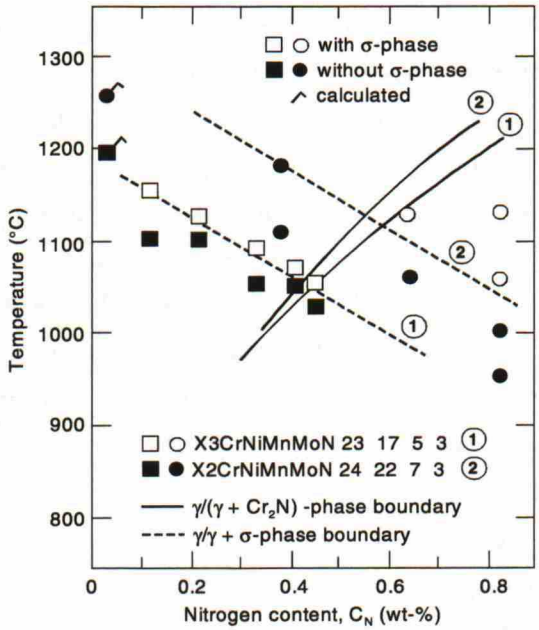

Figure 11. Effect of nitrogen content on the $\gamma / (\gamma + \sigma)$ and $\gamma / (\gamma + Cr_2N)$ phase boundary of two nitrogen alloyed austenitic stainless steels (Uggowitzer et al., 1993).

Precipitation of σ phase is controlled by the rate of diffusion of chromium and other σ phase forming alloying elements, as well as by the mode of nucleation. Also, the residual chemical composition of the austenite after nitride precipitation affects the mechanism of σ phase precipitation. Nitrides (mainly Cr_2N) in high nitrogen steels (> 0,4 wt-%N) have been generally reported to precipitate before σ phase, but in steels with lower nitrogen contents (< 0,4 wt-%N) σ phase has been reported to precipitate before nitrides (Brandis et al., 1976A; Uggowitzer et al., 1993). Nitride precipitation consumes nitrogen from the austenite. As a result, the nitrogen content around the nitrides in the austenite falls below a critical value and σ phase precipitation can take place (Brandis et al., 1976A; Barcik, 1988; Uggowitzer et al., 1993). However, σ phase precipitation has been observed to lead enrichment of nitrogen in the austenitic matrix around the σ phase precipitates. It is due to the fact that σ phase cannot dissolve nitrogen due to its tetrahedrally closed packed crystal structure, and thus, Cr_2N precipitation is possible after σ phase precipitation (Thier et al., 1969; Uggowitzer et al., 1993; Jargelius-Petterson, 1994). It is thus assumed, that Cr_2N and σ phase precipitation is an interactive and alternating process independent of which of the two precipitating phases forms first.

σ phase precipitates intergranularly, at triple junctions and ingranularly depending on the temperature in steels with < 0,5 wt-%N. According to Brandis et al. (1976A) σ phase precipitates

intergranularly and at triple junctions, when the exposure temperature is > 1000 °C, but at temperatures < 1000 °C it precipitates also intragranularly. Intragranular precipitation becomes, however, the more difficult the lower the exposure temperature is. This is due to the diffusion of alloying elements becoming slower as the temperature decreases. This behaviour is valid also for the precipitation of other intermetallic phases and Cr_2N. σ phase precipitation depends also on the grain size of the steel. If the grain size is big, σ phase precipitates intergranularly and at triple junctions and intragranularly. Intragranular precipitation takes place at coherent and incoherent twins, slip bands and at carbides, oxides as well as nitrides. If the grain size of the steel is small, σ phase precipitates mainly intergranularly and the amount of intragranularly precipitated σ phase is small. The amount of intergranularly precipitated σ phase is clearly higher the smaller the grain size of the steel is (Brandis et al., 1976A).

Cold work of austenitic stainless steels increases the rate of σ phase precipitation by decreasing the incubation period for σ phase precipitation (Marshall, 1984). On the other hand, if austenitic stainless steels are annealed at a very high temperature, austenite grain size grows, and σ phase precipitation is retarded (Barcik, 1988). Creep has also been observed to accelerate σ phase formation, and to extend its range to lower temperatures (Minami et al., 1986). In general, the precipitation of intermetallic phases is approximately 100 times slower in the austenite than in the ferrite. This is mainly due to the ability of the alloying element atoms to diffuse faster in ferrite than in austenite. Therefore, if an austenitic stainless steel contains delta ferrite, the risk for σ phase precipitation is increased (Brandis et al., 1976A).

Other intermetallic phases

In addition to different nitrides and σ-phase, other intermetallic phases may precipitate in nitrogen alloyed austenitic stainless steels during exposure to elevated temperatures (> 550 °C) or during solution annealing, i.e., due to too low solution annealing temperature, or due to too slow cooling from the solution annealing temperature. These phases have been identified as chi (χ), eta, Laves and T phases (Thier et al., 1969; Brandis et al., 1976A; Heubner et al., 1989; Jargelius-Petterson, 1993A; 1994; Simmons, 1995A; Simmons et al., 1996). Austenitic stainless steels containing molybdenum have a higher risk for precipitation of these phases, since molybdenum has been observed to increase the stability of chi and Laves phases (Maziasz, 1978; Kearns and Deverell, 1987; Wallis, 1990; Jonsson et al., 1999). Manganese has also been observed to promote precipitation of other intermetallic phases besides σ phase. Tungsten has been observed to promote the precipitation of Laves phase in steels where molybdenum has been partially replaced by tungsten (Jonsson et al., 1999). On the other hand, nickel has been observed to retard the

precipitation of chi and Laves phases when its content is increased together with the nitrogen content of the steel (Heubner et al., 1989). The composition of chi and Laves phase in austenitic stainless steels has been observed to be close to $Fe_{36}Cr_{12}Mo_{10}$ and Fe_2Mo, respectively (Thier et al., 1969; Marshall, 1984).

Nitrogen of content austenitic stainless steels affects the occurrence of these intermetallic phases during the exposure to elevated temperatures. As the nitrogen content increases from 0 - 0,2 wt-%N to 0,2 - 0,5 wt-%N, eta phase (M_5SiN) has been observed to precipitate in addition to Laves phase at low annealing temperatures (600 °C - 850 °C). At higher annealing temperatures (from 850 °C to solution annealing temperature), chi and Laves phases have been observed to be initially precipitated intergranularly in addition to σ phase, as compared with the intragranular precipitation of chi and Laves phases in the steels with low nitrogen contents (0 - 0,2 wt-%N) (Thier et al., 1969; Brandis et al., 1976A; Jargelius-Petterson, 1993A; 1994). As the annealing time is prolonged, chi and Laves phases in the steel with the low nitrogen content have been observed to transform to σ phase, i.e., they are transient phases, whereas in the steels with higher nitrogen content (0,2 - 0,5 wt-%N), chi and Laves phases have been observed to grow and to be accompanied with transient π nitrides and T phase. According to Brandis et al. (1976A) chi phase is precipitated only intergranularly and is transformed to σ phase during exposure to elevated temperatures in steels with 0,33 - 0,44 wt-%N. According to Thier et al. (1969), chi phase is replaced by M_6C carbide in steels with higher carbon content as the nitrogen content of the steel increases up to ~ 0,25 wt-%N, when the steel is exposed to elevated temperatures.

In the steels with higher nitrogen contents, intragranular precipitation of clusters composed of either chi and Laves phases or Cr_2N and Laves phase have been observed, when the annealing time at elevated temperatures is further increased. The precipitation of Cr_2N and Laves phase adjacent to each other is explained to be related to a decrease in the nitrogen content of the surrounding austenite matrix around the Cr_2N precipitate, thus making Laves phase precipitation possible (Thier et al., 1969). Chi and Laves phases have been observed to transform to σ phase at the grain boundaries, and the intragranular transient π nitrides and T phase transform to chi phase with increasing nitrogen content of the steel, when the steel is exposed to elevated temperatures (Jargelius-Petterson, 1994).

As a conclusion on the effects of nitrogen on the precipitation behaviour of the studied steels during exposure to elevated temperatures, it has been found that σ phase precipitation is retarded, whereas chi and Laves phase precipitation is stabilised by nitrogen. According to Brandis et al. (1976A) nitrogen alloying broadens the stability range of chi phase to higher temperatures and accelerates its precipitation. Intragranular precipitation of all intermetallic phases has been observed to begin later in the steels with increasing nitrogen content, as the exposure temperature is

increased. Additionally, as the nitrogen content of the steel is increased, the temperature for the fastest precipitation of other intermetallic phases in addition to σ phase is decreased (Thier et al., 1969; Heubner et al., 1989; Jargelius-Petterson, 1993A; 1994; 1996). However, according to Brandis et al. (1976A), increasing the nitrogen content of the steel results in an increase in temperature for the fastest precipitation of chi phase.

1.6.3 Mechanisms of retardation of intermetallic phase precipitation by nitrogen

The retarding effect of nitrogen on σ phase precipitation has been considered to be due to the low solubility of nitrogen in σ phase, leaving its composition and free enthalpy unaffected. On the other hand, nitrogen lowers the free enthalpy of austenite and stabilizes it. As a result, the difference in free enthalpy necessary for precipitation is reached only at lower temperatures. This is valid only as long as nitrogen is interstitially dissolved in the austenite lattice. The reason for nitrogen to retard the precipitation of σ and Laves phases, is due to their inability to dissolve nitrogen (and carbon), since they have tetrahedrally close packed crystal structures. All the phases have so small tetrahedral interstices that nitrogen atoms are too big to be dissolved into them. Similar behaviour has been also observed for carbon in carbon alloyed austenitic stainless steels (Wiegand and Doruk, 1962; Thier et al., 1969; Brandis et al. 1976A; Uggowitzer et al., 1993). Chi phase, on the other hand, is able to dissolve some nitrogen, which according to Brandis et al. (1976A; 1976B) means that nitrogen does not retard chi phase precipitation.

1.7 Effect of precipitates on properties of nitrogen alloyed austenitic stainless steels

Successful utilization of high-nitrogen austenitic stainless steels in engineering applications requires that their microstructure and its effect on mechanical properties and corrosion resistance is thoroughly understood. Austenite stability is especially of major importance. High-nitrogen austenitic stainless steels are thermally unstable and susceptible to nitride precipitation. Therefore, the nitride precipitation susceptibility of high-nitrogen austenitic stainless steels and the effects of nitrides on mechanical properties and corrosion resistance, i.e., embrittlement and sensitization, should be clearly known. In addition to nitride precipitation, high-nitrogen austenitic stainless steels are susceptible to intermetallic phase precipitation. Intermetallic phases deteriorate toughness and ductility properties, as well as the corrosion resistance of austenitic stainless steels.

1.7.1 Mechanical properties

Tensile properties

Only a few studies on the effects of precipitates on the tensile properties of nitrogen alloyed austenitic stainless steels have been published (Simmons, 1995A; 1995B; Simmons et al., 1996; Rayaprolu and Hendry, 1988, Tailard, 1999). Additionally, they are focused only on the effects of Cr_2N precipitation. Intermetallic phases also affect tensile properties, i.e., they decrease the tensile ductility of nitrogen alloyed austenitic stainless steels. On the other hand, the extent of intermetallic phase precipitation in austenitic stainless steels containing high amounts of nitrogen has been observed to be minor compared to that of Cr_2N precipitation, and thus, the effect of intermetallic phase precipitation on tensile properties has not been considered to be significant.

Cr_2N precipitation as a result of isothermal annealing at elevated temperatures has not been observed to markedly affect the yield and ultimate tensile strength of solution annealed high-nitrogen steel (Simmons, 1995A; Simmons et al., 1996B). In Figure 12, the effect of isothermal annealing at 700 and 900 °C for up to 10 h on yield and ultimate tensile strength of a steel with nominal composition of Fe-19Cr-5Mn-5Ni-3Mo-0,69N is shown. The yield strength of the steel was slightly increased, whereas the ultimate tensile strength was not affected at all by nitride precipitation. This is in contrast to the large differences taking place in the microstructure of the steel as a result of the annealing. The increase in yield strength has, in general, been observed to be greater the lower the annealing temperature is in the temperature range where Cr_2N precipitation has been observed (i.e., from 600 - 650 °C to solution annealing temperature) (Simmons, 1995A; Simmons et al., 1996B). At the lower temperatures (600 - 700 °C), Cr_2N precipitates only intergranularly, whereas at higher temperatures (≥ 900 °C) it precipitates sequentially intergranularly, by cellular precipitation, and by intragranular precipitation as the annealing time is increased. Therefore, according to Simmons (1995A) and Simmons et al. (1996B) an increase in the yield strength of steels annealed at low temperatures (600 - 700 °C) is likely to be due to an increased resistance of Cr_2N containing grain boundaries to dislocation motion. The increase in yield strength of steels annealed at higher temperatures (≥ 900 °C) is also considered to be due to the grain boundary Cr_2N precipitates resisting dislocation motion. At the same time, the amount of interstitial nitrogen of the austenite matrix is reduced due to the large volume of Cr_2N precipitation, and thus, solid solution strengthening via interstitial nitrogen is smaller than in steels annealed at lower temperatures. Taillard et al. (1999) have observed the yield strength of a steel with nominal composition of Fe-18Cr-19Mn-0,9N to decrease as a result of exposure to 800 °C for up to 50 h. This was explained to be due to depletion of nitrogen from the austenite matrix via intergranular and cellular precipitation of Cr_2N.

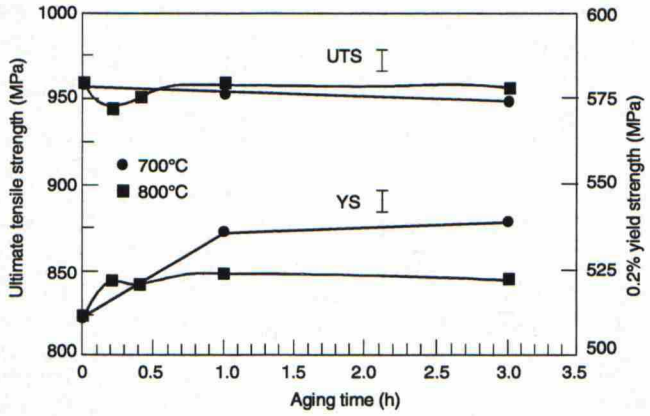

Figure 12. Yield (YS) and ultimate tensile strength (UTS) of solution annealed Fe-19Cr-5Mn-5Ni-3Mo-0,69N steel as a function of annealing time at 700 and 900 °C (Simmons, 1995A).

The tensile ductility of solution annealed high-nitrogen austenitic stainless steels is reduced as a result of annealing at elevated temperatures, and the deterioration is more pronounced as the annealing temperature increases in the temperature range where Cr_2N precipitation has been observed (i.e., from 600 - 650 °C to solution annealing temperature) (Simmons, 1995A; Simmons et al., 1996B; Taillard et al., 1999). Elongation to fracture and reduction of area are reduced, as can be seen from Figure 13, for a steel with nominal composition of Fe-19Cr-5Mn-5Ni-3Mo-0,69N annealed for up to 10 h at 700 and 900 °C. In general, it has been observed that reduction of area values describe ductility better than elongation to fracture values, since reduction of area is mainly determined by the local plasticity of the steel after the onset of necking. Although the elongation to fracture of a steel annealed at low temperatures (600 - 700 °C) is not affected, the ability of a steel to deform plastically is affected, since the true strain at fracture and the true fracture stress are reduced with increasing annealing time, and they are both lower for a steel annealed at high temperatures (≥ 900 °C). The mechanism by which Cr_2N precipitation deteriorates the ductility of a steel annealed at lower temperatures is grain boundary separation, and the fracture morphology is intergranular due to Cr_2N precipitates at grain boundaries. The amount of grain boundary separation has been observed to increase with increasing annealing time due to an increasing amount of intergranular Cr_2N precipitation. Annealing for short times at high temperatures causes similar intergranular separation due to Cr_2N precipitation, whereas at longer annealing times Cr_2N precipitation becomes cellular, and transgranular fracture takes place through the cellular regions (Simmons, 1995A; Simmons et al., 1996B; Taillard et al., 1999).

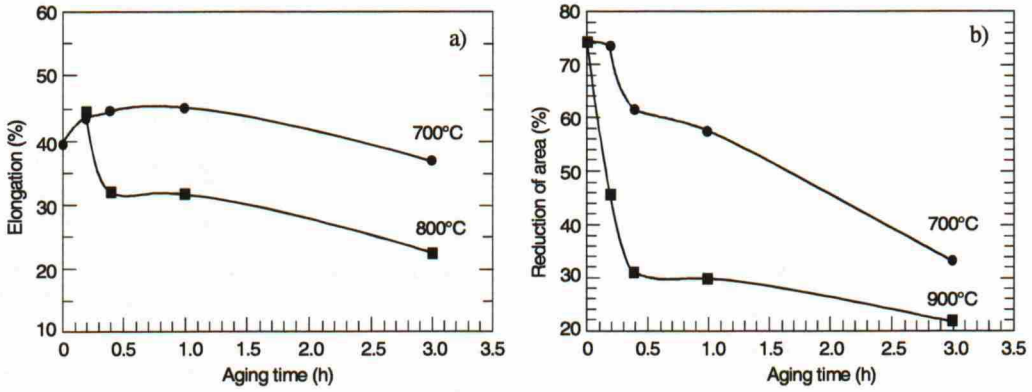

Figure 13. Elongation to fracture a) and reduction of area b) of solution annealed Fe-19Cr-5Mn-5Ni-3Mo-0,69N steel as a function of annealing time at 700 and 900 °C (Simmons, 1995A).

Cold deformation of a high-nitrogen steel prior to annealing at elevated temperatures increases the kinetics of Cr_2N precipitation. According to Simmons (1995A), annealing of a cold-worked (reduction 20 %) steel with the nominal composition of Fe-19Cr-5Mn-5Ni-3Mo-0,69N for up to 10 h at 700 °C and 900 °C decreases the yield and ultimate tensile strength with increasing annealing time, the effect being more pronounced the higher the annealing temperature is. The decrease in yield strength has been observed to be more pronounced than that in ultimate tensile strength, which is explained to be due to recovery occurring during annealing, which increases with increasing annealing time and temperature. On the other hand, Cr_2N precipitation taking place at the same time increases the strength properties slightly. However, recovery compensates for the increase in strength properties caused by Cr_2N precipitation (Simmons, 1995A). The tensile ductility of a cold-worked high-nitrogen steel is affected by isothermal annealing at elevated temperatures, and the effect depends on the annealing time. At short annealing times the tensile ductility of the steels increases, which is due to recovery compensating for the adverse effect of intergranular Cr_2N precipitation. At longer annealing times the tensile ductility of the steels decreases due to rapid intergranular Cr_2N precipitation and cellular or intragranular precipitation, the decrease being far more pronounced as the annealing temperature increases. Fracture morphologies of cold-worked steel annealed at lower temperatures (700 °C) are similar to those of the solution annealed steels annealed at the same temperatures, except that the amount intergranular fracture is larger in the cold-worked steel due to increased Cr_2N precipitation kinetics caused by cold deformation. When a cold-worked steel is annealed at higher temperatures (900 °C), fractographic features of the steel are similar to those of the solution annealed steel when aged for short times. At longer annealing times the cold-worked steel exhibits more transgranular fracture as

compared with the solution annealed steel, due to an increased amount of cellular Cr_2N precipitation (Simmons, 1995A).

Plastic flow behaviour of high-nitrogen austenitic stainless steels is affected by intergranular and cellular Cr_2N precipitation in steels annealed at elevated temperatures (Simmons, 1995B). Annealing at temperatures resulting in intergranular Cr_2N precipitation ($\geq$ 600-650 °C) has no measurable effect on the plastic flow behaviour of the steel below the ultimate tensile strength, i.e., solution annealed steel and the respective steel annealed at low temperatures have basically indistinguishable stress-strain behaviour up to ultimate tensile strength. At this point the ability of a steel to deform plastically is, however, adversely affected by the intergranular nitrides. As the annealing temperature of the steel is increased, cellular precipitation of Cr_2N in addition to intergranular precipitation of Cr_2N takes place, and the plastic flow behaviour of the steel at both low and high strain levels is affected. Cellular precipitation of Cr_2N results in strengthening of the steel matrix in the low strain range ($0{,}001 < \varepsilon < 0{,}03$) and a systematic decrease in the strain hardening exponent (n_1) and strength coefficient (K_1) with increasing annealing time is observed. Cellular precipitation of Cr_2N has also been reported to reduce significantly the ductility of the steel during deformation, promoting premature fracture at lower strain levels. Simmons (1995B) has studied a steel with the nominal composition of Fe-19Cr-5Mn-5Ni-3Mo-0,69N annealed at 700 and 900 °C for up to 10 h. According to his results, the flow curve parameters n_1, K_1, n_2 and K_2 for the steel annealed at 700 °C had values which did not deviate substantially from those of the solution annealed steel, whereas those for the steel annealed at 900 °C were affected by the cellular Cr_2N precipitation as described above. The strain hardening rate ($d\sigma/d\varepsilon$) of high-nitrogen austenitic stainless steels is not affected by annealing of the steel at elevated temperatures. This can be explained by two factors affecting the strain hardening rate at the same time, namely cellular nitride precipitation, and loss of interstitial nitrogen due to nitride precipitation (Simmons, 1995B). Cellular nitride precipitation (Cr_2N) is expected to increase the strain hardening rate. On the other hand, interstitial nitrogen loss due to nitride precipitation is expected to lower the strain hardening capability of the matrix, since the strain hardening rate of austenitic stainless steels has been shown to increase with increasing nitrogen content of the steel. Therefore, it seems that these two phenomena acting simultaneously counteract each other, and cause the strain hardening rate to be similar to that of solution annealed steel.

Impact properties

Chromium nitride and intermetallic phase precipitation during manufacturing, or as a result of exposure to elevated temperatures, deteriorates the impact toughness of nitrogen alloyed austenitic stainless steels. During manufacturing, the impact toughness of nitrogen alloyed

austenitic stainless steels remains at a high level as long as nitrogen is in interstitial solid solution. However, if the nitrogen content of the steel is too high Cr_2N precipitation takes place during cooling from the solution annealing temperatures and the impact toughness of the steel is deteriorated, Figure 16. If the nitrogen content of the steel is such that nitrogen can be interstitially dissolved during solution annealing, Cr_2N can still be precipitated if the solution annealing temperature is not high enough, or if the cooling rate during quenching is not fast enough.

Isothermal annealing of high-nitrogen (> 0,5 wt-%N) austenitic stainless steels at elevated temperatures reduces their impact toughness markedly, mainly due to Cr_2N precipitation. Intermetallic phase precipitation can also take place to a small extent in high-nitrogen steels during isothermal annealing. However, the time needed is longer as compared to Cr_2N precipitation, and thus, it has not been considered to have any major effect on the impact toughness of the steels (Simmons, 1995B; Simmons et al., 1996B). On the other hand, in steels with lower nitrogen contents (< 0,5 wt-%N) the precipitation of intermetallic phases is faster than that of Cr_2N. Therefore, in steels with the lower nitrogen contents the effect of Cr_2N precipitation on impact toughness has been considered to have minor importance (Brandis et al., 1976B).

Generally, the impact toughness properties of isothermally annealed steels follow the same basic trends as ductility in tensile testing, except that the reduced ductility due to Cr_2N and/or intermetallic phase precipitation results in a more pronounced effect on impact toughness properties due to the high strain rate. In other words, the macroscopic plasticity during impact testing is always much less than that during tensile testing. However, generally the fractographic features and failure modes of tensile and impact samples are similar for a given thermal treatment.

Exposure to elevated temperatures of high-nitrogen steels results in intergranular as well as cellular and intragranular precipitation of Cr_2N, depending on the exposure or annealing temperature in the temperature range of Cr_2N precipitation, and impact toughness properties of the steel are deteriorated. The decrease in impact toughness at low annealing temperatures (600 – 700 °C) is related to the extent of grain boundary coverage, and a significant amount of intergranular Cr_2N precipitation is needed before the impact toughness of a steel is significantly affected by the precipitates. Cold working (reduction 20 %) of the steel prior to annealing in the low temperature range results in enhanced kinetics of Cr_2N precipitation, and the amount of intergranular Cr_2N as compared with that of the solution annealed steel is substantially higher. Therefore, the decrease in impact toughness is much faster in the cold-worked steel than in the solution annealed steel. Simmons (1995B) and Simmons et al. (1996B) have studied the effect of isothermal annealing at 700 and 900 °C on the impact toughness properties of solution annealed and cold-worked (reduction 20 %) Fe-19Cr-5Mn-5Ni-3Mo-0,69N steel. The effect of isothermal annealing at 700 °C on the impact toughness of the steel in the solution annealed and solution

annealed + cold rolled (reduction 20 %) state is shown in Figure 14. Annealing of the steel results in a fast reduction in absorbed energy, especially in the cold-worked steel. The cold rolled steel has lower impact toughness than the solution annealed steel, which is due to the fact that the amount of ´´total available plasticity´´ of the steel is consumed during the plastic deformation by cold rolling.

As the annealing temperature of the steel increases up to 900 °C, cellular and intragranular precipitation of Cr_2N takes place in addition to an increased amount of intergranular precipitation of Cr_2N, and the impact toughness of the steel is decreased much faster as compared with the steels annealed at low temperatures (Simmons, 1995B; Simmons et al. 1996B). Prior cold deformation of the steel by cold rolling has no significant effect on the kinetics of Cr_2N precipitation in a nitrogen alloyed austenitic stainless steel during annealing at high temperatures, contrary to steels annealed at low temperatures. This is due to the sufficiently high grain boundary coverage of Cr_2N in solution annealed steel causing a significant decrease in impact toughness. Prior cold deformation, although increasing the kinetics of intergranular Cr_2N precipitation (and cellular and intragranular precipitation), does not have a measurable effect on the impact toughness of the steel. The effect of isothermal annealing at 900 °C on the impact toughness of a Fe-19Cr-5Mn-5Ni-3Mo-0,69N steel in solution anneled and cold-worked (reduction 20 %) condition is shown in Figure 15. The impact toughness of solution annealed steel is reduced very quickly during annealing at 900 °C and it is practically lost after 1 h of annealing at 900 °C, as compared to a ~ 50 % decrease after annealing of the solution annealed steel for 1 h at 700 °C, as shown in Figure 14. At longer annealing times, no differences between the steels annealed at 700 and 900 °C can be noticed.

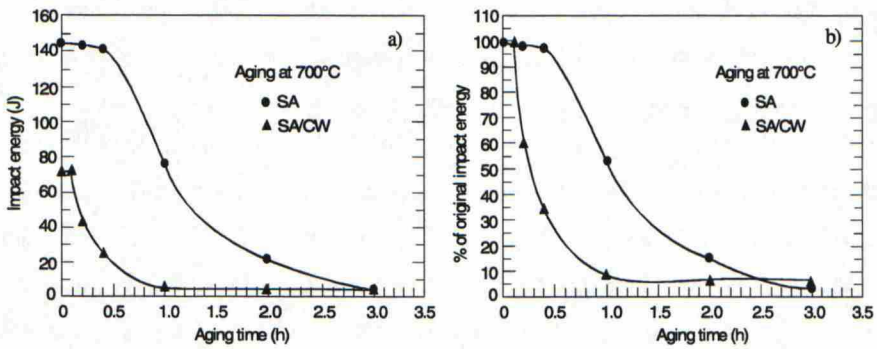

Figure 14. The effect of isothermal annealing at 700 °C on impact toughness properties of a solution annealed and cold-worked (reduction 20 %) Fe-19Cr-5Mn-5Ni-3Mo-0,69N steel: a) measured impact energies and b) ratio of absorbed energies (Simmons, 1995A).

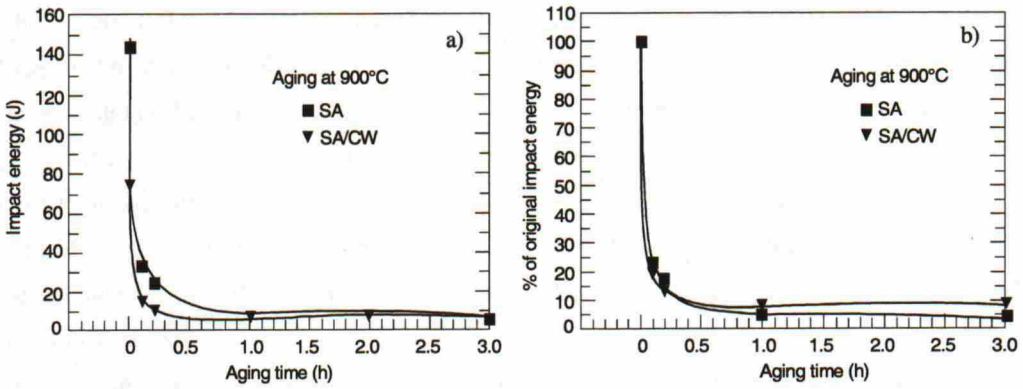

Figure 15. The effect of isothermal annealing at 900 °C on impact toughness properties of a solution annealed and cold-worked (reduction 20 %) Fe-19Cr-5Mn-5Ni-3Mo-0,69N steel: a) measured impact energies and b) ratio of absorbed energies (Simmons, 1995A).

In austenitic stainless steels with lower nitrogen contents (24,5Cr-17Ni-5,5Mn-3,2Mo-0,18Nb-(0,33-0,44N)) nitrogen alloying has been observed to be beneficial with regard to decrease in impact toughness of the steels exposed to temperatures > 950 °C. At lower annealing temperatures (600 - 900 °C) any differences in the decrease of impact toughness between the steels could not be observed (Brandis et al., 1976B). The precipitating phases were intermetallic phases (σ and chi phase (χ)) and Cr_2N and the decrease in impact toughness was due to their intergranular precipitation. According to Brandis et al. (1976B) the reason for the positive effect of increasing nitrogen content of the steel from 0,33 wt-%N to 0,41 - 0,44 wt-%N on the decrease of impact toughness of the steels exposed to temperatures > 950 °C, was due to retardation of σ phase precipitation by increasing nitrogen content of the steel. On the other hand, the reason for the nitrogen content of the steel exposed to the lower temperatures not to have an effect on the decrease of impact toughness is explained to be due to precipitation of chi phase. Chi phase is the first phase to precipitate in the steels during exposure to 600 - 900 °C. According to Brandis et al. (1976A; 1976B) the reason for the fact that increasing nitrogen content of the steel has no positive effect on the decrease in impact toughness is that chi phase can dissolve some nitrogen unlike σ phase. As a result, nitrogen does not retard the precipitation of chi phase. On the contrary, nitrogen broadens the stability range of chi phase to higher temperatures. Cr_2N was also precipitated in the steels during exposure to elevated temperatures, but it was not precipitated in great amounts. Additionally, Cr_2N was precipitated after relatively longer time after the precipitation of intermetallic phases. As a result, Cr_2N was not considered to have any marked effect on the impact toughness (Brandis et al., 1976B).

1.7.2 Resistance to localized corrosion

Cr_2N and intermetallic phases precipitate in nitrogen alloyed austenitic stainless steels during manufacturing or during exposure to elevated temperatures, and deteriorate their excellent localized corrosion resistance. Nitrogen improves the resistance to localized corrosion of austenitic stainless steels as long as it is in interstitial solid solution. As soon as the nitrogen content of the steel is too high, Cr_2N precipitates and deteriorates the localized corrosion resistance. Regardless of whether the precipitating phases are Cr_2N and/or intermetallic phases, the localized corrosion attacks the interface between the precipitated phases and the surrounding austenite matrix, due to Cr (and Mo) depletion at the interface (Sedriks, 1986; Heubner et al., 1989; Jargelius-Petterson, 1996; Simmons et al., 1994; 1996B; Covino et al., 1997). However, according to Wallis (1990) degradation of pitting corrosion resistance takes place at the interface between the intermetallic phase and the austenite matrix, but it is because of impairment of the passive layer due to lattice irregularities at the interface, rather than due to depletion of the alloying elements at the interface.

Cr_2N can precipitate during manufacturing due to too low of a solution annealing temperature, too slow of a cooling rate from the solution annealing temperature, or due to too high of a nitrogen content of the steel making it impossible to perform solution annealing at reasonable temperatures. An example of the last factor can be seen in Figure 16, where the effect of nitrogen content on crevice corrosion resistance of an austenitic stainless steel with a nominal composition of 24Cr-7Mo-(19-22)Ni-7Mn is shown. The critical crevice corrosion temperature of the steel increases with increasing nitrogen content up to approximately 0,9 wt-%N, after which it and the impact toughness of the steel decrease sharply due to Cr_2N precipitation (Uggowitzer et al., 1993).

Thermal exposure to elevated temperatures (from 600-650 °C up to solution annealing temperature) of nitrogen containing austenitic stainless steels results in degradation of their resistance to localized corrosion (pitting and crevice corrosion). This is due to the precipitation of nitrides (mainly Cr_2N) and intermetallic phases. The degradation of the resistance to localized corrosion depends on temperature, time and the composition of the steel.

Nitrogen alloying can reduce the degradation of the localized corrosion resistance of austenitic stainless steels. It has been observed, that at intermediate contents, depending on the chemical composition of a steel, nitrogen has a beneficial or negligible effect on the critical pitting corrosion resistance of a steel exposed to elevated temperatures. This is because of the retarding effect of intermediate nitrogen content on the precipitation of intermetallic phases. However, as the nitrogen content of the steel is increased and the steel is exposed to elevated temperatures, Cr_2N precipitates, and the localized corrosion resistance is lowered. The decrease in the localized corrosion resistance of the steels with high nitrogen contents can be more severe as compared to that in steels with intermediate nitrogen content. The intermediate nitrogen content has been

observed to be ~ 0,2 wt-%N, and high nitrogen contents are ~ 0,5 - 0,7 wt-%N for steels with (20-21)Cr-(5 - 25)Ni-(5 - 10)Mn-(3 - 6)Mo (Kearns and Deverell, 1987; Heubner et al., 1989; Jargelius-Petterson, 1996; Simmons et al., 1994; 1996B; Covino et al., 1997). Manganese has a detrimental effect on the pitting corrosion resistance of nitrogen alloyed austenitic stainless steels if these steels are exposed to elevated temperatures. The decrease in pitting corrosion resistance as a result of exposure to elevated temperatures increases considerably with increasing manganese content of the steel. However, nitrogen alloying was observed to offset the detrimental effect of Mn, especially, when the nitrogen content of the steel was at an intermediate level (Jargelius-Petterson, 1996).

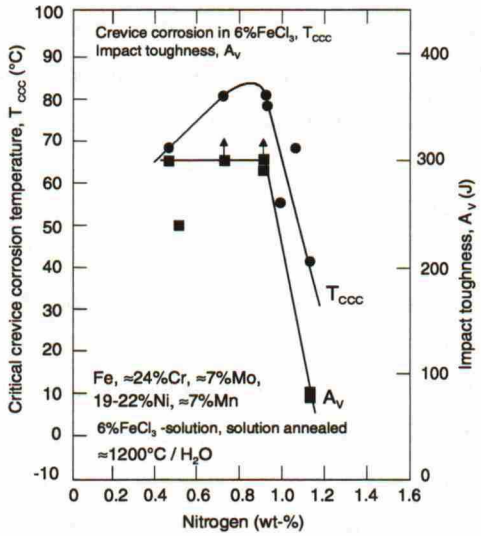

Figure 16. The effect of nitrogen content on the critical crevice corrosion temperature of a 24Cr-7Mo-(19-22)Ni-7Mn austenitic stainless steel (Uggowitzer et al., 1993).

Degradation of the pitting corrosion resistance of nitrogen alloyed austenitic stainless steels exposed to elevated temperatures depends also on the exposure temperature. The decrease in localized corrosion resistance of steels with high and intermediate nitrogen contents is more severe when the steels are exposed to 600-700 °C than when exposed to higher temperatures. This is explained by more severe Cr-depletion around the precipitates formed during exposure to 600-700 °C, than during exposure to higher temperatures. The localized corrosion resistance of the steels exposed to 800 °C is first deteriorated, but as the exposure time at 800 °C is prolonged, the localized corrosion resistance increases. This is called ´´healing´´, which is a result of diffusion of chromium into the Cr-depleted zones around the precipitates leading to a high enough Cr-content (> 14 wt-% Cr) so that sensitization is no longer observed. Healing takes place faster, the higher the nitrogen content of the steel is. Annealing at 900 °C and 1000 °C has not been observed to result in degradation of the localized corrosion resistance, especially in the steels with high nitrogen contents. This can be explained by a high enough chromium content in the Cr-depleted zones

around the Cr_2N precipitates despite the higher amount of inter- and intragranular Cr_2N, as compared with that in the steels exposed to lower temperatures and/or with lower nitrogen contents (Heubner et al., 1989; Jargelius-Petterson, 1996; Simmons et al., 1994; 1996B; Covino et al., 1997). The above mentioned effects of exposure temperature, time, and nitrogen content on the localized corrosion resistance due to exposure to 800 °C and 900 °C for various times of an austenitic stainless steel with a basic composition of 20Cr-18Ni-4,5Mo and with the amounts of manganese and nitrogen varying between 0,2 - 10 wt-%Mn and 0,01 - 0,5 wt-%N, are shown in Figure 17. Annealing at 800 °C is clearly more detrimental to pitting corrosion resistance than annealing at 900 °C. A similar trend was observed in the Streicher test, where the effect of precipitating phases on the degree of sensitization were evaluated by weight loss measurements. Simmons et al. (1994; 1996B) and Covino et al. (1997) have studied the effect of isothermal heat treatments at 400-1000 °C on sensitisation of a steel with the nominal chemical composition of 19Cr-5Mn-5Ni-3Mo-0,7N, and they observed similar results as Jargelius-Petterson (1996) for a steel with the basic composition of 20Cr-18Ni-4,5Mo, and with the amounts of manganese and nitrogen varying between 0,2 - 10 wt-%Mn and 0,01 - 0,5 wt-%N. However, they also observed, that the localized corrosion resistance of the steel annealed at 800 °C for a long enough time was recovered, and that the localised corrosion resistance of the steel annealed at 600-700 °C was deteriorated even after prolonged annealing.

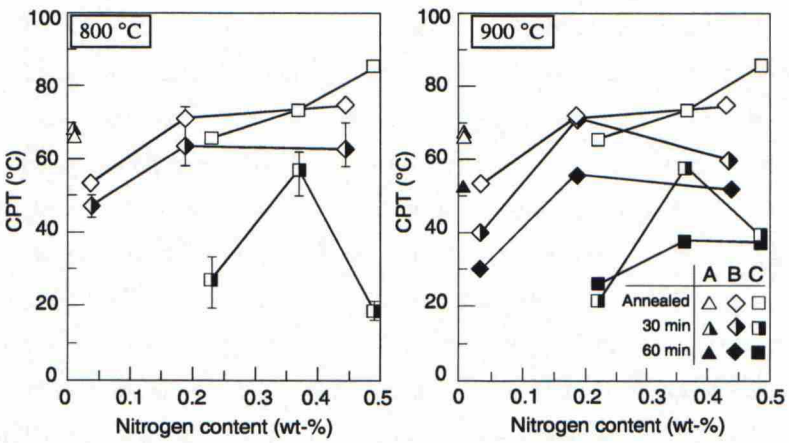

Figure 17. Critical pitting corrosion temperature in 0,2 mol/dm^3 NaCl solution at +600 mV(SCE) as a function of nitrogen content after sensitising heat treatments at 800 °C and 900 °C of steels with the basic composition of 20Cr-18Ni-4,5Mo and with the amounts of Mn and N varying between 0,2 - 10 wt-% and 0,01 - 0,5 wt-%, respectively. Steels annealed at 800 °C for 300 min were omitted since their critical pitting corrosion resistance was below 20 °C. A = steels with the nominal composition of Fe-0,2Mn-20Cr-18,5Ni-4,8Mo-0,005N, B = steels with the nominal composition of Fe-5,3Mn-20Cr-18,5Ni-4,6Mo-(0,04-0,44)N and C = steels with the nominal composition of Fe-10Mn-20Cr-18,5Ni-4,7Mo-(0,004-0,5)N (Jargelius-Petterson, 1996).

2 AIM OF THE STUDY

The aim of this study is to determine the effects of nitrogen content on the microstructure and properties of solution annealed and further isothermally at elevated temperatures (450 °C and 750 °C) annealed nitrogen alloyed P/M austenitic stainless steels. The studied P/M austenitic stainless steels have the nominal composition of 24Cr-22Ni-7,3Mo-3,5Mn-0,3...1,15N and they are manufactured by HIP (Hot Isostatic Pressing) from gas atomized powders. The nitrogen content of the steels is varied by nitrogen alloying of the atomized melt, and by further solid state nitriding of the powders in a fluidized bed furnace when nitrogen contents exceeding nitrogen solubility in the liquid state are needed. The effects of nitriding process variables and powder characteristics on the nitriding process are studied. All of the powders are subsequently consolidated by HIPing, after which the steels are solution annealed.

The steels are annealed at 450 °C and 750 °C in order to study the precipitation reactions in the steels. The above mentioned temperatures were chosen according to literature data from studies on nitrogen alloyed austenitic stainless steels annealed in the temperature range of 500 - 1000 °C (Their et al., 1969; Maziasz, 1978; Kearns and Deverell, 1987; Heubner et. al., 1989; Wallis, 1990; Jargelius-Petterson, 1993A; 1994; Simmons, 1995A; Simmons et al., 1996). However, the steels of the earlier studies had lower chromium, molybdenum and nitrogen contents. Therefore, 450 °C was chosen in order to study if the higher chromium and molybdenum contents of these steels as compared to those of the earlier studies result in precipitation reactions already at this low temperature. Precipitation reactions in the earlier studies have been reported to occur most rapidly around 700 - 950 °C. Additionally, the temperature of the most rapid precipitation has been reported to decrease with increasing nitrogen content of the steel. The nitrogen contents of the steels in this study are at the same level or higher than in the earlier studies reported in the literature, and thus, 750 °C was chosen as the annealing temperature.

The effect of nitrogen content on the microstructure and properties of solution annealed as well as further isothermally at elevated temperatures (450 °C and 750 °C) annealed steels is studied with optical microscopy, transmission electron microscopy, dilatometric analyses, tensile testing, Charpy-V impact testing, hardness measurements, and localized corrosion testing (pitting and crevice corrosion).

3 EXPERIMENTAL

3.1 Experimental materials

The studied experimental steels were manufactured by Hot Isostatic Pressing (HIP) of inert gas atomized powders. The powders were supplied by Rauma Materials Technology Oy. Hot Isostatic Pressing of the powders was supplied by Rauma Materials Technology Oy and VTT Manufacturing Technology. The chemical compositions of the steels are shown in Table 1. The nitrogen content of the steels was varied by alloying the melt prior to atomizing (SMO 0,3N and SMO 0,5N1 and SMO 0,5N2) and when nitrogen contents above the solubility limit of nitrogen in the molten steel were required by solid state nitriding of the powder in a fluidized bed furnace (SMO 0,7N, SMO 0,9N and SMO 1,15N). The steels were solution annealed for 1 h at 1200 - 1250 °C, depending upon the nitrogen content of the steel, and quenched in water. The steel billets had equal sizes in the solution annealing heat treatment.

Table 1. Chemical compositions of the studied P/M steels in wt-% (oxygen content in ppm).

Material	C	Si	Mn	Cu	Cr	Mo	Ni	N	O
SMO 0,3N	0,009	0,26	1,89	0,46	24,4	7,0	22,1	0,34	40
SMO 0,5N1	0,009	0,32	2,12	0,44	24,7	7,4	20,8	0,48	110
SMO 0,5N2	0,015	0,1	3,4	0,35	23,4	8,25	22,0	0,47	160
SMO 0,7N	0,013	0,21	3,54	0,45	24,5	7,31	21,6	0,73	290
SMO 0,9N	0,013	0,21	3,54	0,45	24,5	7,31	21,6	0,92	310
SMO 1,15N	0,012	0,35	2,93	0,37	24,1	7,0	20,3	1,15	390

3.2 Experimental methods

3.2.1 Chemical compositions

The chemical compositions of the HIPed steels were determined through standard optical emission spectroscopy. Nitrogen and oxygen contents of the steel powders and HIPed steels were measured with a LECO TC - 136 residual gas analyser at VTT Manufacturing Technology and at Rautaruukki Raahe Steel Research Center. The analysed samples weighed 0,3 – 1,0 g. The accuracy of the analyser is 0,005 wt-%N up to 0,3 wt-%N and 0,05 - 0,03 wt-%N for nitrogen contents of 0,3 – 1,15 wt-%N.

3.2.2 Optical microscopy and scanning electron microscopy

Optical microscopy was performed with a Nikon Epiphot optical microscope. The samples were ground with SiC water grinding papers and polished with diamond pastes. After polishing the samples were etched by electrolytic etching in a 12 vol-% HNO_3 solution.

Scanninng electron microscopy of the fracture surfaces of the tensile and Charpy V-notch samples was performed with a Zeiss DSM 962 digital scanning electron microscope.

3.2.3 Transmission electron microscopy

Analytical transmission electron microscopy of the steels was performed at Tampere University of Technology with a JEOL JEM 2010 microscope equipped with a Tracor EDS analyser. The samples for analytical transmission electron microscopy were prepared with the window technique. Electrolytic thinning of the samples was performed in a mixture of HNO_3 and methanol.

The different phases were analysed with EDS and SAD (Selective Area Diffraction) analysis. The diffraction patterns in the SAD analyses were photographed from a low index direction. The d-spacings ,i.e., interplanar spacings were calculated with the following formula:

$$Rd = \lambda L \tag{3}$$

where R = distance between the diffraction spot and the incident electron beam, d = interplanar spacing (= d-spacing), λ = wavelength of the electron beam (= 0,0251) and L = effective camera length (= 100 cm). The diffraction patterns were indexed by comparing the measured d-spacings and d-spacing values available in the literature (JCPDS, 1978; Andrews et al., 1967).

The figures of the different phases were formed from the transmitted electron beam by cropping the diffracted spots with the aperture of the microscope.

3.2.4 Dilatometric analysis

Dilatometric analyses were performed at VTT Manufacturing Technology with a Netzsch 402E dilatometer in 90 %Ar-10 $\%H_2$ atmosphere controlled by a personal computer. The samples used in the dilatometric analyses were machined round bars (length 30 mm, diameter 4 mm). Following machining, the samples were solution annealed for 1 h at 1200 - 1250 °C, depending on the nitrogen content of the steel, and subsequently quenched in water. Heating and cooling rates in the thermal cycles were 5, 10 and 20 °C/min. In the isothermal analyses at 450 and 750 °C, the heating and cooling rate was 5 °C/min.

3.2.5 Solid state nitriding

Solid state nitriding of the powder was performed in a gas fluidized bed furnace at VTT Manufacturing Technology. The fluidized bed furnace consisted of a transferable fluidized bed unit, a heating unit for rapid heating of the powder, and a separate cooling unit. Nitrogen gas and a gas with 88 % nitrogen and 12 % hydrogen were used as the fluidizing and nitriding gas. The gas flow rate was ~ 2,0 - 3,0 m^3/h. The particle size of the powder batches was 45 - 250 µm.

3.2.6 Mechanical properties

Tensile strength, yield strength (YS, 0,2%-proof stress), percentage elongation to fracture and percentage reduction of area were measured with an MTS 810 servohydraulic mechanical test machine according to standard SFS-EN 10 002-1 at room temperature (23 °C). The test bars were round bars manufactured according to standard SFS-EN 10 002-1 (1990). Percentage (total) elongation to fracture was measured with an extensometer. Percentage reduction of area was determined by measuring the diameter of the test bar before and after fracture. Yield strength was determined from the force/extension diagram by drawing a line parallel to the straight portion of the curve and at a distance from this equivalent to the prescribed non-proportional percentage, i.e., 0,2 %. The point at which this line intersects the curve gives the force corresponding to the desired yield strength. The latter is obtained by dividing this force by the original cross-sectional area of the test piece.

Charpy-V impact toughness (CVN) properties were tested with an impact hammer according to standard SFS-EN 10 045-1. The specimens used had dimensions of 7,5 x 10 x 55 mm^3 and 10 x 10 x 55 mm^3, machined according to standard SFS-EN 10 045-1. The specimens had a V notch in the middle of the sample. In the sample with the dimensions of 7,5 x 10 x 55 mm^3 the V notch was cut in one of the narrow faces. In the test the sample was broken by one blow from a swinging pendulum of the impact hammer machine. The samples lied on the supports so that the tip of the striker hit the side opposite the notch of the test piece. The machine had a nominal machine energy of 300 ± 10 J. The energy absorbed by the sample during testing is a measure of the impact strength of the material.

3.2.7 Pitting and crevice corrosion resistance

Resistance to pitting and crevice corrosion was determined in 6% $FeCl_3$-solution according to a modified standard ASTM G48 - 76. The ferric chloride solution was prepared by dissolving 100 g of $FeCl_3 \cdot 6H_2O$ in 900 ml distilled water. 18,61 g/litre of Na_2EDTA was added to the

solution as sequestering (chelating) agent. Solution was mixed using magnetic mixer for 24 h. Solution was then poured into a glass beaker through filter paper to remove insoluble particles.

The specimen size was 25 x 50 x 3 mm. The specimen faces were wet ground to a uniform finish using 800 grit SiC abrasive paper. The specimen edges and corners were rounded and wet ground using 1200 grit SiC abrasive paper. The crevice corrosion specimens had a 10 mm hole in the middle of the specimens.

Prior testing the samples were washed in acetone using ultrasonic washer and air dried. After that each sample was weighed 5 times. Teflon multiple crevice washers were fastened to the crevice corrosion specimens by passing sleeved bolt through the hole in the specimen. The torque on the bolt was adjusted to 0,3 Nm using an adjustable torque limiting screwdriver. Thereafter the crevice specimens were assembled on specimen holders.

The ferric chloride solution containing glass beakers were transferred into a constant temperature water bath and allowed to come to the equilibrium temperature with the water bath. Specimens were held for 24 hours in the solution at a constant temperature, after which they were removed from the solution, rinsed in water and distilled water. After that the specimens were washed in acetone using ultrasonic washer and air dried. Thereafter, the samples were weighed for 3 times/specimen and visually examined. If pitting or crevice corrosion was observed in the sample, it was removed from the test. If the sample had not suffered either pitting or crevice corrosion, the temperature of the water bath (and the ferric chloride solution) was increased with 2,5 °C and allowed to stabilize. After that the specimens were put into the ferric chloride containing glass beakers and held there for 24 h. The 24 h periods with 2,5 °C temperature steps were repeated until pitting or crevice corrosion in the specimens was observed. The highest experimented pitting-free and crevice-free temperature was reported as the critical pitting corrosion temperature (CPT) or critical crevice corrosion temperature (CCT), respectively.

4 RESULTS

4.1 Fluidized bed nitriding

Nitriding parameters used in the processing of powders in a fluidized bed furnace before subsequent HIPing of SMO 0,7N, SMO 0,9N and SMO 1,15N, are shown in Table 2 along with the nitrogen and oxygen contents of the HIPed steels before and after powder nitriding. The nitrogen content of the powder (and HIPed steel) increased with increasing nitriding temperature and time. The oxygen content of the powder (and HIPed steel) also increased with increasing nitriding time and temperature.

Table 2. Nitriding parameters, nitrogen and oxygen contents of HIPed SMO 0,7N, SMO 0,9N and SMO 1,15N steels before and after powder nitriding in a fluidised bed furnace.

Material	Nitriding parameters	Nitrogen content before fluidised bed nitriding (wt-%N)	Nitrogen content after fluidised bed nitriding (wt-%N)	Oxygen content before fluidised bed nitriding (ppm)	Oxygen content after fluidised bed nitriding (ppm)
654 SMO 0,7N	760 °C/40 min	0,46	0,74	160	290
654 SMO 0,9N	760 °C/50 min	0,46	0,89	160	310
654 SMO 1,15N	800 °C/1 h 30 min	0,46	1,15	160	390

The nitrogen content of the fluidized bed furnace nitrided powder batch depends upon the particle size of the powder sample, shown in Figure 18, for the powder nitrided at 760 °C for 40 min. The nitrogen content increases as the particle size range decreases. Both the nitrogen and oxygen contents of the fluidized bed furnace nitrided powder increased with decreasing particle size. This can be observed from Figure 19, which shows the nitrogen and oxygen contents of SMO powder (0,46 wt-%N and 160 ppm oxygen) nitrided at 800 °C for 120 min. A deviation from the general trend is observed for oxygen content in the particle size range of 297 - 420 µm. Nitrogen content as a function of particle size range does not show any major deviations from the general trend.

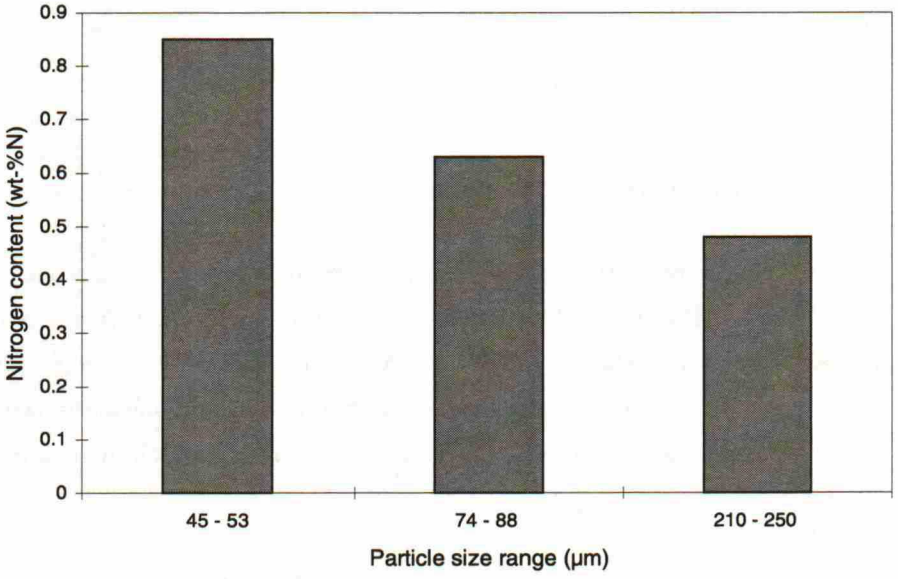

Figure 18. Effect of particle size range on nitrogen content of powder fluidised bed nitrided at 760 °C/40 min.

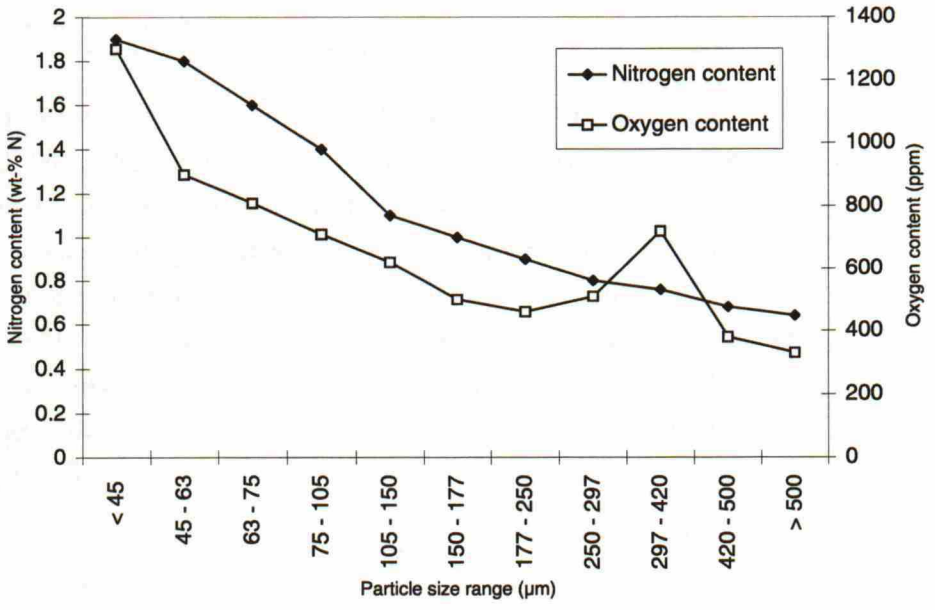

Figure 19. Effect of particle size range on nitrogen and oxygen contents of powder fluidised bed nitrided at 800 °C for 120 min.

4.2 Microstructure

4.2.1 Optical microscopy

All the solution annealed steels had an austenitic microstructure except for the steel with 1,15 wt-%N. The microstructure of SMO 0,7N is shown in Figure 20, and that of SMO 1,15 wt-%N in Figure 21. The microstructure of SMO 1,15 wt-%N consists of an austenitic matrix, but with irregular grain boundaries due to precipitation. The average grain sizes of the materials were 30 - 48 µm, as shown in Table 3.

Table 3. Grain sizes of the studied steels.

Material	Average grain size (µm)
SMO 0,3N	33
SMO 0,5N1	30
SMO 0,7N	32
SMO 0,9N	33
SMO 1,15N	48

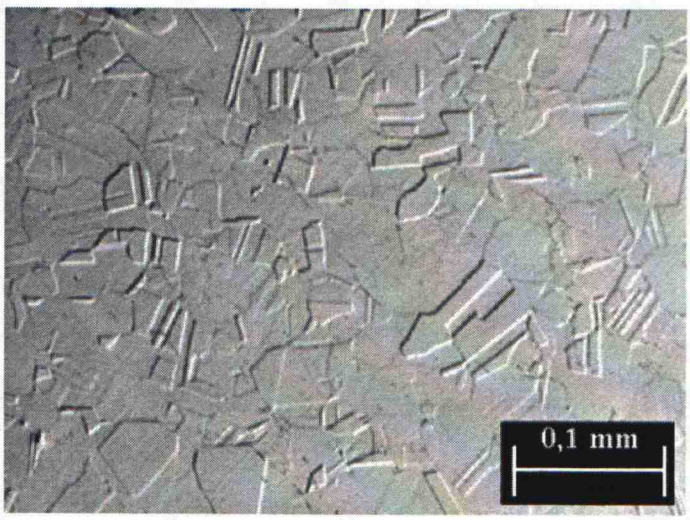

Figure 20. Microstructure of solution annealed SMO 0,7N.

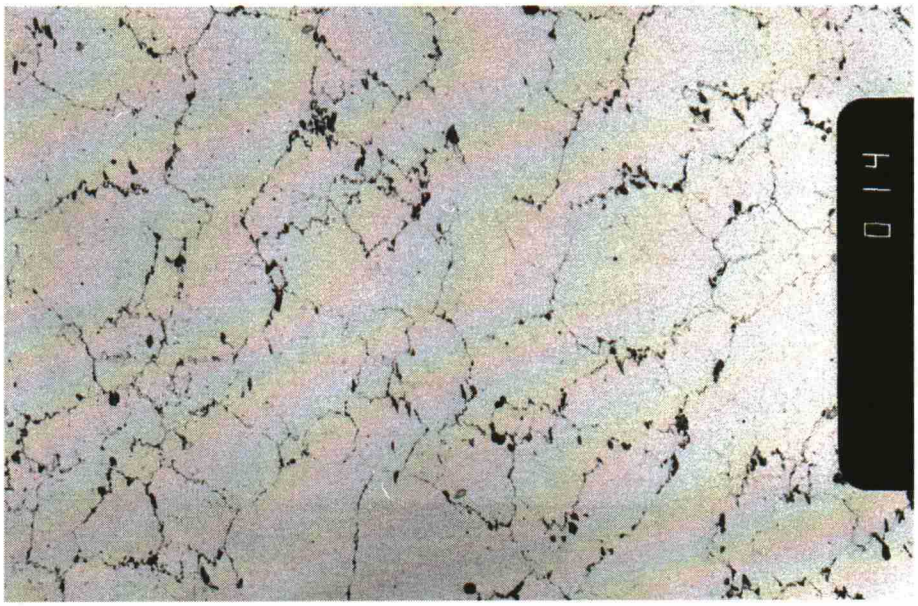

Figure 21. Microstructure of SMO 1,15N showing intergranular precipitation. Magnification 220 x.

The microstructures of the steels annealed at 450 °C for up to 500 h were, in general, similar to those of the solution annealed steels. The only exception was SMO 0,3N, which was observed to contain precipitates on part of the grain boundaries, Figure 22.

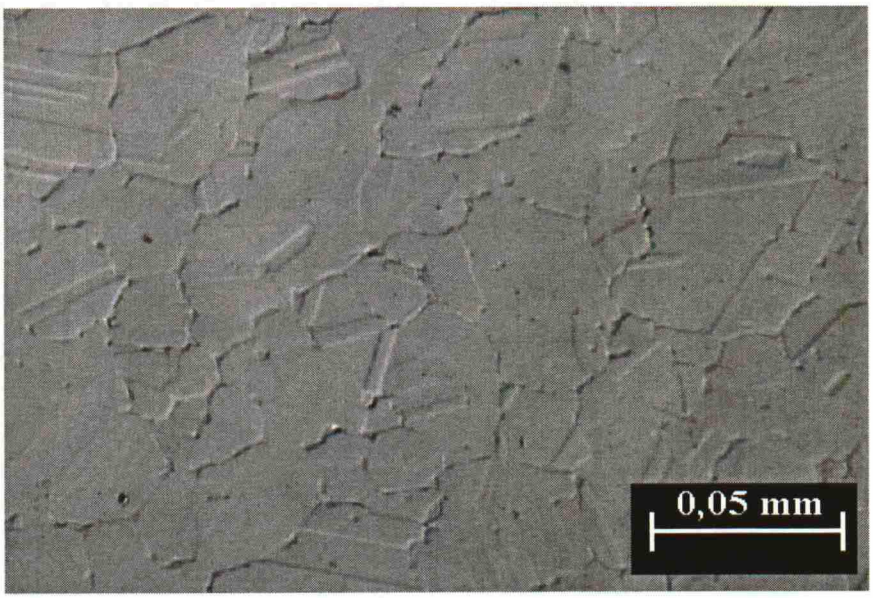

Figure 22. Microstructure of SMO 0,3N annealed for 500 h at 450 °C showing intergranular precipitation.

The microstructures of all of the steels annealed at 750 °C consisted of an austenitic matrix with inter- and intragranular precipitates. The form of the precipitates depended upon the annealing time. After 1 h of annealing precipitation was observed to have taken place mainly intergranularly, but with some intragranular precipitation. As the annealing time was increased, the amount of intragranular precipitation increased. This can be seen in Figure 23, where the microstructures of steels with 0,3 wt-%N and 0,9 wt-%N are shown. After 1 h of annealing, the grain boundaries are more clearly defined due to precipitation, as compared to those of the solution annealed steels. As the annealing time is increased up to 10 h, the grain boundaries are even more clearly defined due to precipitation, and in both steels the amount of intragranular precipitation is increased. After 72 h of annealing, the amount of intragranular precipitation is clearly increased, and the grain boundaries are covered with precipitates to form a continuous film. As the nitrogen content of the steel increases, the amount of both inter- and intragranular precipitation is decreased, Figure 23. Similar trend was observed in the steels with 0,5 and 0,7 wt-%N annealed at 750 °C, Appendix D. Especially after 1 h of annealing, the amount of grain boundary precipitation seems to be less pronounced in the steel with 0,9 wt-%N, as compared to that of the steel with 0,3 wt-%N, Figure 23. Also, in the steel with 0,3 wt-%N, intragranular precipitation can be seen, but not in the steel with 0,9 wt-%N. After 10 h of annealing, the amount of intergranular precipitation seems to be more pronounced in the steel with 0,3 wt-%N than that in the steel with 0,9 wt-%N. Intragranular precipitation has taken place in both steels, but no clear differences in the amount of intragranular precipitation between the steels can be observed. After 72 h of annealing, the grain boundaries of both steels are covered with precipitates. The intergranular precipitates in the steel with 0,3 wt-%N consist mainly of a phase (darkest phase) which is not found in the steel with 0,9 wt-%N. Similar observations can be made when the microstructures of the steels with 0,5 and 0,7 wt-%N are examined, Appendix D. The amount of intragranular precipitates is clearly smaller in the steel with 0,9 wt-%N than that in the steel with 0,3 wt-%N when annealed for 72 h at 750 °C, Figure 23. Similar trend can also be seen from Figure 24, where the microstructures of the steels with 0,7 and 0,9 wt-%N annealed for 72 h at 750 °C are compared. The amount of intragranular precipitation is lower, in general, the higher the nitrogen content of the steel is. Especially if the steels annealed for 72 h are compared, the microstructures of the steels annealed at 750 °C can be divided into two groups consisting of different type of microstructures. The first group consists of the steels with 0,3 and 0,5 wt-%N, and the second group consists of the steels with 0,7 and 0,9 wt-%N, each sharing a similar type of microstructure.

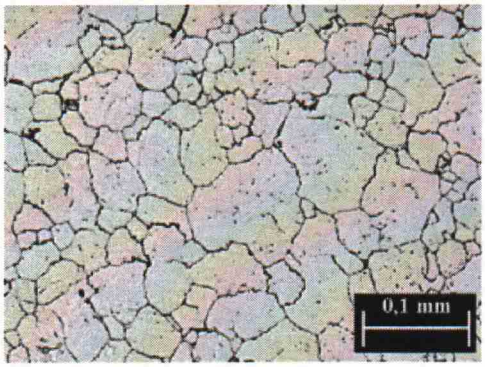

a) SMO 0,3N: 750 °C/1 h.

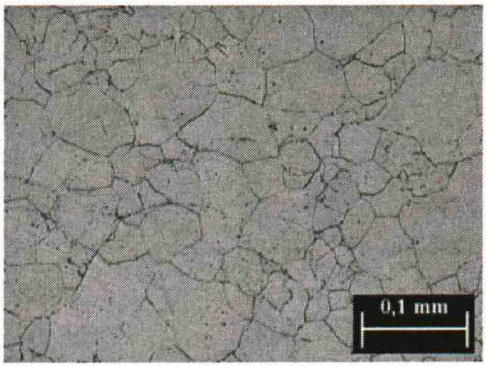

d) SMO 0,9N: 750 °C/1 h.

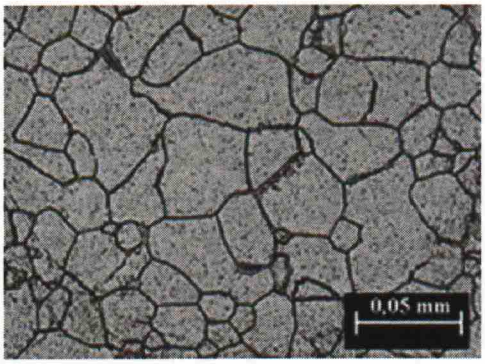

b) SMO 0,3N: 750 °C/10 h

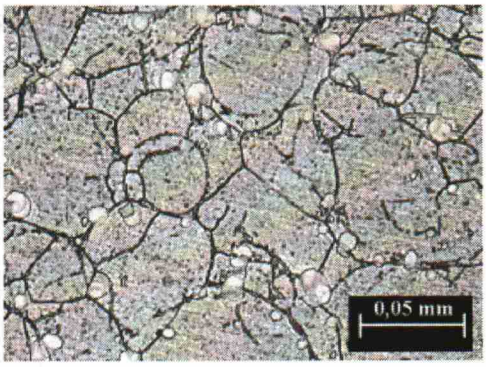

e) SMO 0,9N: 750 °C/10 h.

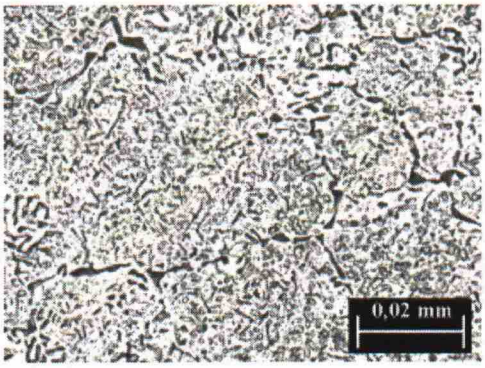

c) SMO 0,3N: 750 °C/72 h.

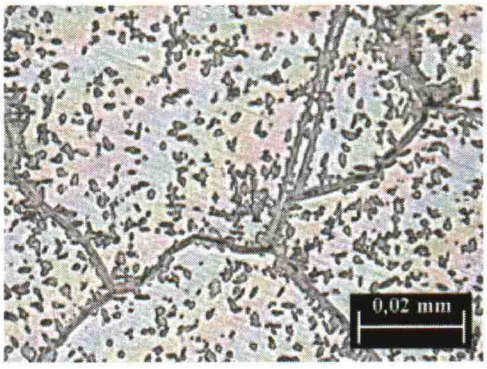

f) SMO 0,9N: 750 °C/72 h.

Figure 23. Microstructures of SMO 0,3N and SMO 0,9N annealed at 750 °C for up to 72 h.

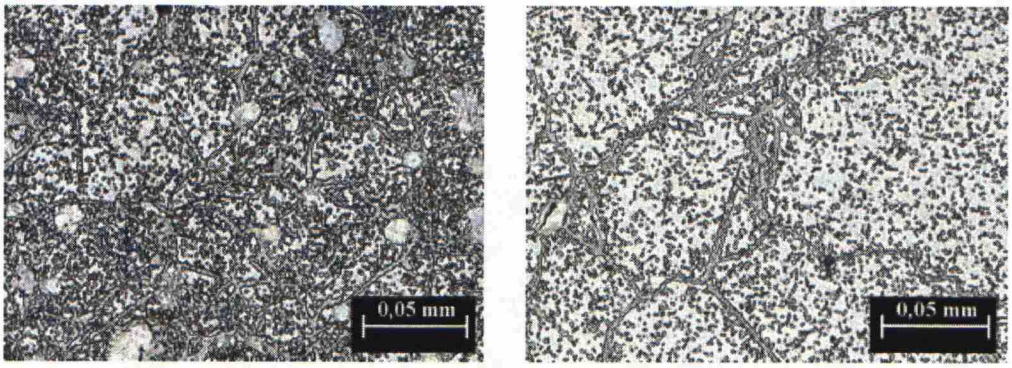

a) b)

Figure 24. Microstructures of a) SMO 0,7N and b) SMO 0,9N annealed at 750 °C for 72 h.

4.2.2 Transmission electron microscopy

The intermetallic phases and nitrides observed by TEM in the solution annealed, as well as subsequently at 450 and 750 °C annealed steels, are shown in Table 4. In the solution annealed steels, σ phase particles were found at grain boundaries in steels with ≤ 0,5 wt-%N. Their amount was higher in the steel with 0,3 wt-%N, as compared to that in the steel with 0,5 wt-%N, Figure 25. In the steel with 1,15 wt-%N, Cr_2N was observed mainly at the grain boundaries and to some extent also inside the grains, Figure 26. The steels with 0,7 and 0,9 wt-%N were not observed to contain any precipitates, i.e., neither intermetallic phases nor Cr_2N were observed at the grain boundaries or inside the grains. In all the solution annealed steels, isolated manganese oxide particles were observed, especially in the steels with nitrogen contents of 0,7 and 0,9 wt-% N. The manganese oxides had a relatively high chromium content. Additionally, in the steel containing 0,5 wt-%N, iron oxides of the type Fe_3O_4 were observed.

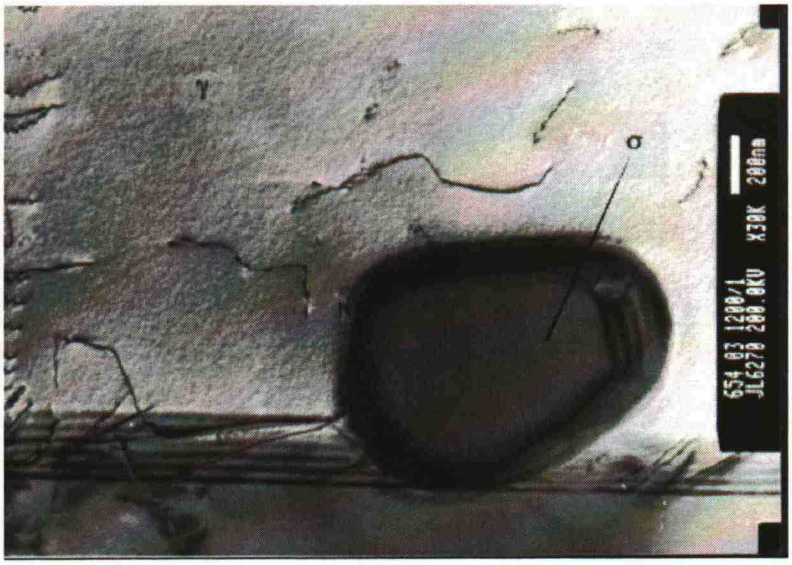

Figure 25. σ phase at the grain boundary in SMO 0,3N.

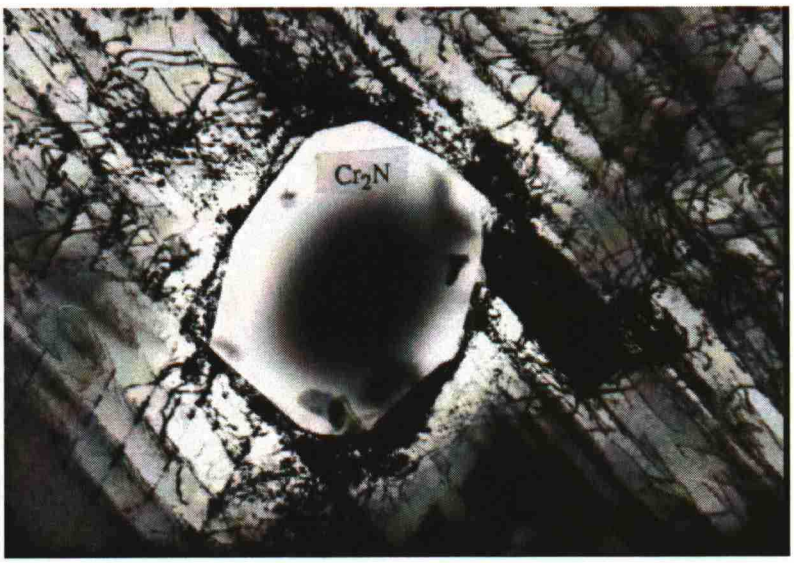

Figure 26. Intragranular Cr_2N precipitate in SMO 1,15N. Magnification 18500 x.

Typical selected area diffraction (SAD) patterns of the observed intermetallic phases and Fe_3O_4 are shown in Figure 27. Selected area diffraction pattern of Cr_2N is not shown, since any clear pattern could not be observed. In Figures 27 c) and d) the selected area diffraction patterns for Laves phase are also shown. The diffraction pattern in Figure 27 c) is similar to that reported by Jargelius-Petterson (1994). The Laves phase was observed to be distorted, which can be seen as

streaks in the diffraction pattern in Figure 27 c). Jonsson et al. (1999) have observed highly distorted Laves phase in steels with similar chemical compositions as those in this study. They explained that the diffraction patterns showed streaks due to highly distorted crystal structure of the Laves phase. Jonsson et al. (1999) also observed rotational symmetries in the selected area diffraction patterns of Laves phase similar to that in Figure 27 d) for steels with similar chemical compositions as those in this study. In Table 5 the d-spacings measured from Figure 27 for the observed intermetallic phases and Fe_3O_4 compared with the respective d-spacings found in the literature (Andrews et al., 1967; JCPDS, 1978) are shown. In Table 6 typical chemical compositions of the intermetallic phases and Cr_2N observed after isothermal annealing up to 72 h at 750 °C are shown.

Table 4. Results of TEM-analyses of the steels annealed at 450 °C and 750 °C.

Material	Heat treatment	Precipitated phases
SMO 0,3N	1200 °C/1h	σ
	1200 °C/1h + 450 °C/500 h	σ, λ
	1200 °C/1h + 750 °C/1 h	σ, λ, Cr_2N*
	1200 °C/1h + 750 °C/72 h	σ, λ
SMO 0,5N1	1200 °C/1h	σ
	1200 °C/1h + 450 °C/1 h	σ
	1200 °C/1h + 450 °C/72 h	σ
	1200 °C/1h + 450 °C/500 h	σ
	1200 °C/1h + 750 °C/1 h	σ, λ
	1200 °C/1h + 750 °C/72 h	σ,λ
SMO 0,7N	1225 °C/1h	-
	1225 °C/1h +450 °C/72 h	-
	1225 °C/1h +750 °/1 h	λ , Cr_2N
	1225 °C/1h +750 °C/72 h	σ, λ , Cr_2N
SMO 0,9N	1250 °C/1h	-
	1250 °C/1h +450 °C/72 h	-
	1250 °C/1h +450 °C/500 h	-
	1250 °C/1h +750 °/1 h	λ , Cr_2N
	1250 °C/1h +750 °C/72 h	σ, λ , Cr_2N
SMO 1,15N	1250 °C/1h	Cr_2N

*) Only very few and small isolated particles were found.

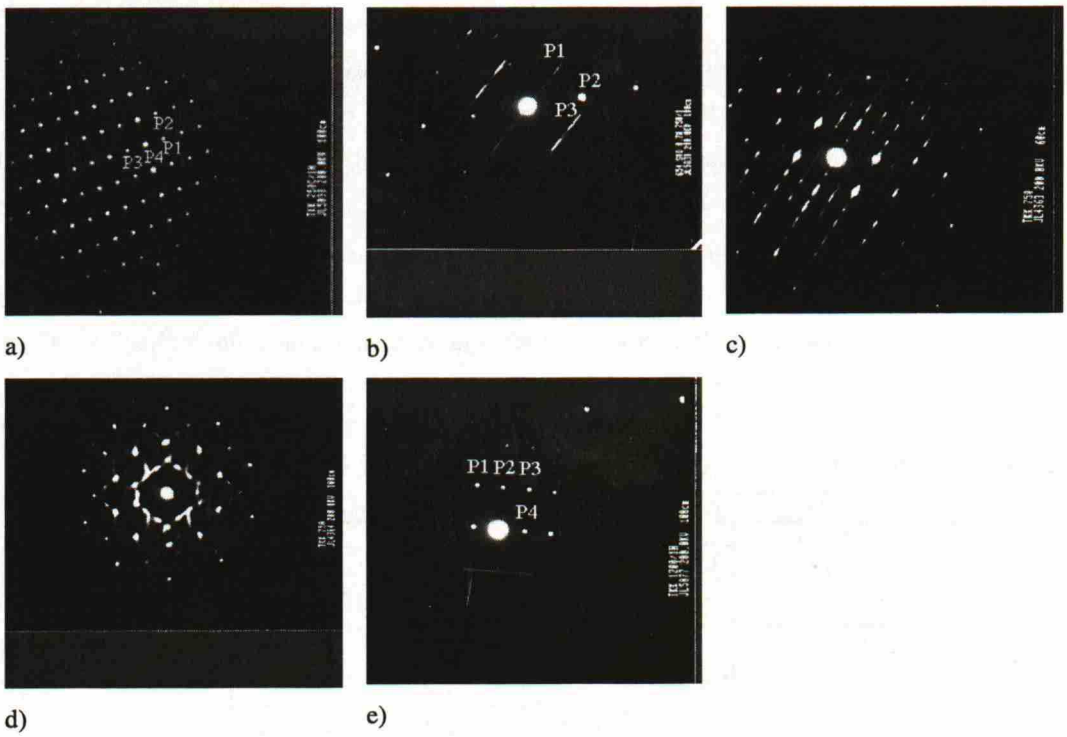

Figure 27. Selected area diffraction (SAD) patterns of σ phase a), Laves phase b), c), d) and Fe_3O_4 e). The incident electron beam was parallel to: a) [$\bar{1}$ 1 0], c) [0 0 0 1], d) [1 1 $\bar{2}$ 0] and e) [$\bar{1}$ 1 2].

Table 5. Comparison of d-spacings measured from Figure 27 for σ and Laves phase as well as for Fe_3O_4 compared with the respective values found in the literature (JCPDS, 1978; Andrews et al., 1967).

Analysed phase		d-spacing measured (Å)	d-spacing literature (Å)	hkl
σ	P1	3,75	3,669; 3,866*	111
	P2	6,12	6,222; 6,496*	110
	P3	3,69	3,669; 3,866*	111
	P4	4,65	4,544; 4,812*	001
Laves	P1	2,40	2,365	110
	P2	1,80	1,750	014
	P3	1,96	1,98	201
Fe_3O_4	P1	2,49	2,53	311
	P2	4,74	4,85	111
	P3	2,49	2,53	311
	P4	2,95	2,966	220

*) first value = σ Fe-Cr; second value = σ Fe-Mo

Table 6. Typical chemical compositions in wt-% of the observed intermetallic phases and Cr_2N in the studied steels annealed isothermally up to 72 h at 750 °C.

Phase	Fe	Cr	Ni	Mn	Mo
σ	37 ± 3	33 ± 1	11 ± 2	2 ± 1	18 ± 2
Laves	33 ± 5	14 ± 2	13 ± 3	2 ± 1	43 ± 4
Cr_2N	5 ± 1	82 ± 1	4 ± 1	2 ± 1	6 ± 1

Annealing at 450 °C for 500 h resulted in σ phase precipitation at the grain boundaries in the steels with nitrogen contents of 0,3 and 0,5 wt-%N. In Figure 28, σ phase precipitated at the grain boundaries in the steel containing 0,5 wt-%N is shown. Additionally, in the steel containing 0,3 wt-%N, both Laves (λ) and σ phase were observed to precipitate after 500 h of annealing at 450 °C, Figure 29. The TEM sample of the steel in Figure 29 was made from a tensile test bar, and therefore the microstructure of the steel contains a high density of dislocations. Intermetallic phases were not found in the steels containing 0,7 and 0,9 wt-%N which were isothermally annealed at 450 °C. Cr_2N did not precipitate in the steels isothermally annealed at 450 °C. Isolated manganese oxide particles with relatively high chromium content were also found in all the steels isothermally annealed at 450 and 750 °C. They were especially noticed in the steels with nitrogen contents of 0,7 and 0,9 wt-% N. Iron oxides of the type Fe_3O_4 were also observed in the steel containing 0,5 wt-%N, Figure 30.

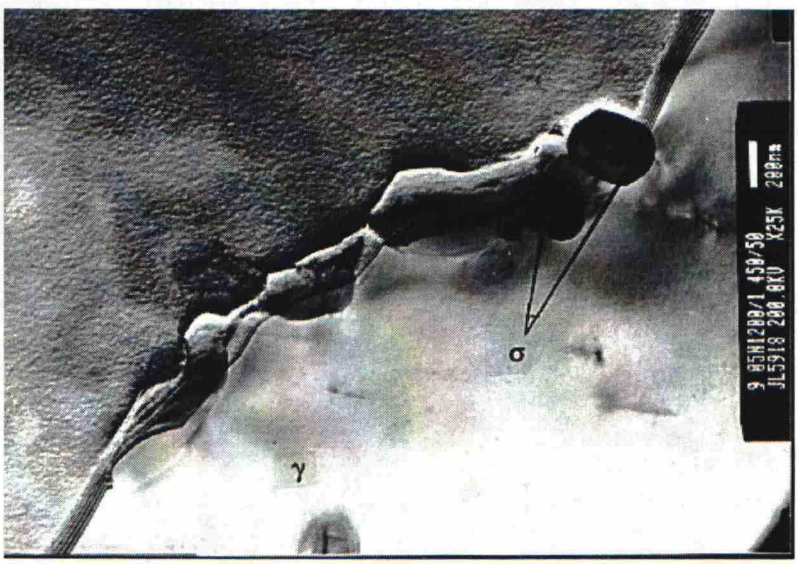

Figure 28. Intergranular σ phase in SMO 0,5N1 isothermally annealed at 450 °C for 500 h.

Figure 29. Intergranular σ phase in SMO 0,3N isothermally annealed at 450 °C for 500 h.

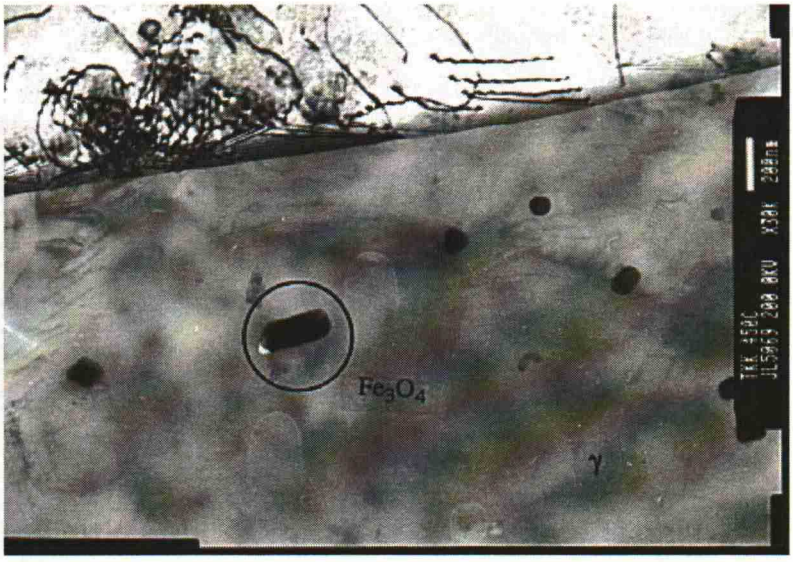

Figure 30. Fe-oxides of type Fe_3O_4 in SMO 0,5N1 isothermally annealed at 450 °C for 1 h.

In steels annealed at 750 °C mainly intermetallic phases (σ and Laves phase) were observed when the nitrogen content of the steel was ≤ 0,5 wt-% N. However, in the steel containing 0,3 wt-%N very few isolated particles with high Cr-content being most likely Cr_2N had precipitated intragranularly after 1 h of annealing at 750 °C, but not in the steel containing 0,5 wt-%N. The

amount of intermetallic phase precipitation increased with increasing annealing time at 750 °C, Figure 31.

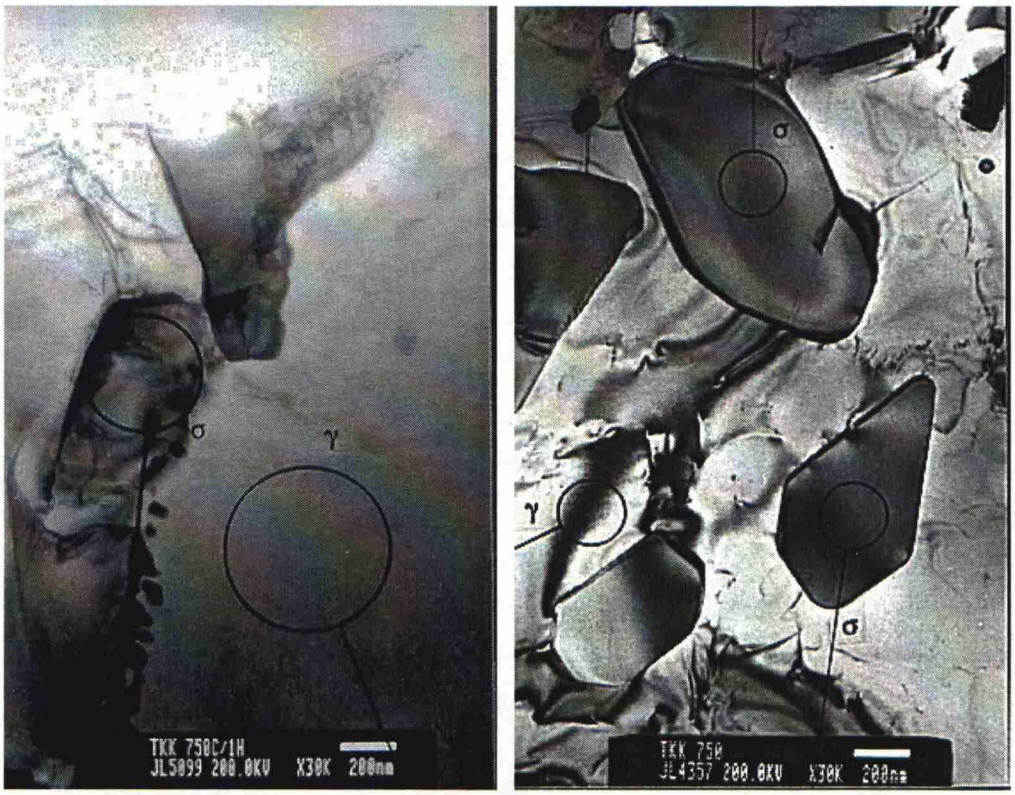

a) b)

Figure 31. Inter- and intragranular σ phase in SMO 0,5N1 isothermally annealed at 750 °C for a) 1 h and b) 72 h.

Annealing at 750 °C resulted in Cr_2N precipitation in addition to intermetallic phase precipitation in steels with nitrogen contents of 0,7 and 0,9 wt-%N, with the amount of Cr_2N precipitation increasing with increasing annealing time. After 1 h of annealing at 750 °C, Laves phase and Cr_2N had precipitated adjacent to each other mainly at the grain boundaries, Figure 32. σ phase was not observed in the steels annealed for 1 h at 750 °C. In addition to intergranular precipitation, intragranular precipitation of Cr_2N and intermetallic phases took place, with the amount of intragranular precipitates increasing as the annealing time at 750 °C increased up to 72 h, Figure 33. In the steels with 0,7 and 0,9 wt-%N, Cr_2N had precipitated intragranularly adjacent to Laves phase after 72 h of annealing at 750 °C, Figure 34.

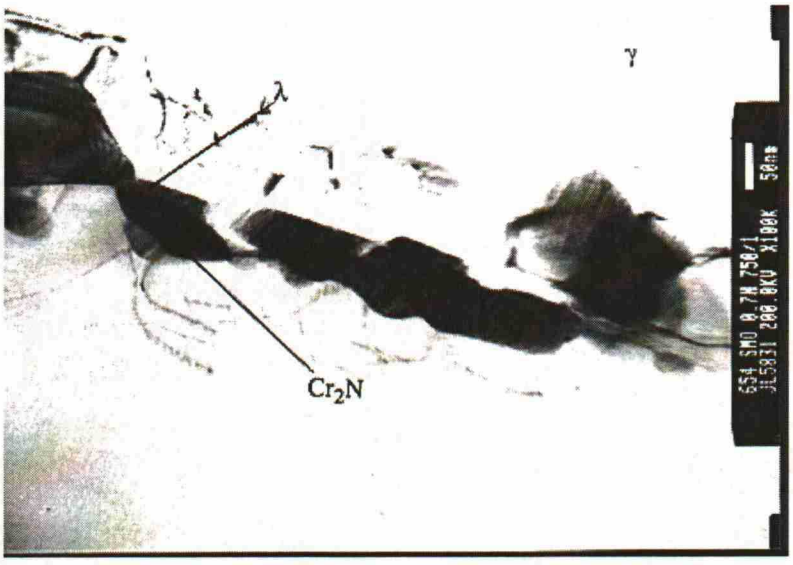

Figure 32. Intergranular Laves phase and Cr_2N in SMO 0,7N isothermally annealed at 750 °C for 1 h.

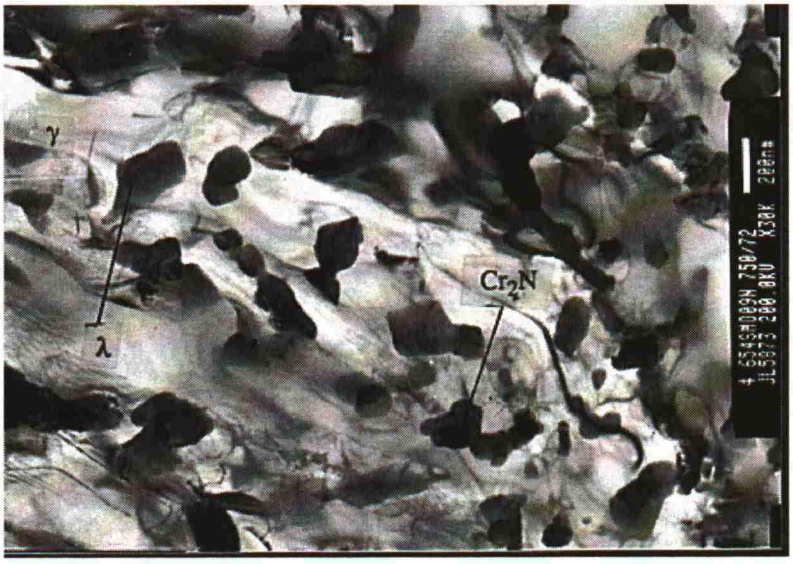

Figure 33. Intragranular Laves phase and Cr_2N in SMO 0,9N isothermally annealed at 750 °C for 72 h.

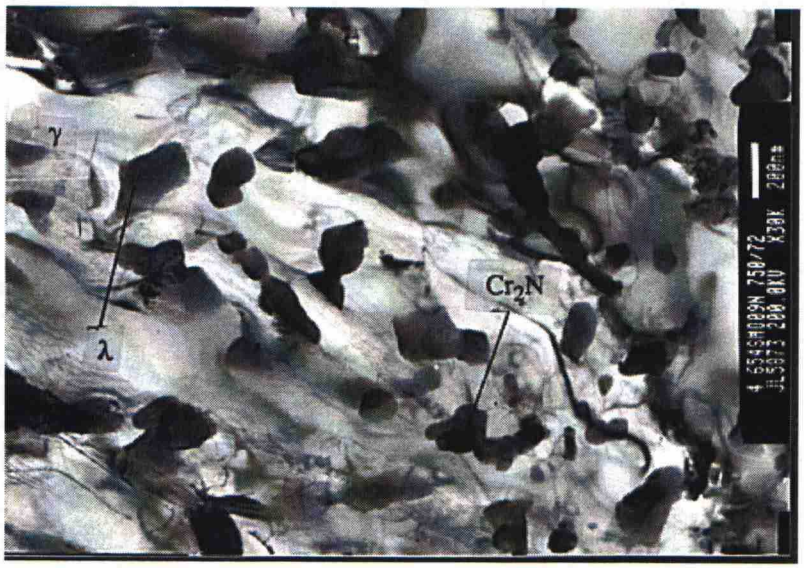

Figure 34. Intragranular adjacently precipitated Laves phase and Cr_2N in SMO 0,9N isothermally annealed at 750 °C for 72 h.

The austenite matrix adjacent to the precipitates in all of the steels annealed at 750 °C was observed to have lower chromium, and especially, lower molybdenum content as compared to that of solution annealed steels, Table 7. As the annealing time at 750 °C increased, the molybdenum and chromium contents in the austenite matrix adjacent to the precipitates decreased.

Table 7. Chemical composition of precipitation free solution annealed austenite matrix and the austenite matrix adjacent to intermetallic phase or intermetallic phase and Cr_2N precipitates in SMO 0,3N and SMO 0,9N isothermally annealed up to 72 h at 750 °C.

	Fe	Cr	Ni	Mn	Mo
Solution annealed austenite matrix: SMO 0,3N	42,8	24,2	23,7	2,5	6,8
Austenite matrix adjacent to Laves phase: SMO 0,3N	44,6	20	29,3	2,9	3,2
Solution annealed austenite matrix: SMO 0,9N	42,4	24,4	22,1	3,6	7,4
Austenite matrix adjacent to Laves phase and Cr_2N: SMO 0,9N	49,1	16,9	26,3	4,7	2,9

4.3 Dilatometric analyses

4.3.1 Heating and cooling analyses

Typical dilatometric curves during heating and cooling (dL/l_o and dL/dt) for SMO 0,5N1 are shown in Appendix E. All of the studied steels had similar dilatometric curves during heating and

cooling. From the derivative of the expansion curves) (dL/dt) in Appendix E and Figure 36 it can be seen, that the increase in the length of the sample is decelerated beginning at ~ 420 - 450 °C and at ~ 720 - 750 °C. The minimum increase rate of the length of the samples takes place at ~ 550 - 600 °C and ~ 950 °C, respectively. In Figure 35 the expansion curves (dL/l_o) with heating rates of 5, 10 and 20 °C/min are shown for the steel with 0,7 wt-%N. Dilatation increases with decreasing heating rate for the steel, and the slope of the curve changes for all the heating rates at about 550 °C. This change is most pronounced for the curve with the heating rate of 5 °C/min. The difference in dilatation due to the different heating rates decreases with increasing temperature. In general, the difference in dilatation for the different heating rates became negligible above ~ 600 °C. No major differences between the materials were observed in the heating analyses at any of the heating rates, Figure 36.

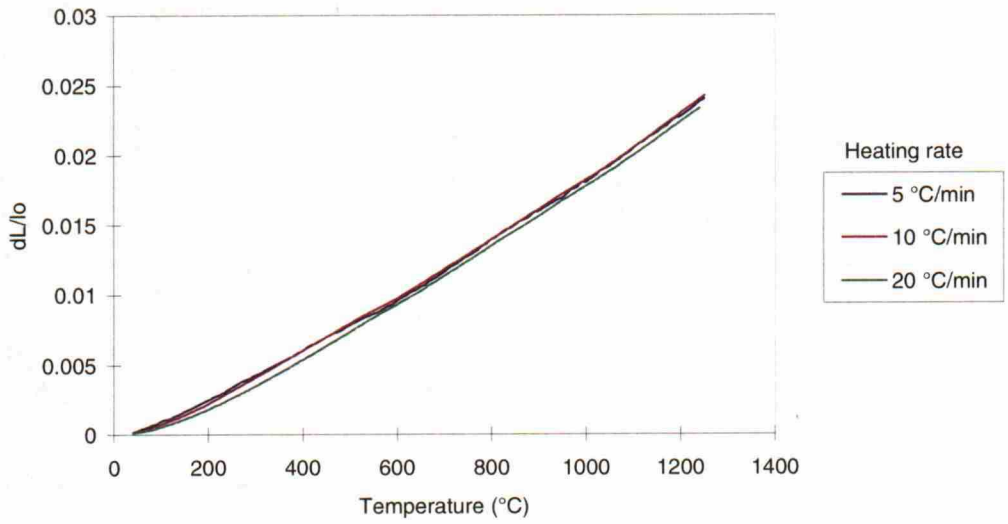

Figure 35. Dilatometric curves during heating for SMO 0,7N. Heating rates: 5, 10 and 20 °C/min.

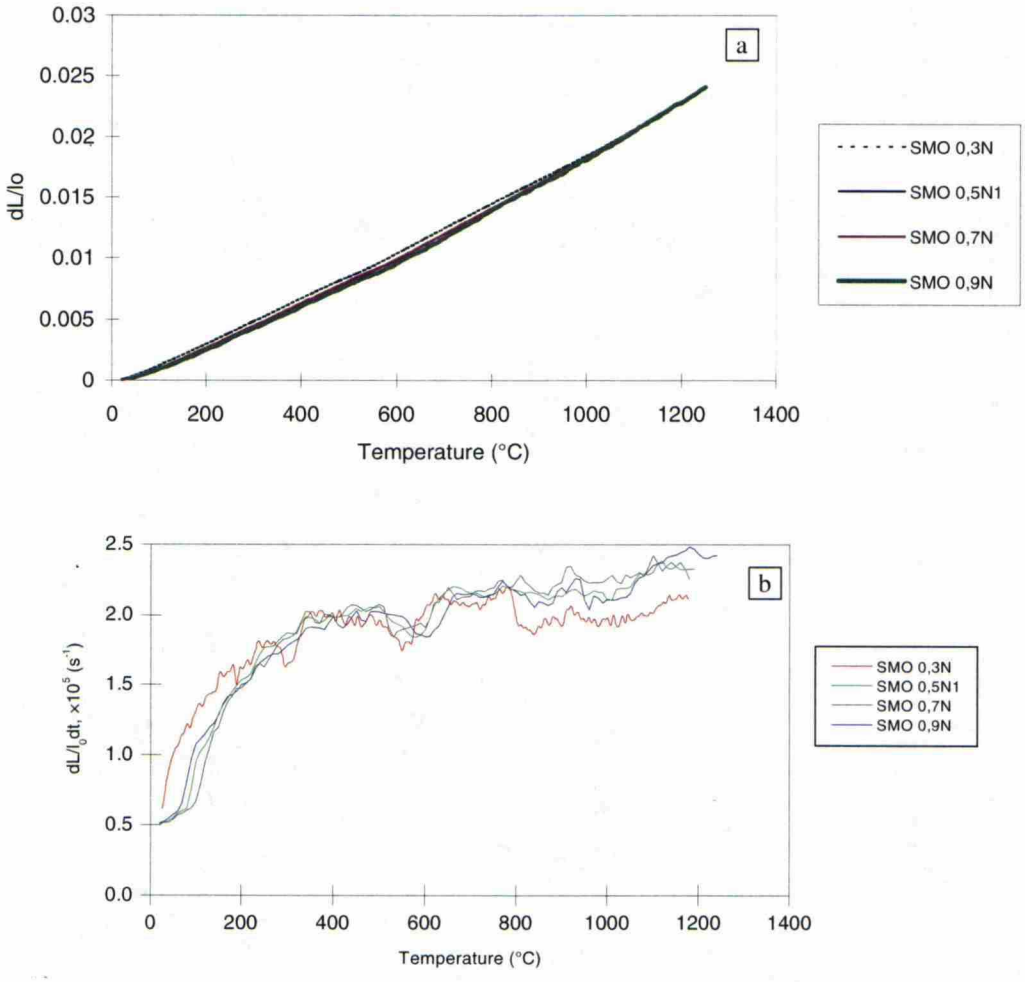

Figure 36. Dilatometric curves during heating for the studied steels: a) dilatation, heating rate 5 °C/min and b) derivative of heating curves.

In Figure 37, the shrinking curves with the cooling rates of 5, 10 and 20 °C/min for the steel with 0,5 wt-%N are shown. As in the case of the dilatometric curves during heating, shrinking is more rapid with decreasing cooling rate. Likewise, a change in the slope of the curves takes place at approximately 550 °C. In Figure 38, the cooling curves with the cooling rate of 10 °C/min for the steels are compared. The cooling curves for the steels are similar to each other. Similar behaviour was observed in the analyses of the cooling rates of 5 and 10 °C/min.

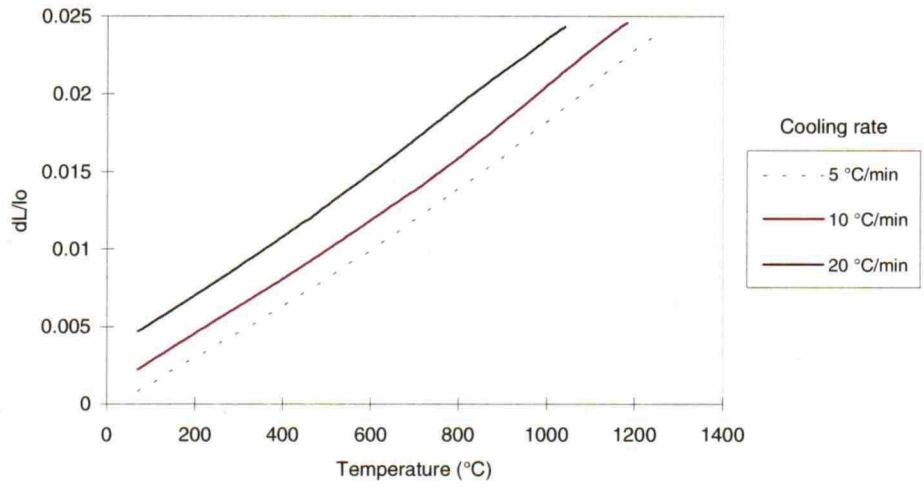

Figure 37. Dilatometric curves during cooling for SMO 0,5N1. Cooling rates: 5, 10 and 20 °C/min.

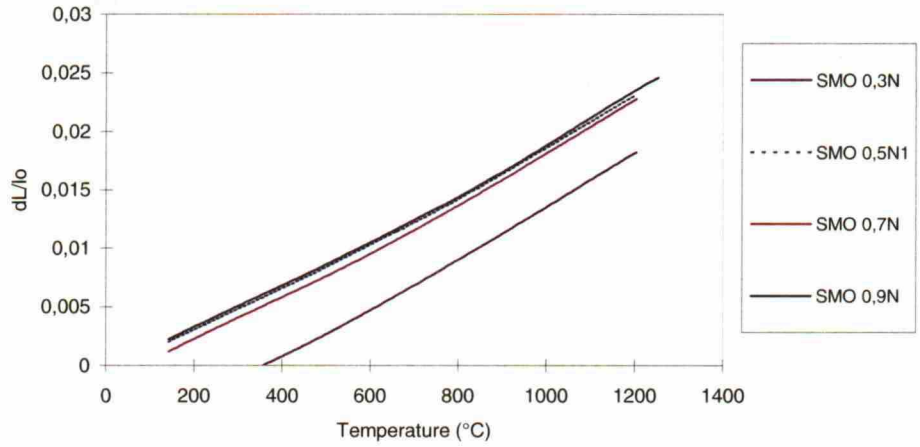

Figure 38. Dilatometric curves during cooling for the studied steels. Cooling rate: 10 °C/min.

4.3.2 Isothermal analyses

Isothermal analysis was performed at 450 and 750 °C. These temperatures were chosen based on the literature data on isothermal annealing of nitrogen alloyed austenitic stainless steels and on the dilatometric curves during heating. Especially, the derivative dilatometry (dL/dt) showed substantial changes beginning at the proximity of these temperatures. In Figure 39, the effect of annealing for up to 72 h at 450 °C on dilatation is shown. For all the steels dilatation first decreases,

after which it becomes strongly fluctuating, although the overall changes in it become negligible. Dilatation is also fluctuating in the beginning of the analyses, Figure 40, but the fluctuating changes in dilatation are substantially smaller than in the latter stages of the analyses. There appears to be only minor differences in the rate of decrease in dilatation between the steels in the beginning of the analyses.

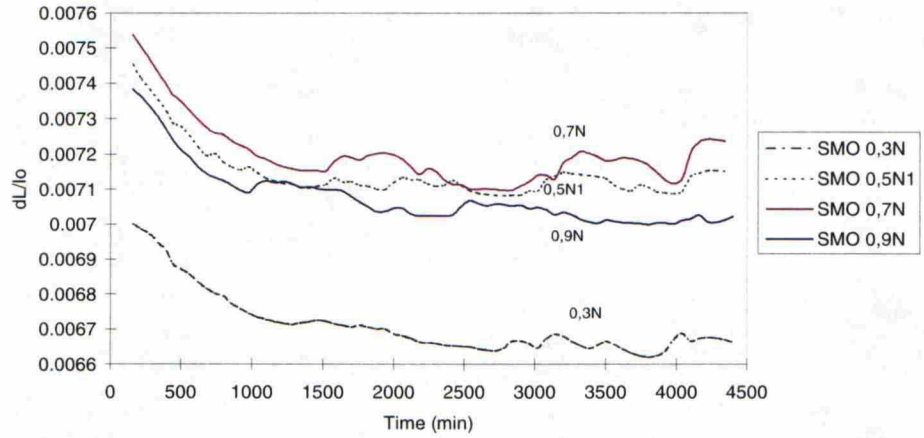

Figure 39. Isothermal dilatometric analysis at 450 °C for the studied steels.

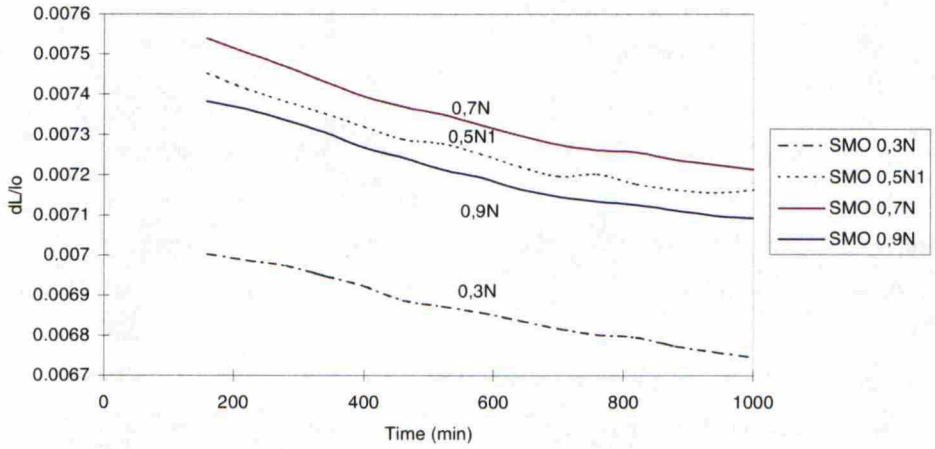

Figure 40. Isothermal dilatometric analysis for the studied steels for the first 840 min at 450 °C.

In Figure 41 the isothermal analysis for the studied steels at 750 °C is shown. For all the steels dilatation decreases constantly with increasing annealing time and is fluctuating during the entire annealing time at 750 °C. As in the case during annealing at 450 °C, the fluctuations in

dilatation become bigger as the holding time increases. In general, the decrease in dilatation with increasing annealing time becomes slower as the nitrogen content of the steel increases. The only exception is SMO 0,3N, which has the smallest decrease in dilatation during the holding time at 750 °C.

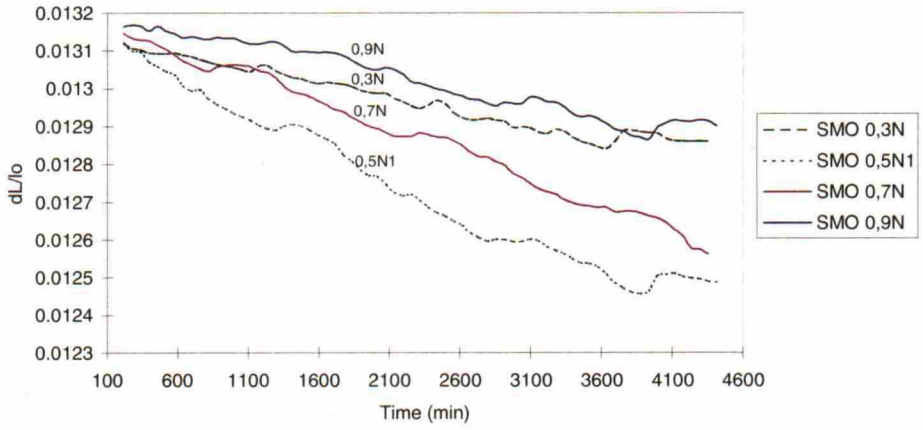

Figure 41. Isothermal analysis at 750 °C for the studied steels.

4.4 Effect of precipitates on mechanical properties

4.4.1 Tensile testing

Results of the tensile tests for the solution annealed steels and the steels further isothermally annealed at 450 °C and 750 °C, are shown in Table 8. The yield and ultimate tensile strength values of the solution annealed steels increased with increasing nitrogen content of the steel, Figure 42. Tensile ductility of the solution annealed steels is high for nitrogen contents of up to 0,5-0,6 wt-%N, but it begins to decrease slowly as the nitrogen content of the steel is increased up to 0,9 wt-%N, Figure 43. When the nitrogen content of the steel reaches 1,15 wt-%N, the tensile ductility of the solution annealed steels deteriorates, Figure 43. The results of earlier studies (Romu et al., 1996; 1997; Tervo et al., 1997; Tervo, 1998) made on these steels are also shown in Figures 42 and 43.

Table 8. Results of the tensile tests performed for studied steels in the solution annealed as well as solution annealed and isothermally at 450 °C and 750 °C annealed conditions.

Material	Heat treatment	$R_{p0,2}$ (MPa)	R_m (MPa)	A (%)	Z (%)
SMO 0,3N	1200 °C/1 h	456, 479	876, 893	55, 57	61, 63
	1200 °C/1 h +450 °C/72 h	468	898	52	43
	1200 °C/1 h + 450 °C/500 h	516, 539	868, 892	17, 19	37, 37
	1200 °C/1 h + 750 °C/1 h	429, 454	850, 865	52, 54	52, 56
	1200 °C/1 h + 750 °C/10 h	512, 525	798, 871	-	10, 10
	1200 °C/1 h +750 °C/72 h	651, 657	899, 993	3	1, 4
SMO 0,5N1	1200 °C/1 h	520, 535	895	50	63, 64
	1200 °C/1 h + 450 °C/1 h	528, 561	918, 927	51, 58	51, 59
	1200 °C/1 h + 450 °C/10 h	556, 535	925, 909	49, 53	54, 57
	1200 °C/1 h + 450 °C/72 h	544, 538	897, 903	51, 52	57, 58
SMO 0,5N2	1200 °C/1 h	503, 507	915, 918	57, 62	54, 62
	1200 °C/1 h + 750 °C/1 h	518, 526	904, 908	68, 70	55, 57
	1200 °C/1 h + 750 °C/10 h	531	914	61, 62	35, 38
	1200 °C/1 h +750 °C/72 h	663, 669	880, 904	6, 7	5, 7
SMO 0,7N	1225 °C/1 h	665	956	54	48
	1225 °C/1 h + 450 °C/1 h	687, 688	989, 1036	57, 60	54, 54
	1225 °C/1 h + 450 °C/10 h	680, 696, 702	963, 978, 989	56, 59, 60	55, 56, 57
	1225 °C/1 h + 450 °C/72 h	680, 717	942, 973	60, 61	52, 53
	1225 °C/1 h + 750 °C/1 h	696	959	48	48
	1225 °C/1 h + 750 °C/10 h	648	975	48	34
	1225 °C/1 h + 750 °C/72 h	695, 708	946	6	4, 5
SMO 0,9N	1250 °C/1 h	798, 801	1003, 1095	46	38, 39
	1250 °C/1 h + 450 °C/1 h	815, 835	1030, 1116	44, 47	40, 40
	1250 °C/1 h + 450 °C/10 h	798, 818, 863	1000, 1024, 1027	48, 52, 55	43, 46, 48
	1250 °C/1 h + 450 °C/72 h	795, 817	1025, 1034	47, 52	39, 45
	1250 °C/1 h + 750 °C/1 h	629, 635	1028, 1040	46, 50	40, 43
	1250 °C/1 h + 750 °C/10 h	661, 663	903, 932	33	27, 28
	1250 °C/1 h + 750 °C/72 h	642	787	16	19
SMO 1,15N	1250 °C/1 h	805, 828	1114, 1145	20, 25	21, 30

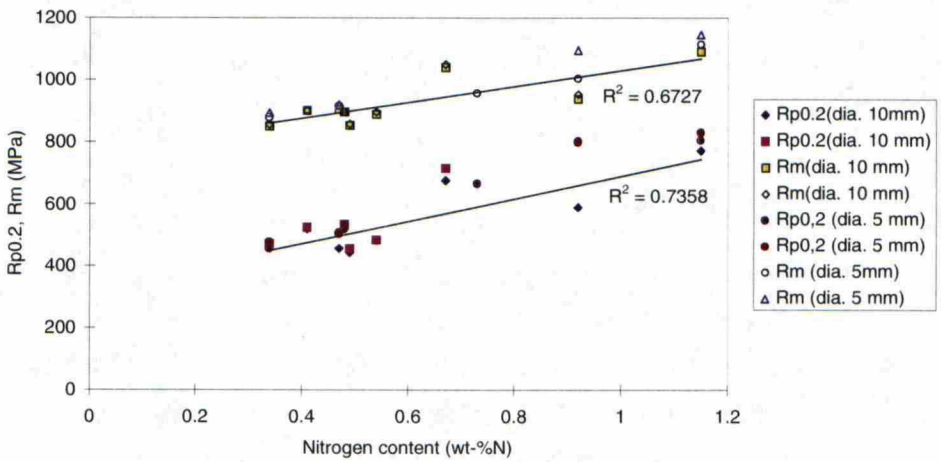

Figure 42. Effect of nitrogen content on yield and ultimate tensile strength of the studied solution annealed steels.

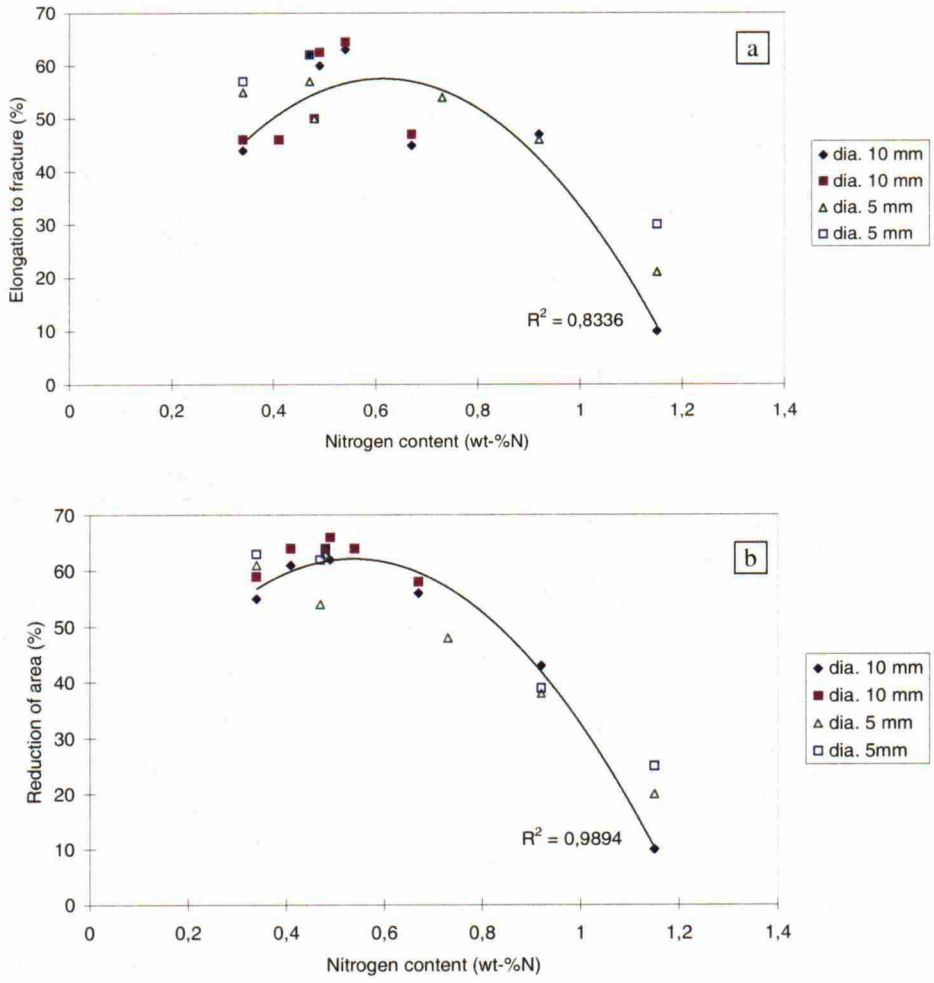

Figure 43. Effect of nitrogen content on tensile ductility of the studied solution annealed steels: a) elongation to fracture and b) reduction of area.

Annealing the steels at 450 °C did not have any major effect on the yield and ultimate tensile strength, or the tensile ductility, except in the steel containing 0,3 wt-% N. The effect of isothermal annealing at 450 °C on the strength properties of the studied steels is shown in Figure 44. Practically speaking, neither the yield nor the ultimate tensile strength of the steels are affected by annealing at 450 °C. The only exception is SMO 0,3N, for which annealing at 450 °C for 500 h increases the yield strength by about 40 - 80 MPa, Table 8. The ultimate tensile strength of SMO 0,3N, however, is not significantly affected by annealing at 450 °C for 500 h.

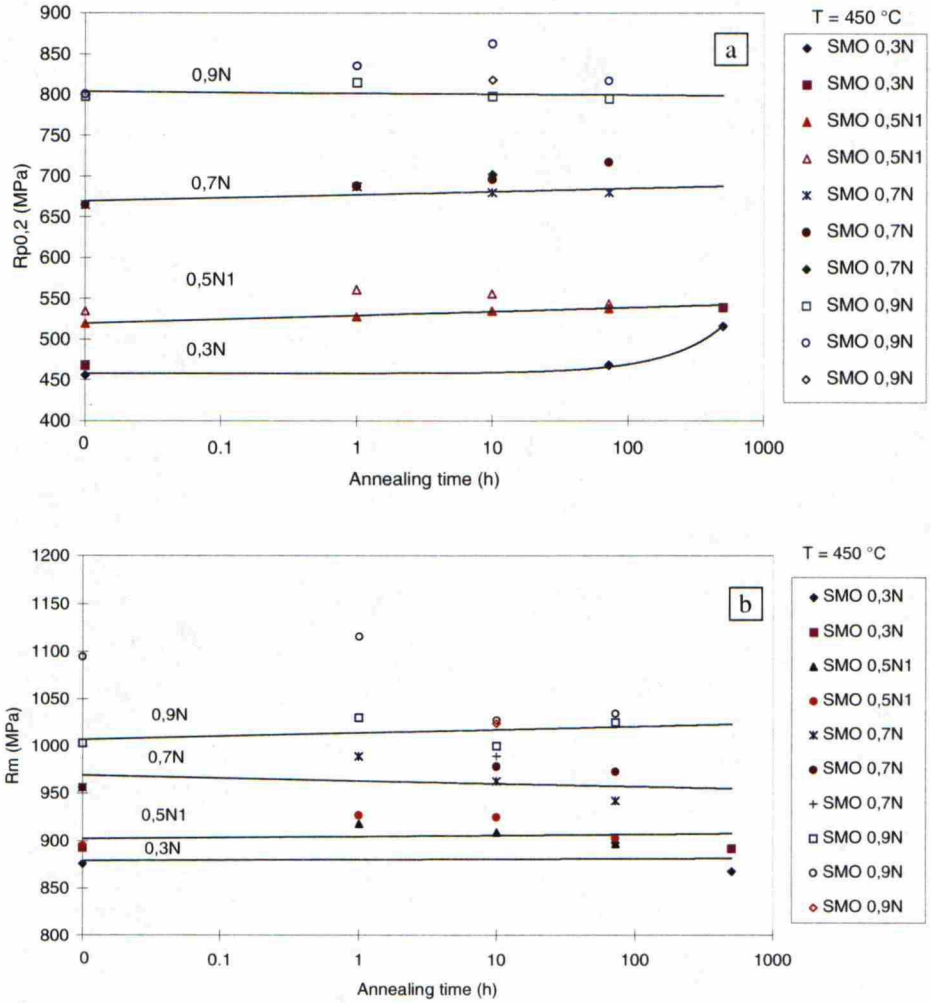

Figure 44. The effect of isothermal annealing at 450 °C on yield strength a) and ultimate tensile strength b) of the studied steels.

The effect of isothermal annealing at 450 °C on the tensile ductility of the studied steels is shown in Figure 45. Both elongation to fracture and reduction of area are not, in general, significantly affected by annealing at 450 °C. However, it can be noticed that annealing for 500 h at 450 °C clearly reduces the tensile ductility of SMO 0,3N. The values of elongation to fracture are decreased to about 30 % and the values of reduction of area are decreased to about 60 % of the originally rather high values of the solution annealed steel. Already after 72 h of annealing at 450 °C, the tensile ductility of SMO 0,3N is reduced to some degree.

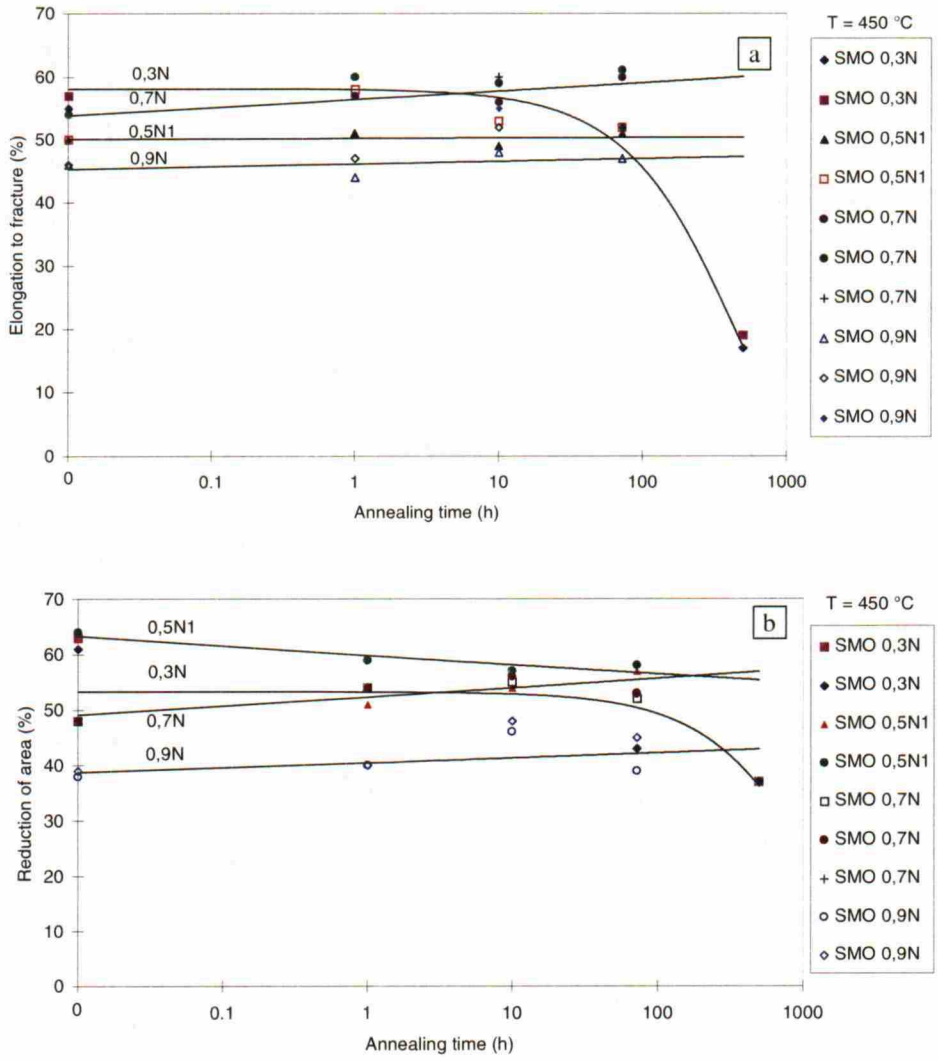

Figure 45. The effect of isothermal annealing at 450 °C on a) elongation to fracture and b) reduction of area of the studied steels.

The effect of isothermal annealing at 750 °C on the tensile properties of the studied steels depended upon the nitrogen content of the steel. The effect of isothermal annealing at 750 °C on the yield and ultimate tensile strength of the studied steels is shown in Figure 46 and in Table 8. The yield strength of SMO 0,3N and SMO 0,5N2 increases with increasing annealing time, whereas that of SMO 0,7N is practically unaffected by the annealing. The yield strength of SMO 0,9N decreases first, i.e., after 1 h of annealing, after which it remains basically at the same level. The effect of annealing at 750 °C on the ultimate tensile strength is, in general, the same as on the yield strength of the studied steels. The ultimate tensile strength of SMO 0,9N, however, decreases with increasing annealing time up to 72 h. Also, the ultimate tensile strength of SMO 0,3N decreases

after 1 to 10 h of annealing at 750 °C, but begins to increase slightly as the annealing time is increased up to 72 h.

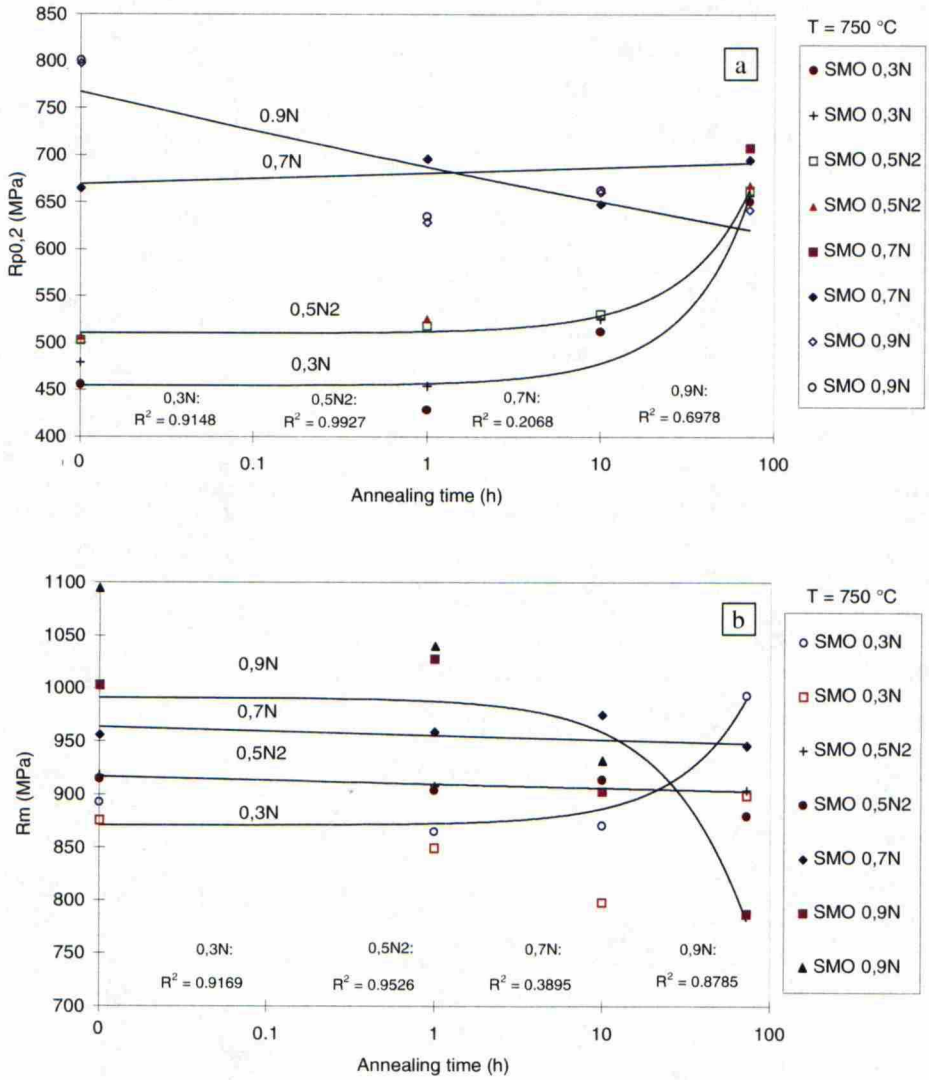

Figure 46. Effect of isothermal annealing at 750 °C on a) yield strength and b) ultimate tensile strength of the studied steels.

The effect of isothermal annealing at 750 °C on tensile ductility is shown in Figure 47. Both elongation to fracture and reduction of area decrease for all the steels with increasing annealing time at 750 °C. The decrease in tensile ductility with increasing annealing time is the smaller the higher the nitrogen content of the steel is. The effect of nitrogen content on the decrease of tensile ductility is clearer in the case of reduction of area, than in the case of elongation to fracture. When

the tensile ductility values, especially the reduction of area values, for the steels annealed at 750 °C for 1 h are compared with those of the solution annealed steels, Table 8, it can be noticed that they are on the same level, or slightly lower. In general, for the steels annealed at 750 °C for 1 h, as the nitrogen content of the steel increases, the tensile ductility values are first lower, but approach and finally reach the values of the respective solution annealed steels.

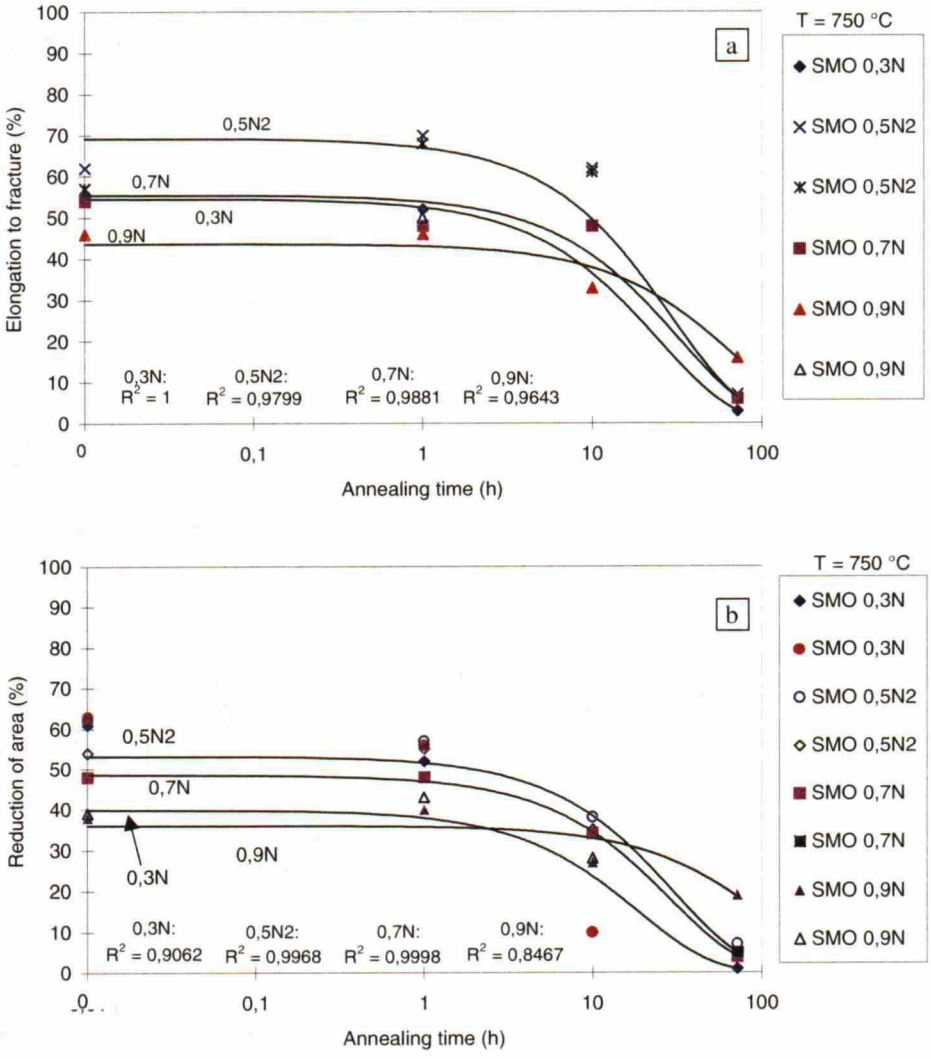

Figure 47. The effect of isothermal annealing at 750 °C on a) elongation to fracture and b) reduction of area of the studied steels.

The fracture surfaces of the solution annealed steels with 0,3 and 0,9 wt-%N are shown in Figure 48. The fracture surfaces of all of the solution annealed steels are characterized by more or less ductile fracture. However, the fracture surface of the solution annealed steel with 0,9 wt-%N

contained few isolated areas of brittle fracture, Figure 48. Also, it seems that although the fracture is ductile, it has propagated intergranularly in addition to transgranular propagation. In steels with nitrogen contents lower than 0,9 wt-%N, the amount of intergranular fracture is much lower, or it was not observed at all. The fracture surfaces of the solution annealed steels with 0,7 and 0,9 wt-%N showed that fracture took place additionally, to some extent, along prior powder particle boundaries.

Figure 49 shows the fracture surfaces of the tensile specimens of the steel with 0,3 wt-%N in the solution annealed condition, as well as for the sample solution annealed and subsequently isothermally annealed at 450 °C for 500 h. The fracture surface of the steel annealed at 450 °C is characterized by a ductile fracture coexisting with areas having a brittle appearance. For the other steels isothermally annealed at 450 °C, no major differences between their fracture surfaces and that of the solution annealed steel samples were observed.

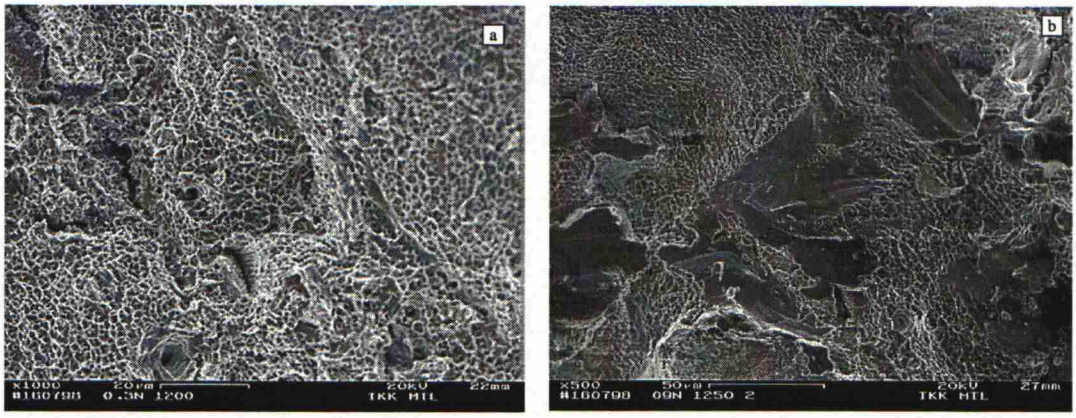

Figure 48. Fracture surfaces of tensile samples of studied solution annealed steels: SMO 0,3N a) and SMO 0,9N b).

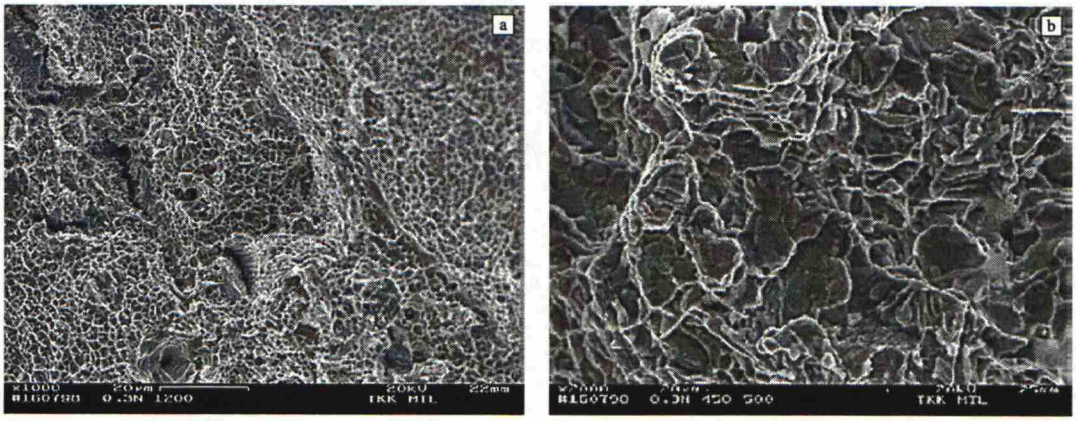

Figure 49. Fracture surfaces of solution annealed a) and for 500 h at 450 °C annealed b) SMO 0,3N.

The fracture surface of the tensile specimen of the steel with 0,5 wt-%N annealed at 750 °C for 1 h, is shown in Figure 50. The fracture surface of the steel consists of transgranular ductile areas and intergranular brittle areas. The fracture surfaces of the other steels annealed at 750 °C for 1 h were similar to that in Figure 50.

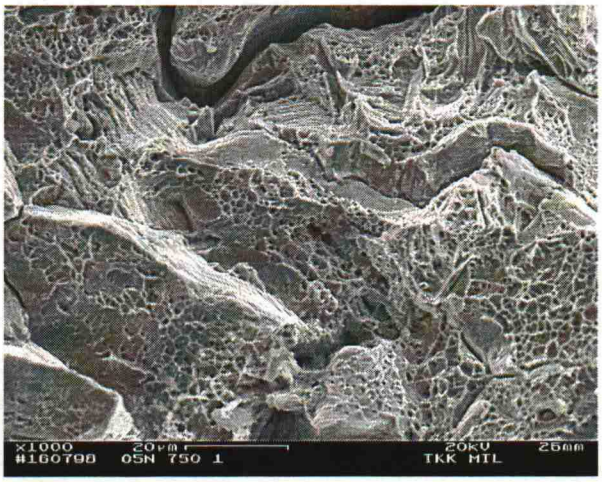

Figure 50. Fracture surface of tensile sample of SMO 0,5N annealed at 750 °C for 1 h.

The fracture surfaces of all of the steels isothermally annealed at 750 °C were characterized, in general, by a gradual change from ductile to brittle fracture mode with increasing annealing time. When the fracture surfaces of the different steels annealed at 750 °C were compared, it was observed that the higher the nitrogen content of the steel, the higher the amount of ductile fracture as the annealing time increased. It was also observed for all of the steels, that as the annealing time at 750 °C increased, the amount of intergranular cracking increased due to an increasing amount of brittle intermetallic phases and Cr_2N at the grain boundaries. Similarly, the amount of transgranular fracture through the regions containing high amounts of intermetallic phases and Cr_2N, increased with increasing annealing time at 750 °C. It was also characteristic, that as the nitrogen content of the steel increased, the fracture morphology changed from both inter- and transgranular to mainly intergranular, when the annealing time was prolonged up to 72 h, Figure 51. In Appendix F the fracture surfaces of the other solution annealed and steels annealed at 750 °C are shown.

Figure 51. Fracture surfaces of tensile samples of the studied steels with 0,3 wt-%N a) and 0,7 wt-%N b) isothermally annealed at 750 °C for 72 h.

4.4.2 Impact toughness

Charpy-V impact test results for the solution annealed steels and steels subsequently isothermally annealed at 450 and 750 °C, are shown in Table 9. The impact energy of the solution annealed steels as a function of nitrogen content is shown in Figure 52. Measurements from earlier studies (Romu et al., 1997) of the steels made on specimens with dimensions of 10 x 10 x 55 mm^3, are also included in Figure 52. The impact energy of the steels increases first as the nitrogen content increases from 0,3 wt-%N to 0,5 - 0,6 wt-%N, but then decreases as the nitrogen content of the steel increases beyond 0,6 wt-%N.

Table 9. Results of Charpy-V impact tests at +20 °C for the studied steels (specimen size: 7,5 x 10 x 55 mm^3).

Material	Heat treatment	Impact energy at +20 °C (J)
SMO 0,3N	1200 °C/1 h	64
	1200 °C/1 h + 450 °C/10 h	66
	1200 °C/1 h + 450 °C/72 h	73
	1200 °C/1 h + 450 °C/500 h	49
	1200 °C/1 h + 750 °C/1 h	23
	1200 °C/1 h + 750 °C/10 h	8
	1200 °C/1 h + 750 °C/72 h	3
SMO 0,5N1	1200 °C/1 h	82,112
	1200 °C/1 h + 450 °C/1 h	92,110
	1200 °C/1 h + 450 °C/10 h	106, 107
	1200 °C/1 h + 450 °C/72 h	89,115
	1200 °C/1 h + 450 °C/500 h	98, 100
	1200 °C/1 h + 750 °C/1 h	55, 59
	1200 °C/1 h + 750 °C/10 h	4, 4
	1200 °C/1 h + 750 °C/72 h	3
SMO 0,7N	1225 °C/1 h	42, 42
	1225 °C/1 h + 450 °C/1 h	43, 43, 43, 56
	1225 °C/1 h + 450 °C/10 h	47, 47, 47, 61
	1225 °C/1 h + 450 °C/72 h	45, 50
	1225 °C/1 h + 750 °C/1 h	14, 20
	1225 °C/1 h + 750 °C/10 h	4, 4
	1225 °C/1 h + 750 °C/72 h	3
SMO 0,9N	1250 °C/1 h	33, 34, 35
	1250 °C/1 h + 450 °C/1 h	38, 40
	1250 °C/1 h + 450 °C/10 h	31, 32, 36, 46
	1250 °C/1 h + 450 °C/72 h	39
	1250 °C/1 h + 450 °C/500 h	50
	1250 °C/1 h + 750 °C/1 h	7, 8
	1250 °C/1 h + 750 °C/10 h	3, 3
	1250 °C/1 h + 750 °C/72 h	2
SMO 1,15N	1250 °C/1 h	4, 4

The effect of isothermal annealing at 450 °C on the impact energy of the studied steels is shown in Figure 53. Annealing at 450 °C for up to 72 h had no effect on the impact energy of the studied steels. With the exception of SMO 0,3N, isothermal annealing at 450 °C for up to 500 h did not have an effect on the impact toughness of the studied steels. For SMO 0,3N the impact energy value was decreased, but not as clearly as in the case of the tensile ductility, Table 9.

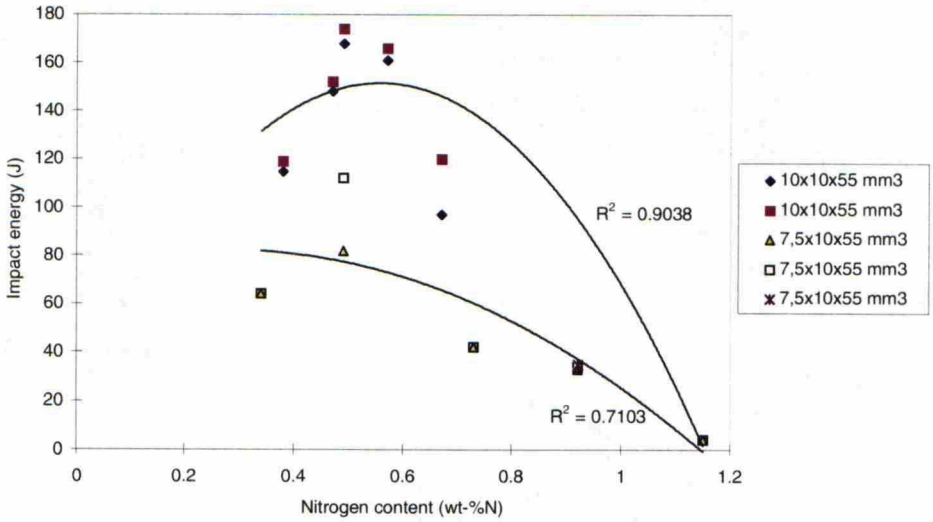

Figure 52. Effect of nitrogen content on impact energy of studied solution annealed steels. Upper curve is for samples with the dimensions of $10x10x55mm^3$ and lower curve for samples with the dimensions of $7,5x10x55\ mm^3$.

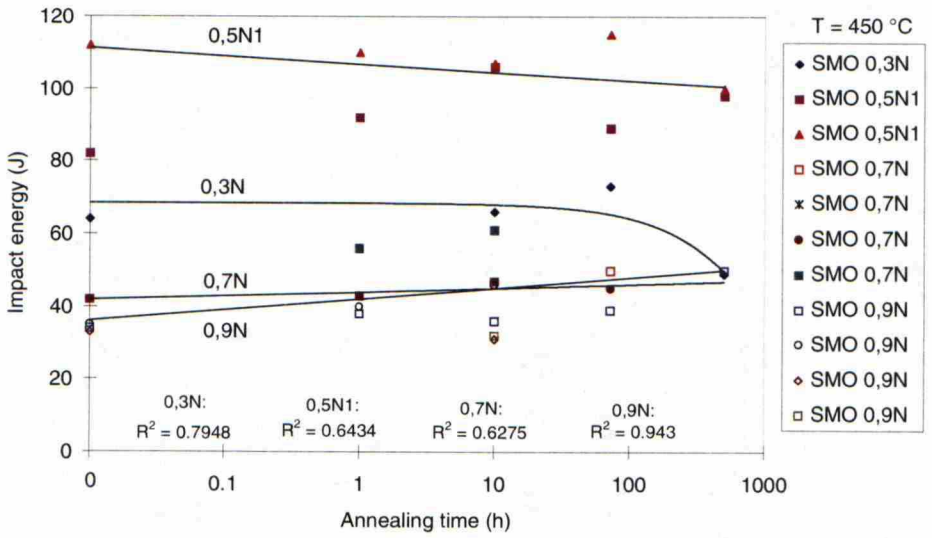

Figure 53. The effect of isothermal annealing at 450 °C on impact energy of the studied steels at +20 °C.

The effect of isothermal annealing at 750 °C on the impact energy of the studied steels is shown in Figure 54. Isothermal annealing at 750 °C deteriorated the impact toughness of the steels of this study. It seems that as the nitrogen content of the steel increases the decrease in impact toughness becomes slower. However, the effect of the nitrogen content of the steel on the decrease in impact energy is not very pronounced. The effect of isothermal annealing at 750 °C for 1 h on the

average impact energy as a percentage of that of solution annealed steel, is shown in Figure 55. The smallest decrease takes place for SMO 0,5N1, and there is no correlation between the decrease in the impact toughness and the nitrogen content of the steel. For longer annealing times at 750 °C, no major differences between the materials could be observed, Table 9. The biggest decrease in impact energy is for SMO 0,9N, and the smallest decrease is for SMO 0,5N1.

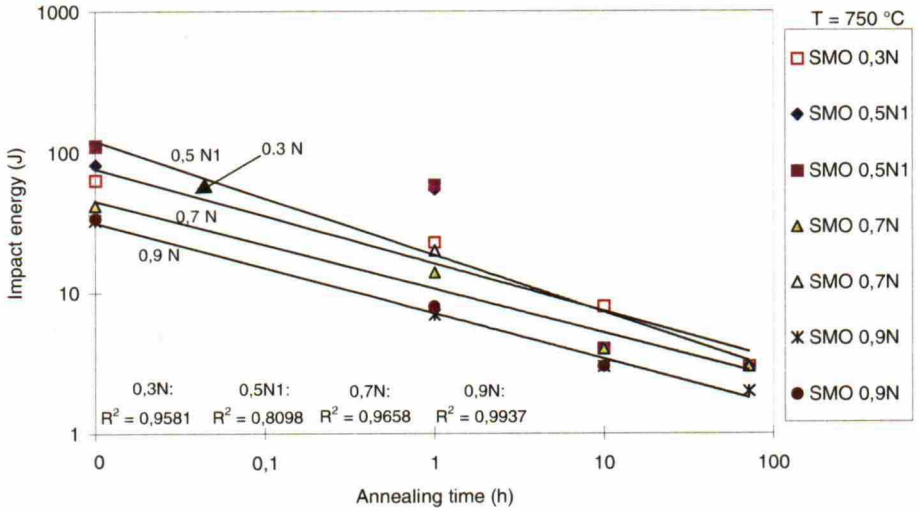

Figure 54. The effect of isothermal annealing at 750 °C on impact energy of the studied steels at +20 °C.

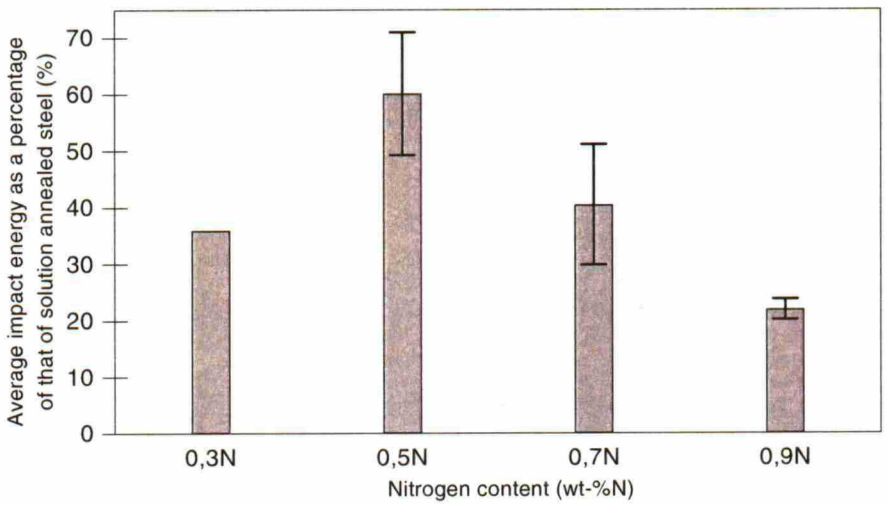

Figure 55. The effect of isothermal annealing at 750 °C for 1 h on average impact energy as a percentage of that of solution annealed steel at +20 °C.

The fracture surface morphology of the solution annealed steels varied with the nitrogen content of the steel. As the nitrogen content of the steel increased, the fracture mode changed from a

mainly ductile fracture, to a combination of ductile and brittle fracture, Figure 56. This combination of ductile and brittle fracture consists of fracture morphology that exhibits brittle-like fracture, but the fracture surfaces have a dimple-like appearance. On the fracture surfaces of the solution annealed steels with 0,3 and 0,5 wt-%N, small areas of brittle fracture were observed. It was also observed that fracture had propagated along prior powder particle boundaries to some extent, and that its amount was highest in the steels with 0,7 and 0,9 wt-%N.

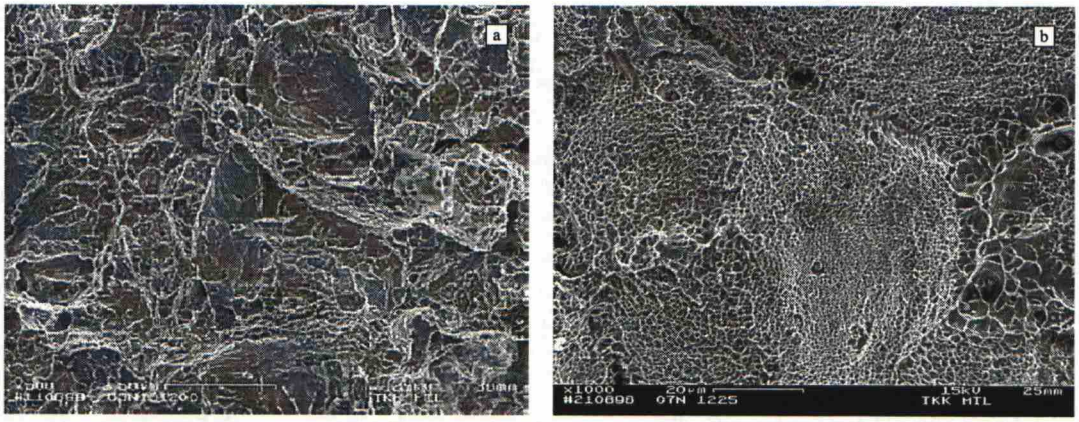

Figure 56. Fracture surfaces of impact test samples of studied solution annealed steels with 0,3 wt-%N a) and 0,7 wt-%N b).

The fracture surfaces of solution annealed and further at 450 °C for 500 h annealed steels with 0,3 wt-%N, are shown in Figure 57. The fracture surface of both the solution annealed steel and the steel subsequently annealed at 450 °C for 500 h, was observed to consist of ductile and brittle fracture.

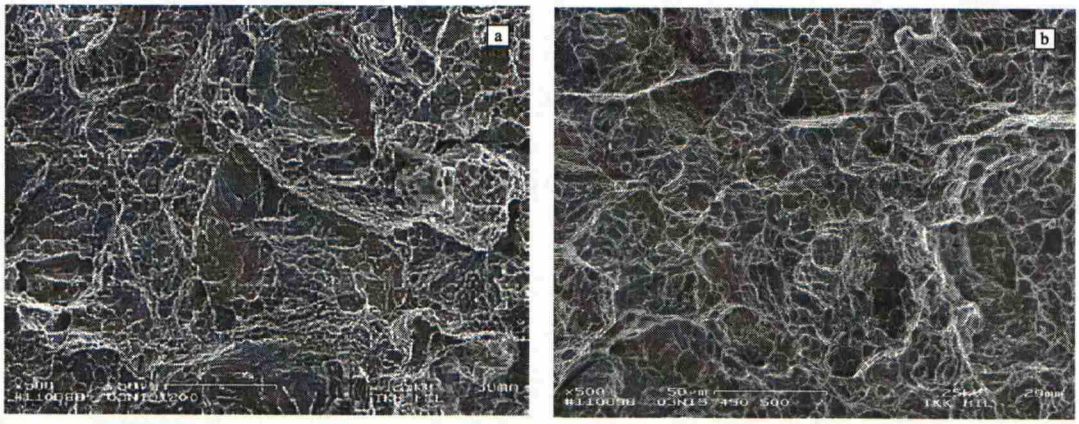

Figure 57. The fracture surfaces of solution annealed a) and at 450 °C for 500 h annealed b) steel with 0,3 wt-%N.

The fracture surfaces of the studied steels annealed at 750 °C showed an increasing amount of brittle fracture and a decreasing amount of ductile fracture as the annealing time increased.

Additionally, the higher the nitrogen content of the steel, the higher was the amount of ductile fracture with increasing annealing time at 750 °C. The fracture surface of the steel with 0,9 wt-%N annealed at 750 °C for 72 h still had a small amount of ductile fracture, whereas the fracture surfaces of the other steels were completely brittle, Figure 58. It was also characteristic, that as the nitrogen content of the steel increased, the fracture morphology changed from both inter- and transgranular to mainly intergranular, Figure 58. The amount of ductile fracture in the impact samples annealed at 750 °C was clearly lower than that in the respective tensile samples. In Appendix G, the fracture surfaces of the other solution annealed and at 750 °C annealed steels are shown.

Figure 58. Fracture surfaces of impact samples of steels SMO 0,5N1 a) and SMO 0,9N b) annealed isothermally at 750 °C for 72 h.

4.4.3 Hardness measurements

The results of the hardness measurements are shown in Table 10. Hardness as a function of the nitrogen content of the solution annealed steel is shown in Figure 59. Hardness increases with increasing nitrogen content in the solution annealed steel. Isothermal annealing at 450 °C for up to 500 h clearly increased the hardness of the steel with 0,3 wt-%N, but not the hardness of the steels with higher nitrogen contents, Figure 60. Isothermal annealing of the steels at 750 °C increased the hardness of all of the steels as the annealing time increased, Figure 60. After 1 h of annealing, the hardness of the steels was not, in general, affected very much as compared to the hardness of the respective solution annealed steels. However, as the annealing time at 750 °C increased, the hardness of all of the steels clearly increased.

Table 10. Results of hardness measurements of the studied steels in solution annealed as well as solution annealed and subsequently isothermally at 450 and 750 °C annealed condition.

Material	Heat treatment	Hardness (HV 30)	Average hardness (HV 30)
SMO 0,3N	1200 °C/1 h	281, 282, 284, 286, 290	285
	1200 °C/1 h + 450 °C/1 h	235, 238, 241, 242, 251	241
	1200 °C/1 h + 450 °C/10 h	232, 237, 238, 239, 246	238
	1200 °C/1 h + 450 °C/72 h	236, 237, 238, 242, 242	239
	1200 °C/1 h + 450 °C/500 h	339, 341, 345, 346, 350	344
	1200 °C/1 h + 750 °C/1 h	235, 245, 250, 253, 258	248
	1200 °C/1 h + 750 °C/10 h	278, 278, 281, 283, 285	281
	1200 °C/1 h + 750 °C/72 h	373, 377, 380, 381, 382	379
SMO 0,5N1	1200 °C/1 h	222, 232, 239, 247, 249	238
	1200 °C/1 h + 450 °C/1 h	243, 245, 248, 252, 254	248
	1200 °C/1 h + 450 °C/10 h	238, 245, 246, 247, 248	245
	1200 °C/1 h + 450 °C/72 h	259, 268, 276, 276, 280	272
	1200 °C/1 h + 450 °C/500 h	272, 276, 279, 279, 285	278
	1200 °C/1 h + 750 °C/1 h	242, 243, 244, 250, 253	246
	1200 °C/1 h + 750 °C/10 h	312, 313, 317, 320, 320	316
	1200 °C/1 h + 750 °C/72 h	384, 386, 386, 387, 394	387
SMO 0,7N	1225 °C/1 h	302, 312, 324, 333, 342	322
	1225 °C/1 h + 450 °C/1 h	259, 266, 267, 268, 308	273
	1225 °C/1 h + 450 °C/10 h	268, 277, 279, 288, 290	280
	1225 °C/1 h + 450 °C/72 h	332, 341, 346, 351, 360	346
	1225 °C/1 h + 450 °C/500 h	302, 303, 306, 315, 319	309
	1225 °C/1 h + 750 °C/1 h	366, 367, 368, 372, 377	370
	1225 °C/1 h + 750 °C/10 h	380, 382, 383, 385, 389	384
	1225 °C/1 h + 750 °C/72 h	381, 384, 387, 394, 394	388
SMO 0,9N	1250 °C/1 h	288, 290, 295, 296, 307	295
	1250 °C/1 h + 450 °C/1 h	313, 317, 320, 321, 324	319
	1250 °C/1 h + 450 °C/10 h	317, 349, 350, 357, 360	347
	1250 °C/1 h + 450 °C/72 h	342, 343, 344, 345, 347	344
	1250 °C/1 h + 450 °C/500 h	334, 351, 355, 360, 375	355
	1250 °C/1 h + 750 °C/1 h	296, 297, 299, 300, 302	299
	1250 °C/1 h + 750 °C/10 h	302, 315, 320, 323, 325	317
	1250 °C/1 h + 750 °C/72 h	364, 380, 388, 392, 394	384
SMO 1,15N	1250 °C/1 h	398, 409, 415, 433, 434	418

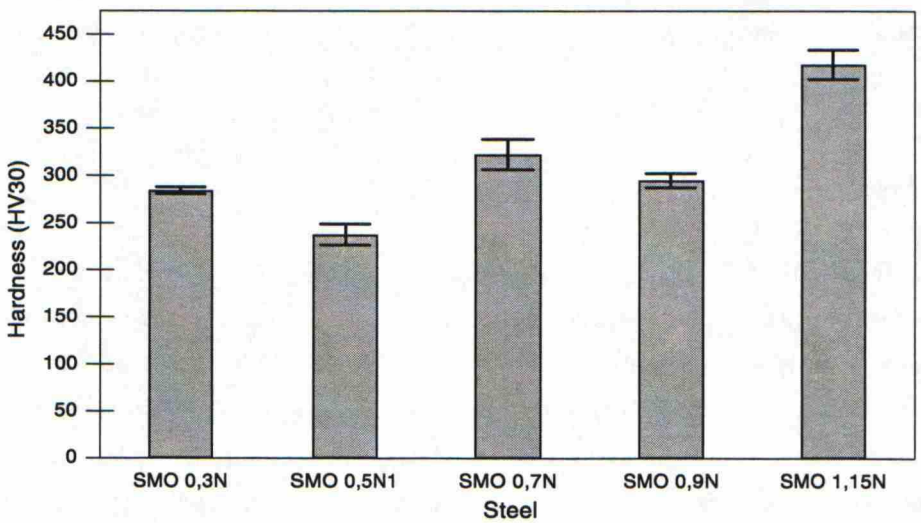

Figure 59. Hardness of the studied steels in the solution annealed condition.

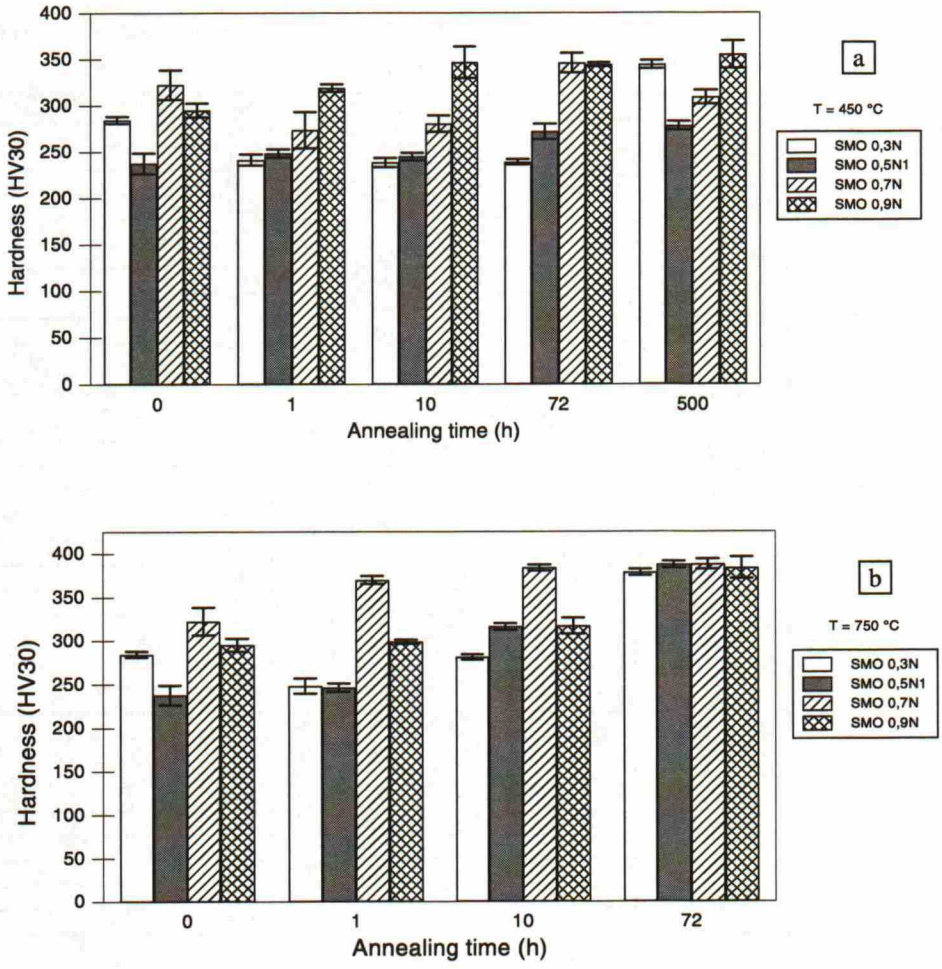

Figure 60. Effect of isothermal annealing at 450 °C a) and 750 °C b) on average hardness (HV30) of the studied steels.

4.5 Localized corrosion resistance

The results of pitting and crevice corrosion tests for the solution annealed steels and those further isothermally annealed at 450 °C and 750 °C, are shown in Table 11. The localized corrosion resistance of the solution annealed steels was high, Figure 61. In Figure 61, results from earlier studies (Romu et al., 1996; 1997) made on these steels are also shown. The critical pitting corrosion temperature of the solution annealed steels of this study was, in general, ≥ 97,5 °C. Variation in the test results becomes almost negligible when the nitrogen content of the steel is 0,5 - 0,9 wt-%N. The critical crevice corrosion resistance of the studied solution annealed steels depends upon the

nitrogen content of the steel. The highest critical crevice corrosion temperatures are achieved when the nitrogen content of the steel is about 0,5 - 0,7 wt-%N. Both the pitting and the crevice corrosion resistance of the steel with 1,15 wt-%N is deteriorated.

Table 11. Localized corrosion resistance in 6 % $FeCl_3$ solution (ASTM G48 and ASTM G76) of the studied solution annealed as well as solution annealed and isothermally at 450 °C and 750 °C annealed steels.

Material	Heat treatment	Critical pitting corrosion temperature (°C)	Critical crevice corrosion temperature (°C)
SMO 0,3N	1200 °C/1 h	≥ 97,5, ≥ 97,5	55, 62,5, 67,5
	1200 °C/1 h + 450 °C/1 h	90, 92,5	62,5, 65
	1200 °C/1 h + 450 °C/10 h	92,5, 95	60, 65
	1200 °C/1 h + 450 °C/72 h	90, 92,5	52,5, 60, 70
	1200 °C/1 h + 450 °C/500 h	85, 90	45, 52,5
	1200 °C/1 h + 750 °C/1 h	20	22,5, 30
	1200 °C/1 h + 750 °C/10 h	20, 20	10, 12,5
	1200 °C/1 h + 750 °C/72 h	10, 27.5	5, 7,5
SMO 0,5N1	1200 °C/1 h	70, 74	72,5, 80
	1200 °C/1 h + 450 °C/1 h	70, 72,5	72,5, 75
	1200 °C/1 h + 450 °C/10 h	75, 77,5	62,5, 75
	1200 °C/1 h + 450 °C/72 h	75, 75	60, 67,5, 67,5, 80
	1200 °C/1 h + 450 °C/500 h	40, 47,5, 50, 82,5	47,5, 55, 60, 72,5
	1200 °C/1 h + 750 °C/1 h	30, 42,5	25, 30
	1200 °C/1 h + 750 °C/10 h	15, 20	10, 17,5
	1200 °C/1 h + 750 °C/72 h	15, 15	5, 5
SMO 0,7N	1225 °C/1 h	≥ 97,5, ≥ 97,5	75, 80
	1225 °C/1 h + 450 °C/1 h	≥ 97,5, ≥ 97,5	67,5, 77,5
	1225 °C/1 h + 450 °C/10 h	≥ 97,5, ≥ 97,5	67,5, 67,5
	1225 °C/1 h + 450 °C/72 h	≥ 97,5, ≥ 97,5	67,5, 70
	1225 °C/1 h + 450 °C/500 h	≥ 97,5, ≥ 97,5	67,5, 75
	1225 °C/1 h + 750 °C/1 h	30, 40	15, 32,5, 35
	1225 °C/1 h + 750 °C/10 h	12,5, 22,5, 32,5	5, 12,5
	1225 °C/1 h + 750 °C/72 h	10,17,5, 25	10, 20
SMO 0,9N	1250 °C/1 h	≥ 97,5, ≥ 97,5	67,5, 67,5
	1250 °C/1 h + 450 °C/1 h	≥ 97,5, ≥ 97,5	65, 65
	1250 °C/1 h + 450 °C/10 h	≥ 97,5, ≥ 97,5	67,5, 72,5
	1250 °C/1 h + 450 °C/72 h	≥ 97,5, ≥ 97,5	67,5, 72,5
	1250 °C/1 h + 450 °C/500 h	≥ 97,5, ≥ 97,5	70, 75
	1250 °C/1 h + 750 °C/1 h	32,5, 45, 52,5	32,5, 42,5, 55
	1250 °C/1 h + 750 °C/10 h	15, 37,5	12,5
	1250 °C/1 h + 750 °C/72 h	7,5, 12,5	7,5, 17,5
SMO 1,15N	1250 °C/1 h	< 5	< 5

With the exception of the steels with 0,3 and 0,5 wt-% N, isothermal annealing at 450 °C for up to 500 h did not have an effect on the resistance to localized corrosion in the steels of this study. In the case of the steels with 0,3 and 0,5 wt-%N, both pitting and crevice corrosion resistance was decreased, especially for the steel with 0,5 wt-%N. However, both the crevice and pitting corrosion resistance of those steels remained practically unaffected by isothermal annealing at 450 °C for up to 72 h, as can also be seen in Figure 62. As can be seen in Table 10, there are large variations in the test results of the steel with 0,5 wt-%N which was annealed at 450 °C for 500 h.

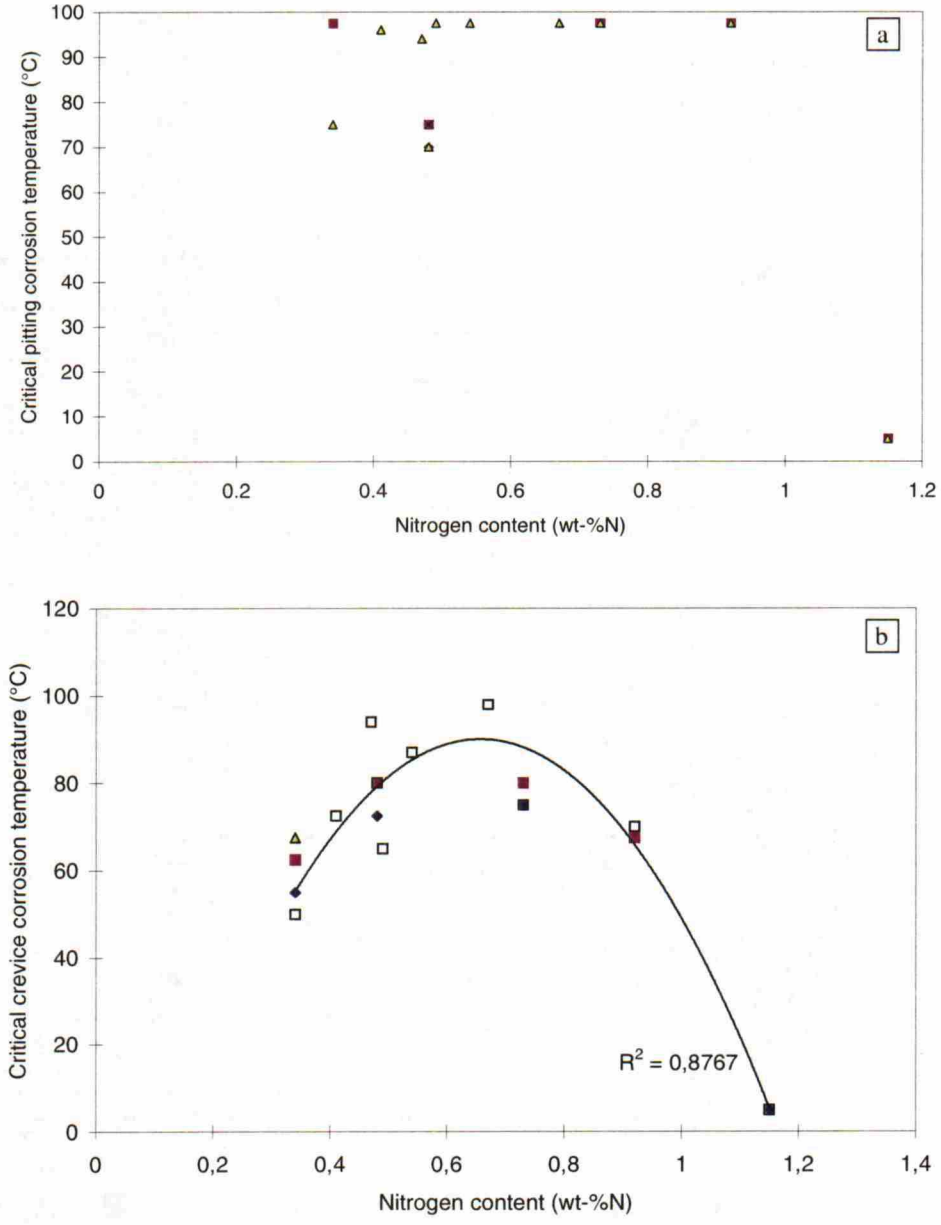

Figure 61. Pitting a) and crevice b) corrosion resistance of the studied solution annealed steels in 6 % $FeCl_3$ solution (modified ASTM G48 and ASTM G76).

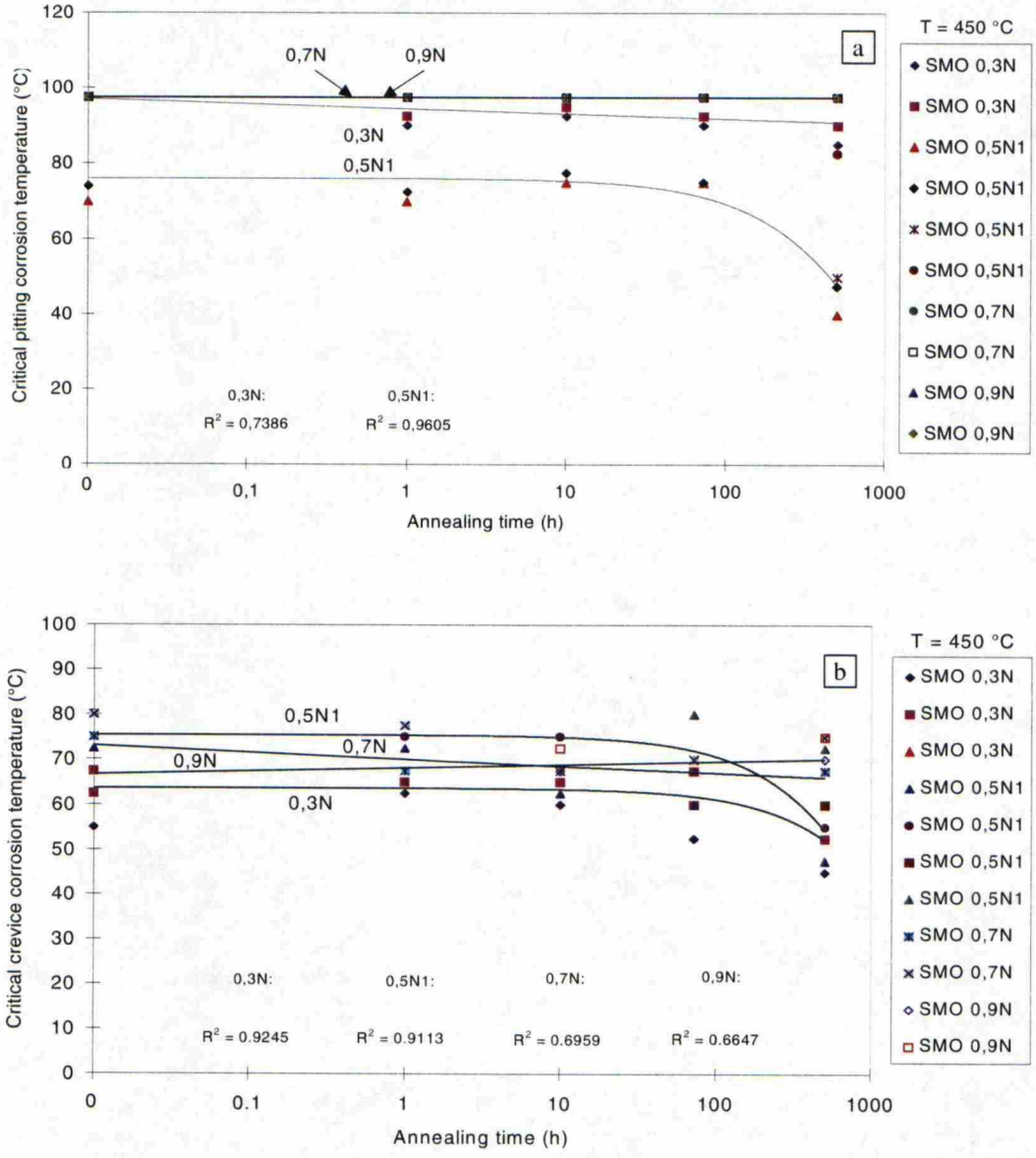

Figure 62. The effect of isothermal annealing at 450 °C on a) pitting corrosion resistance and b) crevice corrosion resistance of the studied steels in 6 % $FeCl_3$ solution (modified ASTM G48 and ASTM G76).

The adverse effect of isothermal annealing at 750 °C on the localized corrosion resistance of the studied steels is clear already after 1 h of annealing. Both the pitting and crevice corrosion resistance decreased with increasing holding time at 750 °C, as shown in Figure 63. Both the pitting and crevice corrosion resistance seem to decrease, in general, with increasing annealing time, the more slowly the higher the nitrogen content of the steel is. This is especially true for crevice

corrosion resistance. The crevice corrosion resistance of the steel with 0,9 wt-% N seems to decrease more slowly than that of the other steels do as the holding time at 750 °C increases, Figure 63. The difference is more clear, when the crevice corrosion resistance of the studied steels annealed at 750 °C for 1 h are compared.

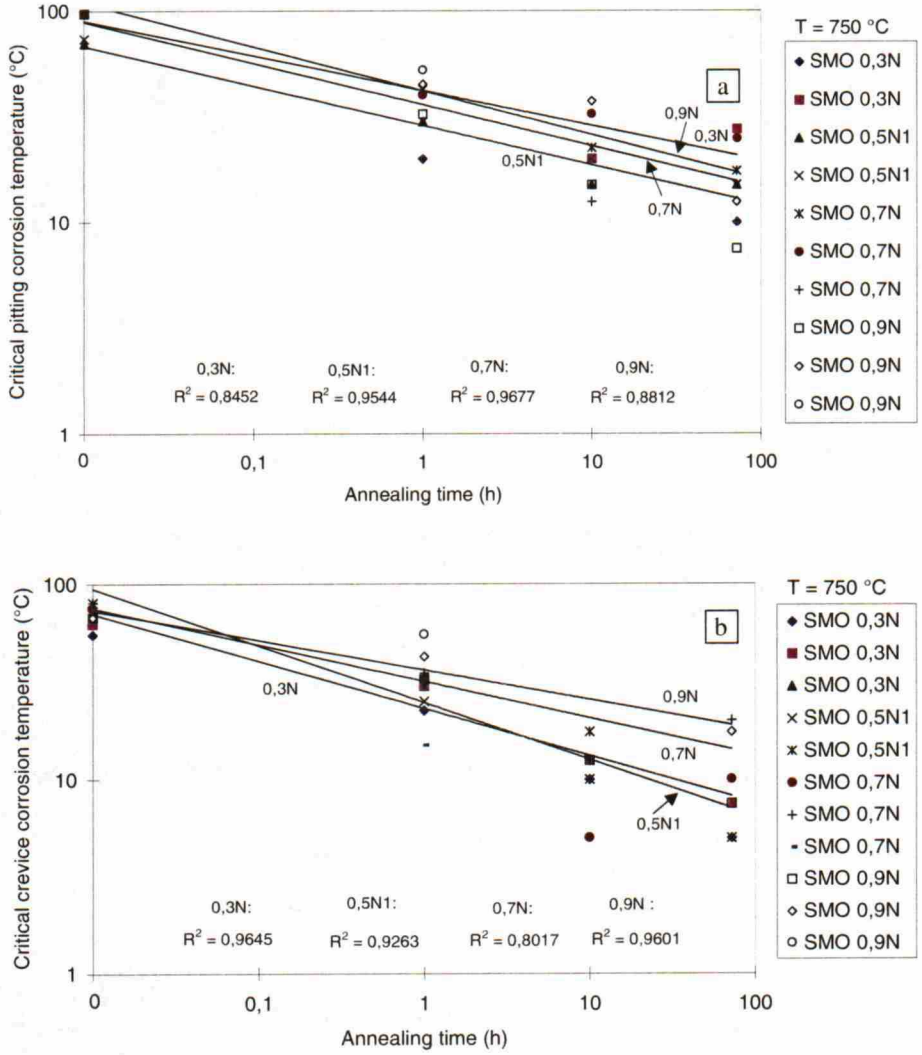

Figure 63. The effect of isothermal annealing at 750 °C on a) pitting corrosion resistance and b) crevice corrosion resistance of the studied steels in 6 % $FeCl_3$ solution (modified ASTM G48 and ASTM G76).

5 DISCUSSION

In this chapter the experimental findings of the work are discussed and they are compared with previously published studies. The types and mechanisms of precipitation reactions taking place in the powder metallurgically manufactured nitrogen alloyed austenitic stainless steels during solution annealing and subsequent isothermal annealing, are discussed. The effects of nitrogen content on the mechanical properties and corrosion resistance of the solution annealed steels and steels subsequently isothermally annealed at 450 °C and 750 °C are considered in detail.

5.1 Fluidised bed furnace nitriding of powders

The effect of average particle size on the nitriding behaviour of the gas atomized powders can be explained by the specific surface area of the powder particles. The smaller the particle size is the larger the specific surface area of the powder particles, and therefore, the higher the resulting nitrogen content. As the average particle size decreases, there is more surface area for nitrogen atoms to diffuse into the powder particles, and thus, the nitrogen content of the powder increases. The thickness of the surface oxide film on the powder particles may also influence the particle size effect on the nitrogen content of the powder. It has been reported for water atomized austenitic stainless steel powders, that as the particle size decreases, the thickness of the surface oxide layer decreases (Nyborg et al., 1990). It has also been reported, that according to ESCA- and Auger-analyses for gas atomized martensitic steel powders, the surface oxide thickness of the powder particles is independent of the particle size (Nyborg and Olefjord, 1988). Similar results have been obtained for gas atomized AISI 304L powder (Bracconi and Gasc, 1994). Therefore, as the thickness of the oxide layers on the surface of the as-atomized powder particles has not been determined quantitatively as a function of particle size, the effects of the oxide layers on the kinetics of nitrogen absorption into the gas atomized powder particles in this study cannot be discussed in more detail.

The increase in the oxygen content of the powders during/after fluidised bed nitriding is a result of an increase in the amount of surface oxides. Surface oxidation most likely takes place during the nitriding treatment due to insufficient gas shielding of the powder batch in the fluidised bed furnace chamber. The oxides on the surfaces of the powder particles have been reported earlier to be mainly Cr- and Mn-oxides, or combinations thereof (Romu, 1994; Romu et al., 1996). However, the origin of the oxygen contamination is not known precisely, and therefore, a more thorough investigation on the factors affecting the purity of the nitriding atmosphere is needed. It is

possible that the dew point of the nitriding atmosphere is not low enough and thus, oxides are formed on the surface of the powder particles during nitrogen absorption. Nitrides also form on the surface layers of the powder particles, due to the relatively high amounts of nitrogen present at the surface (Romu, 1994; Romu et al., 1996).

The effect of the average powder particle size on the oxygen content of the fluidised bed nitrided powders can be explained in the same way as for the nitrogen content of the powder particles. As the average particle size of the powder decreases, the higher the specific surface area of the powder and, consequently, more oxygen can diffuse into the surface layers of the powder particles. It should be pointed out, however, that the oxygen content of the powders, as well as that of the HIPed samples, is not only a result of the surface oxide films of the powder particles. The powder particles also contain inclusions, which are usually Si- and Al-oxides or their combinations, and which may also contain some other impurity elements. These inclusions are most likely entrapped into the molten steel from the refractory linings of the melt crucible of the gas atomizing equipment. The entrapment of inclusions within the powder may also explain the deviation of the oxygen content in the powder particle size range 297 - 420 μm from the general trend shown in Figure 19. However, metallographical analyses did not reveal the reason for the above mentioned deviation, i.e., the powder particles in the particle size range 297 - 420 μm did not contain a higher amount of oxide inclusions as compared to other particle size ranges. Surface oxidation during nitriding is not likely to cause the deviation, since no deviation in the nitrogen content of the powder particles as a function of powder particle size range was observed.

5.2 Microstructure

The microstructures of the solution annealed steels varied with the nitrogen content of the steels. The steels with 0,3 and 0,5 wt-%N were observed to contain σ phase at the grain boundaries of an otherwise austenitic matrix. The steels with 0,7 and 0,9 wt-%N were fully austenitic and did not contain any precipitates. The σ phase at the grain boundaries of the steels with ≤ 0,5 wt-%N is formed due to their high chromium and molybdenum contents, which makes it difficult to avoid σ phase precipitation during cooling from the solution annealing temperatures. Nitrogen has been explained to retard the precipitation of intermetallic phases during the manufacturing of austenitic stainless steels. In this study, it seems, that the nitrogen content of the steels had to be ≥ 0,5 wt-%N in order to avoid σ-phase precipitation during water quenching. The intergranular precipitates observed with both optical microscopy and TEM in the steel with 1,15 wt-%N, were Cr_2N. Cr_2N precipitated due to the nitrogen content of the steel exceeding the nitrogen solid solubility limit.

Isothermal annealing for 500 h at 450 °C resulted in both σ and Laves phase precipitation in the steels containing ≤ 0,5 wt-% N. This is due firstly to the fact that these steels contain small, isolated σ phase particles on the grain boundaries already in the solution annealed condition thus providing favorable conditions for the further growth of the σ phase with increased annealing time. Secondly, it seems that there is a high driving force for σ and Laves phase precipitation already at 450 °C, especially in the steel with 0,3 wt-%N, due to high chromium and molybdenum contents of the steels. In steels with > 0,5 wt-% N, intermetallic phase precipitation was not observed during annealing at 450 °C. It is believed to be due to the combination of two factors. Firstly, due to the high nitrogen content of the steels they do not contain intermetallic phases in the solution annealed condition. Secondly, the high nitrogen content of the steels results in retardation intermetallic phase precipitation during annealing at 450 °C.

At 750 °C, intermetallic phases such as σ and Laves phase are precipitated both inter- and intragranularly in all the steels due to the high amounts of chromium and molybdenum of the steels and due to the high driving force for their precipitation. It is also possible that χ phase may have precipitated in the steels. It is difficult to distinguish whether an intermetallic phase is either σ or χ phase, if a clear diffraction pattern cannot be obtained. Also, it is well known that the Fe-, Cr- and Mo-contents of σ phase can vary in a wide range, which further complicates the identification of the precipitated phases. However, in the TEM-analyses χ phase was not observed to have precipitated in the steels. In steels containing ≤ 0,5 wt-% N, Cr_2N was not generally observed to precipitate at 750 °C (only one isolated particle most likely being Cr_2N was found from the steel with 0,3 wt-%N in TEM-analyses), whereas in steels with > 0,5 wt-%N, Cr_2N precipitated both inter- and intragranularly in addition to intermetallic phases. In the samples analysed, the amount of Cr_2N increased with increased annealing time at 750 °C. This can be explained by the higher driving force for the precipitation of intermetallic phases than that for Cr_2N precipitation in the steels with < 0,5 wt-% N, whereas in steels with > 0,5 wt-% N, the driving force for Cr_2N precipitation increases enough to cause Cr_2N to precipitate in addition to the intermetallic phases.

The total amount of precipitates in the steels annealed at 750 °C was observed to decrease with increasing nitrogen content of the steel, according to optical microscopy and TEM. The amount of intragranular precipitates in the steels annealed for 72 h was especially the lower, the higher the nitrogen content of the steel was. Also, for the shorter annealing times at 750 °C, the amount of grain boundary precipitation decreased with increasing nitrogen content of the steel. This is a result of the retarding effect of nitrogen on the precipitation of intermetallic phases becoming more pronounced as the nitrogen content of the steel increases, despite of the increasing amount of Cr_2N precipitation.

The Cr_2N precipitation in the steels annealed at 750 °C was both inter- and intragranular. Precipitation of Cr_2N began intergranularly at short annealing times, but as the annealing time increased, the amount of intragranular precipitation increased. Precipitation began intergranularly because grain boundaries are the energetically most favourable sites for precipitation to take place, and subsequently, precipitation continued intragranularly at annealing twins or at other favorable structural irregularities, such as oxides etc.. Cellular precipitates, i.e., precipitates consisting of lamellae of Cr_2N and austenite having lower nitrogen and chromium content than the supersaturated austenite, were not observed. This is consistent with observations of Simmons (1995A) and Simmons et al. (1996B) for a high nitrogen steel (Fe-19Cr-5Mn-5Ni-3Mo-0,69N) and Rayaprolu et al. (1988; 1989) for a steel with lower nitrogen content (Fe-21Cr-12Ni-5Mn-2Mo-0,2Nb-0,2V-0,24N). Taillard et al. (1999) have also observed similar results for a high nitrogen austenitic stainless steel (Fe-18Cr-19Mn-0,9N). According to Simmons (1995A) and Rayaprolu et al. (1988; 1989) cellular precipitation of Cr_2N was not observed to take place at all or was observed only in extremely small quantities in nitrogen alloyed austenitic stainless steels isothermally annealed below 900 - 1000 °C. According to Taillard et al. (1999) cellular precipitation takes place in nitrogen alloyed austenitic stainless steels at temperatures above 800 °C. It seems, however, that the temperature range for cellular precipitation decreases with increasing nitrogen content of the steel. In this study, a strong tendency for intermetallic phase precipitation and the low annealing temperature of 750 °C seemed to inhibit cellular precipitation of Cr_2N. In general, when compared to the studies by Simmons (1995A), Simmons et al. (1996B), Rayaprolu et al. (1988; 1989) and Taillard et al. (1999), the tendency for intermetallic phase precipitation is stronger in the studied steels due to their higher chromium and molybdenum contents.

In steels with > 0,5 wt-%N, precipitation of σ phase was not observed after 1 h of annealing at 750 °C, whereas after 72 h of annealing it was observed to have precipitated. Some σ phase was, however, observed after 1 h of annealing at 750 °C in steels with $\leq$ 0,5 wt-% N. Thus, increasing nitrogen content of the steel retards the precipitation of σ phase and stabilizes Laves phase during annealing at 750 °C. Similar trend has been observed in the studies by Jargelius-Petterson (1994; 1996) for steels with the nominal composition of 20Cr-18Ni-(0,2-10)Mn-4,5Mo-(0,03-0,5)N. In her study it was observed that, as the nitrogen content of the steel increased, precipitation of σ phase was retarded and χ and Laves phase were stabilized when the steels were annealed at 700 and 900 °C. Brandis et al. (1976A) have observed, that nitrogen alloying retards σ phase precipitation and stabilizes χ phase precipitation in steels with the nominal composition of 24,5Cr-17Ni-5,5Mn-3,2Mo-0,18Nb-(0,33-0,44N)). Retardation of σ phase and stabilization of Laves phase precipitation with increasing nitrogen content of the steel, when the steels of this study were annealed at 750 °C for 1 h, can be possibly explained by Cr_2N precipitation. As Cr_2N precipitated in steels with 0,7 and

0,9 wt-%N, chromium was consumed from the surrounding austenite matrix. Since σ phase contains high amounts of chromium, its precipitation then becomes more difficult. At the same time, the molybdenum content of the austenite matrix is increased locally and the precipitation of Laves phase then becomes easier. Additionally, allthough Cr_2N precipitation consumes nitrogen from the austenite matrix, it seems that the nitrogen content of the matrix is still high enough to delay σ phase precipitation. However, the actual mechanism how nitrogen retards σ phase precipitation remained unclear. Laves phase and Cr_2N were observed to precipitate adjacent to each other at the grain boundaries in the steel with 0,7 wt-%N after 1 h of annealing at 750 °C. This can be explained by the fact, that at the same time, as Laves phase is precipitated intergranularly, the nitrogen concentration adjacent to it increases and facilitates Cr_2N precipitation. The reason for the nitrogen content to increase adjacent to the Laves phase, is the low solubility of nitrogen in the Laves phase.

The reason for intragranular precipitation of Cr_2N adjacent to Laves phase in the steel with 0,9 wt-%N, can most likely also be explained by the above mentioned mechanisms, i.e., due to molybdenum enrichment in the austenite matrix adjacent to Cr_2N precipitates and nitrogen enrichment adjacent to Laves phase. It seems that, although the nitrogen content of the austenite matrix decreases due to Cr_2N precipitation, the nitrogen content of the austenite matrix is high enough to delay σ phase precipitation and to make the precipitation of Laves phase more favorable. As Laves phase is precipitated, the nitrogen concentration adjacent to it increases and facilitates Cr_2N precipitation. The concurrent precipitation of Laves and Cr_2N is similar to the interactive and alternating formation of σ phase and Cr_2N in nitrogen alloyed austenitic stainless steels during cooling from solution annealing temperature described by Uggowitzer et al. (1996). In that study, the molybdenum content of the steel was lower, and thus, the precipitation of Laves phase was not favored over σ phase. Jargelius-Petterson (1994) observed that Cr_2N and Laves phase or χ and Laves phase precipitate intragranularly in clusters in an austenitic stainless steel with the nominal composition of 20Cr-18Ni-4,5Mo-10Mn-0,49N when isothermally annealed at 900 °C. Thier et al. (1969) have also observed intragranular clusters of Cr_2N and Laves phase in a steel with the nominal composition of 17Cr-13Ni-5Mo-0,25N isothermally annealed at 550 - 1000 °C.

In Table 12 the precipitated phases and the time needed for their appearance in the studied steels are compared with those in austenitic stainless steels with lower alloying element content reported in the literature are shown. As can be seen, intermetallic phase precipitation in the studied steels takes place faster than in steels with lower contents of alloying elements. The time for the onset of Cr_2N precipitation in the studied steels with 0,7 and 0,9 wt-%N is in the same range as reported in the literature for steels with similar nitrogen contents.

Table 12. Intermetallic phase and Cr_2N precipitation and time needed for their appearance during isothermal annealing at 700 - 800 °C in the studied steels and in steels reported in the literature.

Steel	Precipitating phases	Temperature (°C)/time	Reference
SMO 0,3N	σ, Laves	750/1 h	-
SMO 0,5N1	σ, Laves	750/1 h	-
SMO 0,7N	Laves, Cr_2N	750/1 h	-
SMO 0,9N	Laves, Cr_2N	750/1 h	-
17Cr-13Ni-5Mo-0,145N (0,05C)	Laves	750/100 h	Thier et al., 1969
	$M_{23}C_6$	750/30 min	
	M_6C	750/1 h	
17Cr-13Ni-5Mo-0,25N (0,05C)	Laves	750/200 h	Thier et al., 1969
	$M_{23}C_6$	750/50 min	
	M_6C	750/1 h	
24,5Cr-17Ni-5,5Mn-3,2Mo-0,18Nb-0,33N	χ	750/20 h	Brandis et al., 1976A
	σ	750/100 h	
	Cr_2N	750/100 h	
24,5Cr-17Ni-5,5Mn-3,2Mo-0,18Nb-0,41N	χ	750/5h	Brandis et al., 1976A
	σ	750/100 h	
	Cr_2N	750/100 h	
	Z phase (NbCrN)	750/1 h	
24,5Cr-17Ni-5,5Mn-3,2Mo-0,18Nb-0,44N	χ	750/5 h	Brandis et al., 1976A
	σ	750/100 h	
	Cr_2N	750/100 h	
	Z phase (NbCrN)	750/1 h	
Fe-17Cr-9Mn-4,4Ni-0,27N	Cr_2N	750/20 min	Mielityinen-Tiitto, 1979
25Ni-21Cr-6Mo-(0,14-0,19)N	χ	750/15 min	Heubner et al., 1989
18Ni-20Cr-6Mo-0,21N	χ	750/15 min	Heubner et al., 1989
Fe-19Cr-5Mn-5Ni-3Mo-0,69N	Cr_2N	700/5 min	Covino et al., 1997
	Laves	750/20 h	
Fe-18Cr-19Mn-0,9N	Cr_2N	800/< 1 h	Taillard et al., 1999
	intermetallic phases	not precipitated after 50 h at 800 °C	

5.3 Dilatometric analyses

In the dilatometric analyses it was observed that according to the derivative dilatometry the expansion rate of all the studied steels was slowed down during heating beginning at about 420 - 450 °C and about 720 - 750 °C and had their minima at 550 - 600 °C and 950 °C, respectively. At about 720 - 750 °C, it was due to precipitation of intermetallic phases and Cr_2N, depending on the nitrogen content of the steel. As precipitation processes take place in the studied steels, the length of the sample increases more slowly with the increasing temperature, since alloying elements (Cr, Mo, Fe, N) are removed from the lattice and are forming different compounds.

The heating and cooling (shrinking) curves for the studied steels were observed to be similar to each other indenpendently of the nitrogen content of the steel. This can be explained by the effect of nitrogen content on the elastic constants of austenitic stainless steels. These constants are determined by the interatomic force constants and are nearly independent of the nitrogen content of the steel (Ledbetter and Austin, 1985). Nitrogen lowers the elastic stiffness of AISI type 304 austenitic stainless steel by approximately 0,5 % per atomic per cent of solute. According to Ledbetter and Austin (1985), it means, that other interatomic force constants determined physical constants, such as thermal expansivity and specific heat, are also nearly independent of the nitrogen content of the steel. This explains why there are no significant differences between the heating and cooling curves of the studied steels.

At 450 °C no massive formation of either intermetallic phases or Cr_2N is believed to take place, since the time for which the studied samples were at 400 - 500 °C was rather short. It remained unclear what is exactly taking place in the above mentioned temperature range. One explanation is that, internal stresses formed in water quenching of the samples from the solution annealing temperature, were relaxed.

In the isothermal analyses at 450 °C for up to 72 h no major differences between the materials were observed. Dilatation in all the steels first decreased until changes in it became negligible. This is due to the fact that neither intermetallic phases nor Cr_2N were observed to have precipitated in the steels according to microstructural analysis after 72 h of annealing. It is believed, that if the annealing had been continued up to 500 h, differences between the steels may have been observable.

In the isothermal analyses at 750 °C for up to 72 h, it was observed that dilatation decreased constantly with increasing annealing time for all of the studied steels. This is due to the precipitation of intermetallic phases or intermetallic phases and Cr_2N, depending on the nitrogen content of the steel. It was also observed that, in general, the decrease in dilatation depended on the nitrogen content of the steel. As the nitrogen content of the steel increased, the decrease in dilatation with increasing annealing time became slower. This is related to the type and amount of precipitates forming in the steels during annealing at 750 °C. In steels with < 0,5 wt-%N, intermetallic phases were observed to be the main precipitating phases, and Cr_2N was observed to precipitate only as very few isolated particles. In steels with > 0,5 wt-%N, Cr_2N was observed to precipitate in addition to intermetallic phases, and the amount of Cr_2N increased with increasing nitrogen content of the steel. Although Cr_2N precipitates with increasing nitrogen content of the steel, the retarding effect of nitrogen alloying on intermetallic phase precipitation is also increased. Results of optical microscopy and TEM analyses support this theory. The exception to the above mentioned discussion is the behaviour of the steel with 0,3 wt-%N, having the slowest decrease in dilation with

increasing annealing time. This could be possibly explained by the σ phase observed in the steel after solution annealing affecting the nucleation and growth of the intermetallic phases during isothermal annealing.

5.4 Effect of precipitates on mechanical properties

5.4.1 Tensile properties

In this chapter the effect of the nitrogen content on the tensile properties of solution annealed and the steels further annealed at 450 °C and 750 °C are discussed. The chapter is divided into two sections: strength properties and ductility.

Strength properties

Solution annealed nitrogen alloyed austenitic stainless steels have high tensile properties. Yield and ultimate tensile strength values of the steels increase with increasing nitrogen content of the steel, which is due to solid solution strengthening and grain boundary hardening. Additionally, nitrogen alloying has been observed to enhance the grain size hardening effect (Norström, 1977; Sandström and Bergqvist, 1977; Byrnes et al., 1987; Werner, 1988; Tervo, 1998). In this study the increase in the yield and ultimate strength values with increasing nitrogen content of the steel is due to solid solution strengthening for the steels with 0,3 - 0,9 wt-%N, since they all have similar grain size (30 - 33 μm). The yield strength of the steel with 1,15 wt-%N increased only a little from the values for the steel with 0,9 wt-%N. This can be explained based on the following arguments. Firstly, the Cr_2N precipitates observed in the steel after solution annealing are not able to increase the yield strength effectively. Cr_2N precipitated in the steel with 1,15 wt-%N, due to the nitrogen content exceeding nitrogen solubility in the steel. Secondly, the grain size of the steel with 1,15 wt-%N is larger (48 μm) than that of the other steels (30 - 33 μm), which means that grain size hardening effect is less pronounced in the steel with 1,15 wt-%N. Thirdly, nitrogen solubility in the steel at the solution annealing temperature (1250 °C) used in this study seems to be close to 0,9 wt-%N and thus, further nitrogen alloying does not increase solid solution strengthening. According to Tervo (1998) Cr_2N precipitates were also found in TEM analyses in similar steels with 0,67 and 0,91 wt-%N, but in small amounts and as small isolated precipitates. In that study, Cr_2N began to precipitate as the nitrogen content of the steel was ≥ 0,67 wt-%N. In the TEM analyses of this study, however, no signs of Cr_2N precipitation were observed even in the steel with 0,9 wt-%N. The solution annealing temperature in the earlier study of Tervo (1998) was lower (1175 °C; in this study for the steel with 0,7 wt-%N it was 1225 °C) and the chromium, manganese and molybdenum

contents were somewhat lower than in the steels of this study. This means, that nitrogen solubility was higher in the steels of this study than in those of Tervo (1998).

The increase in the yield strength of the steel with 0,3 wt-% N as a result of isothermal annealing for up to 500 h at 450 °C, is due to the precipitation of σ and Laves phase at the grain boundaries. The increase in yield strength is due to dispersion strengthening effect of the precipitates, which is more effective than the loss of solid solution strengthening by chromium and molybdenum.

The yield and ultimate tensile strength of the studied steels were observed to increase, decrease or remain practically unaffected by isothermal annealing at 750 °C, depending on the nitrogen content of the steel. In steels with ≤ 0,5 wt-% N, Cr_2N was not, in general, observed to precipitate, at least not in large amounts. Isolated particles (only one particle was found in the TEM-analyses) of Cr_2N had precipitated in the steel with 0,3 wt-%N as a result of annealing at 750 °C for up to 72 h, but it is believed that Cr_2N does not have any major effect on tensile properties of the steel. It is most likely that solid solution strengthening due to interstitially dissolved nitrogen was not lost, and the increase in the strength properties was due to the precipitation of intermetallic phases during isothermal annealing at 750 °C. In the steel with 0,7 wt-% N, Cr_2N was observed to precipitate, and therefore, the solid solution strengthening effect of nitrogen was partially lost. The loss in strength due to decreased solid solution strengthening by nitrogen is believed to be more or less compensated for by precipitation of Cr_2N and intermetallic phases, which explains why the strength properties remain unaffected by isothermal annealing at 750 °C. Similar behavior has been observed by Simmons (1995A) for a steel with a nominal composition of Fe-19Cr-5Mn-5Ni-3Mo-0,69N. The loss in the strength properties of the steel with 0,9 wt-% N is most likely due to the more severe decrease of solid solution strengthening by nitrogen due to Cr_2N precipitation which could not be compensated for by Cr_2N and intermetallic phase precipitation. Similar behavior was observed by Taillard et al. (1999) for the yield strength of a steel with nominal composition of Fe-18Cr-19Mn-0,9N annealed at 800 °C for up to 50 h.

Ductility

Tensile ductility of the solution annealed steels is at a relatively high level, which is typical for P/M austenitic stainless steels. The decrease in tensile ductility of the steels, especially when the nitrogen content of the steel was ≥ 0,7 wt-%N, is due to the fact that, as the nitrogen content of the steels becomes high enough the ductile-to-brittle transition temperature approaches room temperature. The tensile ductility of the steel with 1,15 wt-%N is deteriorated due to Cr_2N precipitation at the grain boundaries. The oxygen content of the steels HIPed from fluidized bed furnace nitrided powders (0,7, 0,9 and 1,15 wt-%N) was higher due to surface oxidation of the

powders, which increased the amount of fracture along prior particle boundaries, and thus decreased the tensile ductility of the steels somewhat. However, the amount of fracture along prior particle boundaries was not observed to be very high. The differences in the fracture surfaces of the tensile samples of solution annealed steels can also be explained by the effect of the nitrogen content of the steel on their fracture behavior, i.e., ductile-to-brittle transition temperature approaches room temperature as the nitrogen content of an austenitic stainless steel increases high enough. Therefore, the appearance of small areas of brittle fracture in the steel containing 0,9 wt-%N, as well as the fracture surface of the steels with 0,7 and 0,9 wt-%N showing a combination of brittle and ductile fracture, is due to the ductile-to-brittle transition temperature raising due to increasing nitrogen content of the steel.

The decrease in the tensile ductility of the steel with 0,3 wt-%N annealed at 450 °C for 500 h, is due to the brittle intergranular σ and Laves phase, which could be observed as brittle areas in the fracture surface of the steel.

The tensile ductility of all of the steels decreased due to precipitation of intermetallic phases or Cr_2N and intermetallic phases during annealing at 750 °C. The positive effect of increasing nitrogen content of the steel, on the decrease of tensile ductility resulting from isothermal annealing at 750 °C, can be explained by three mechanisms. Firstly, as the nitrogen content of the steel increases > 0,5 wt-%N, Cr_2N precipitation takes place, and the decrease in tensile ductility is slower. This could mean, that Cr_2N precipitates are less harmful for tensile ductility than the intermetallic phase precipitates. Secondly, as Cr_2N is precipitating, the nitrogen content of the remaining austenite matrix decreases. Therefore, ductility of the austenite matrix is likely to increase due to the ductile-to-brittle transition phenomenon. Thirdly, and most likely, although Cr_2N is precipitating, the nitrogen content in the solid solution of the steels still remains high enough to retard intermetallic phase precipitation. Especially, the amount of intragranular precipitation was observed to decrease with increasing nitrogen content of the steel. Additionally, the retarding effect of nitrogen on intermetallic phase precipitation seems to be more effective the higher the nitrogen content of the steel is, despite Cr_2N precipitation. This is most likely due to the amount of interstitially dissolved nitrogen of the austenite matrix remaining high enough, despite Cr_2N precipitation. The fracture surfaces of the tensile samples were observed to contain an increasing amount of ductile areas with increasing nitrogen content of the steel as the annealing time at 750 °C increased. This supports the above mentioned explanations, but whether it was due to any of the mechanisms described above alone or if all of them were involved simultaneously, could not be determined by fractography.

The tensile ductility values of the steels annealed at 750 °C for 1 h were at the same level, or slightly lower than those of the solution annealed steels. It is most probable that tensile ductility is

not very sensitive to small amounts of intergranular precipitates. The observed trend of the tensile ductility values of the steels annealed for 1 h at 750 °C being lower at first, but approaching and finally reaching the values of the respective solution annealed steels as the nitrogen content of the steel increases, can be explained by the amount and type of intergranular precipitation in the steels. As observed by the microstructural analysis using optical microscopy and TEM, the amount of intergranular precipitation of the steel annealed at 750 °C for 1 h decreased with increasing nitrogen content of the steel. In the microstructural analysis it was also observed that, as the nitrogen content of the steel annealed for 1 h at 750 °C increased > 0,5 wt-%N, the precipitation of σ phase in the steel was delayed. Therefore, it seems that σ phase is more detrimental than Cr_2N when tensile ductility is considered.

The tendency to intergranular cracking with increasing annealing time at 750 °C, increased as a function of the amount of intermetallic phases and Cr_2N at the grain boundaries. The amount of transgranular fracture also increased with increasing annealing time at 750 °C, and was due to an increased amount of intragranular precipitation of intermetallic phases and Cr_2N. The amount of transgranular fracture was more pronounced in the steels with ≤ 0,5 wt-%N than in steels with higher nitrogen content. This is due to the smaller amount of intragranular precipitation in the steels with > 0,5 wt-%N. Both fracture mechanisms are similar to those observed by Simmons (1995A) for a steel with nominal composition of Fe-19Cr-5Mn-5Ni-3Mo-0,69N isothermally annealed at 700 and 900 °C.

5.4.2 Impact toughness

The difference in the impact toughness values and in the fracture surface appearance of the impact toughness samples of solution annealed steels can be explained in the same way as in the case of the tensile test samples. As the nitrogen content of the steel increases, the amount of brittle fracture increases because the ductile-to-brittle transition temperature approaches room temperature. The fracture surface of the steel with 0,3 wt-%N also contained brittle areas, which are due to the intergranular σ phase observed in the TEM analyses. The steels of this study contained high amounts of Ni (21 - 22 wt-%) and some Mn (1,9 - 3,5 wt-%). According to Uggowitzer et al. (1992) and Ilola et al. (1996) the ductile-to-brittle transition is more pronounced in Mn alloyed than in Ni alloyed austenitic stainless steels, where the decrease in impact toughness with decreasing temperature is less pronounced. Additionally, according to Uggowitzer et al. (1992) the ductile-to-brittle transition temperature and deterioration of impact toughness increase with increasing nitrogen content of the steel. Therefore, it seems that the relatively small amount of manganese together with the high nitrogen content is capable of decreasing the impact toughness of the steel at room temperature, despite its high nickel content. Therefore, the impact toughness of the solution

annealed steels decreases as their nitrogen content increases. The fracture appearance of the impact toughness samples of the solution annealed steels showed crack propagation along prior particle boundaries. This was more pronounced in the steels HIPed from fluidized bed furnace nitrided powders which had oxidised more during the nitriding treatments. As a result, the impact toughness of the steels with 0,7 and 0,9 wt-%N is reduced somewhat due to oxide inclusions on the prior particle boundaries. The ductile-to-brittle transition temperature of nitrogen alloyed austenitic stainless steels has been observed to slightly increase with decreasing grain size of the steel, which is opposite to the case of ferritic steels (Tomota and Endo, 1990). The grain sizes of the studied steels were small (30 - 33 μm), and comparable to those in the study of Tomota and Endo (1990). Therefore, it is possible that the decrease in impact toughness of the studied steels, especially of the steels with 0,7 and 0,9 wt-%N, can be at least partly explained by the effect of the small grain size of the steels increasing the ductile-to-brittle transition temperature. The low impact toughness of the steel with 1,15 wt-%N is due to the above mentioned mechanisms and additionally due to the intergranular Cr_2N precipitates.

If the values of tensile ductility and impact toughness of the solution annealed steels are compared, it can be observed that the decrease in the tensile ductility values is smaller than that of the impact toughness values. According to Uggowitzer et al. (1992), and Simmons et al. (1996), the ductile-to-brittle transition temperature is lower in the tensile test as compared with impact toughness testing due to the lower strain rate during tensile testing.

The reason for the decrease in impact toughness of the steel with 0,3 wt-%N as a result of annealing at 450 °C for 500 h, is intergranular precipitation of brittle σ and Laves phases during annealing. This could be seen in the TEM, and in SEM analyses of the fracture surfaces of the impact test samples.

The decrease in the impact toughness values of the steels annealed at 750 °C for 1 h as compared to those of the solution annealed steels (average impact energy as a percentage of that of solution annealed steel, Figure 55) was observed to vary depending on the nitrogen content of the steel, but no clear trend was observed. It seems that, although the amount of intergranular precipitation decreases with increasing nitrogen content of the steel, the decrease in impact toughness does not follow this trend. That means that it is not only the amount of intergranular precipitation, but also the type of the intergranular precipitates that determines the decrease in impact toughness values from those of the solution annealed steels. Microstructural analyses showed that, after 1 h of annealing at 750 °C only intermetallic phases (σ and Laves phase) precipitated in steels with ≤ 0,5 wt-%N, whereas in the steels with > 0,5 wt-%N, Cr_2N and Laves phase precipitated (no σ phase was observed). Thus, it seems that Cr_2N precipitation is more detrimental than intermetallic phases when the impact toughness of the steels is considered.

The nitrogen content of the steel was not observed to have any clear effect on the decrease in impact toughness after annealing at 750 °C for a time over 1 h. It seems that both Cr_2N and intermetallic phases are detrimental to the impact toughness of the studied steels, and that no difference in their effect on impact toughness can be determined. Similar results have been observed by Brandis et al., 1976B) for a steel with the nominal chemical composition of 24,5Cr-17Ni-5,5Mn-3,2Mo-0,18Nb-(0,33-0,44N)) isothermally annealed < 950 °C. This is most likely due to the fact that the amount of both intergranular Cr_2N and intermetallic phases becomes so high, that no difference in their effect on deterioration of impact toughness can be observed.

Cr_2N precipitation decreases the nitrogen content of the austenite matrix in steels with 0,7 and 0,9 wt-% N, and should result in an increase in the toughness of the matrix. However, this does not seem to have a positive effect on the impact toughness since no major differences in the decrease of the impact energy values of the studied steels annealed at 750 °C were observed. The amount of ductile fracture decreased in all of the steels with increasing annealing time at 750 °C, but as the annealing time at 750 °C increased up to 72 h, the amount of ductile fracture became higher as the nitrogen content of the steel increased. This can be explained by the same arguments as in the case of tensile test samples. It is due to the retardation of intermetallic phase precipitation as the nitrogen content of the steel increases, because the nitrogen content of the austenite matrix is still high enough despite the Cr_2N precipitation. Therefore, it seems that in impact toughness testing, the intergranularly precipitated brittle intermetallic phases and Cr_2N control the fracture mode, and the austenite matrix does not seem to have as great an effect as in the case of tensile tests. Although the amount of intragranular precipitation was observed to decrease with increasing nitrogen content of the steel, it seems to have no effect on the decrease in impact toughness with increasing annealing time at 750 °C.

Both inter- and transgranular cracking increased with increasing amount of precipitation as a result of annealing at 750 °C. The amount of intergranular cracking increased with increasing annealing time at 750 °C. This was due to the increasing amount of intermetallic phases, or intermetallic phases and Cr_2N at the grain boundaries, depending upon the nitrogen content of the steel. The amount of transgranular fracture increased with increasing annealing time at 750 °C, due to the increased amount of intragranular precipitation of intermetallic phases or intermetallic phases and Cr_2N depending on the nitrogen content of the steel. The amount of transgranular fracture was more pronounced in the steels with ≤ 0,5 wt-%N, than in steels with higher nitrogen content. This was due to the smaller amount of intragranular precipitation with increasing nitrogen content of the steel.

5.4.3 Hardness

The hardness of the solution annealed steels increased, in general, with increasing nitrogen content of the steel. Similar behavior has been observed by Tervo (1998) and Biancaniello et al. (1997). The high hardness of the steel with 0,3 wt-%N as compared to those of the other steels can, at least partly, be explained by the isolated brittle σ phase particles found at the grain boundaries in the steel with 0,3 wt-%N. The hardness of the steel with 1,15 wt-%N is clearly higher than that for the other steels, due to Cr_2N precipitation at the grain boundaries.

When the steels were annealed at 450 °C for 500 h, the hardness was observed to increase for the steel with 0,3 wt-%N, but not for the steels with higher nitrogen contents. The reason for the increase in the hardness of the steel with 0,3 wt-%N after 500 h of annealing at 450 °C, is the formation of σ and Laves phase in the steel. σ and Laves phase are brittle and hard phases, and although they are formed only as few isolated particles at the grain boundaries, they increase the hardness of the steels. Although σ phase was observed also to precipitate intergranularly in the steel with 0,5 wt-%N during annealing at 450 °C for up to 500 h, it seems that the amount of the isolated σ phase particles was not high enough to increase the hardness of the steel. The reason for the hardness of the steels with 0,7 and 0,9 wt-%N not increasing as a result of annealing at 450 °C for 500 h, is that neither intermetallic phases nor Cr_2N precipitated in these steels.

Annealing at 750 °C increases the hardness of all of the steels, due to the formation of intermetallic phases, or intermetallic phases and Cr_2N in the steels. The increase in the hardness of all of the steels is of the same magnitude. This means that whether the precipitating phases are merely intermetallic phases, or both intermetallic phases and Cr_2N, the increase in hardness is at practically the same level. The reason for the hardness of the steels to, in general, increase only a little from that of the solution annealed steels after 1 h of annealing at 750 °C, is most likely due to the precipitating phases being mainly intergranular. As the annealing time at 750 °C is increased up to 72 h, the amount of intergranular precipitation increases rapidly, and additionally, intragranular precipitation takes place. As intermetallic phases and Cr_2N are brittle and hard, the hardness of the steels increases with increasing amount of precipitates. When intermetallic phases and Cr_2N are precipitated, the solid solution hardening effect of the alloying elements in the austenite, especially that of nitrogen, is decreased. This decrease, however, is at least to some extent compensated for by the formation of hard precipitates.

5.5 Effect of precipitates on localized corrosion resistance

The localized corrosion resistance of the studied steels in the solution annealed condition was observed to depend upon their nitrogen content. The pitting corrosion resistance of the steels is

high, and in general, above 90 °C in the used tests. The lower pitting corrosion resistance of some of the steels with < 0,5 wt-%N can be partly explained by the observed intergranular intermetallic phases in the steels. The pitting corrosion resistance of the studied steels is best, when their nitrogen content is 0,5 - 0,9 wt-%N, i.e., in the absence of either intermetallic phases or Cr_2N in the steel. The crevice corrosion resistance of the studied steels also depends upon their nitrogen content. Crevice corrosion resistance of the steel with 0,3 wt-%N was lower than that of the other steels, due to σ phase at the grain boundaries. Steels with 0,5 - 0,7 wt-%N have the best crevice corrosion resistance, which is due to the absence of either intermetallic phases or Cr_2N. The crevice corrosion resistance of the steel with 0,9 wt-%N was somewhat lower than that of the steels with 0,5 - 0,7 wt-%N, but since it was not observed to contain Cr_2N (or intermetallic phases), the reason remains unclear. One possible explanation could be that in these localized corrosion tests the observed variation in crevice corrosion resistance results was clearly higher than in those of pitting corrosion. Both pitting and crevice corrosion resistance of the steel with 1,15 wt-%N is deteriorated due to intergranular Cr_2N precipitation, since the nitrogen content of the steel is above its solubility limit in the steel. In general, the crevice corrosion resistance of the studied steels is good due to their high amounts of chromium, molybdenum and nitrogen, and as long as intermetallic phases and/or Cr_2N are absent.

The localized corrosion resistance was observed to decrease after 500 h of annealing at 450 °C for the steels with ≤ 0,5 wt-%N, but not for the steels with > 0,5 wt-%N. The decrease of localized corrosion resistance of the steels with ≤ 0,5 wt-% N as a result of this isothermal annealing, is due to the precipitation of σ and Laves phase. As σ and Laves phase are precipitated, chromium and molybdenum contents in the austenite matrix adjacent to them are decreased. These chromium and molybdenum depleted regions are favorable sites for localized corrosion attack.

Localized corrosion of the studied steels annealed at 750 °C was deteriorated by the precipitation of intermetallic phases, or intermetallic phases and Cr_2N. The chromium, molybdenum and nitrogen contents of the austenite matrix adjacent to both Cr_2N and intermetallic phase precipitates are lowered and localized corrosion attacks these regions as has been described earlier for other nitrogen alloyed austenitic stainless steels (Jargelius-Petterson, 1996; Covino et al., 1997). The nitrogen content of the steel had no clear effect on the decrease of pitting corrosion resistance as a result of isothermal annealing at 750 °C, but crevice corrosion resistance was observed to decrease less with increasing annealing time at 750 °C, as the nitrogen content of the steel increased. Resistance to crevice corrosion was observed to decrease less especially for the steel with 0,9 wt-%N, as compared to that of other steels. In the microstructural analyses, the precipitation of intermetallic phases was observed to be retarded (especially σ phase precipitation in steels with 0,7 and 0,9 wt-%N annealed for 1 h at 750 °C) as the nitrogen content of the steel increased, and thus,

the amount of intermetallic phases was lower. Additionally, although Cr_2N precipitation was observed in the steels as their nitrogen content increased > 0,5 wt-%N, the decrease in crevice corrosion resistance was somewhat lower than in the steels with lower nitrogen contents. This can be explained by the fact that, despite Cr_2N precipitation, the nitrogen content of the austenite matrix remained high enough to retard intermetallic phase precipitation, as observed in the microstructural analyses. Thus, it seems that the crevice corrosion resistance of the studied steels is more sensitive to intermetallic phases, especially to σ phase, than to Cr_2N, which differs from the results of Jargelius-Petterson (1996) for steels with lower chromium, molybdenum and nitrogen contents. It should be noticed that there are large variations in the values of critical pitting and crevice corrosion temperatures, Table 11.

6 CONCLUDING REMARKS

In this study the effects of the nitrogen content on the microstructure and properties of solution annealed and further isothermally at elevated temperatures annealed, powder metallurgically manufactured, nitrogen alloyed, austenitic stainless steels, were studied. This was performed with optical microscopy, transmission electron microscopy, dilatometric analyses, tensile testing, impact toughness testing, and localized corrosion testing. The following conclusions can be drawn:

1. The powder metallurgical manufacturing method allows the manufacturing of an austenitic stainless steel with excellent localized corrosion resistance and mechanical properties.
2. Nitrogen alloying increases the yield and ultimate tensile strength of the studied solution annealed steels. The room temperature ductility and toughness of the steels remain good when their nitrogen content is 0,5 - 0,7 wt-%N.
3. Nitrogen alloying improves the pitting and crevice corrosion resistance of the studied solution annealed steels, when their nitrogen content is 0,5 - 0,9 wt-%N.
4. The microstructure of the solution annealed steels depended on their nitrogen content. The microstructure of the steels was fully austenitic, when their nitrogen content was 0,5-0,9 wt-%N. At lower nitrogen contents, intermetallic phases (mainly σ phase) are precipitated. At higher nitrogen contents, Cr_2N is precipitated.
5. Increasing the nitrogen content of the steel results in retardation of precipitation of intermetallic phases during solution annealing and subsequent exposure to elevated temperatures.
6. Intermetallic phases are precipitated in the steels with $\leq$ 0,5 wt-%N when isothermally annealed at 450 °C for a long time (500 h in this study). Ductility, toughness, and localized corrosion resistance of the steels are deteriorated due to intermetallic phase precipitation. The hardness and strength properties of the steels are increased due to intermetallic phase precipitation. In steels with higher nitrogen contents, intermetallic phases are not precipitated.
7. Depending on the nitrogen content of the steel intermetallic phases, or intermetallic phases and Cr_2N, were precipitated when the steels were isothermally annealed at 750 °C. In steels with $\leq$ 0,5 wt-%N, intermetallic phases were precipitated whereas in steels with > 0,5 wt-%N, both intermetallic phases and Cr_2N were precipitated.

8. The precipitation of σ phase was retarded, and Laves phase was stabilized during annealing at 750 °C when the nitrogen content of the steel was > 0,5 wt-%N.
9. The yield and ultimate tensile strength of the studied steels isothermally annealed at 750 °C increased, remained unaffected or decreased as the nitrogen content of the steel increased. This is due to the balance between the decrease of solid solution strengthening by nitrogen, and an increase in strength due to precipitation of intermetallic phases and Cr_2N.
10. The tensile ductility of the steels annealed at 750 °C decreased with increasing annealing time. The decrease is controlled by the amount and type of the precipitates. The decrease in tensile ductility was the less, the higher the nitrogen content of the steel, which is due to retardation of the precipitation of intermetallic phases with increasing nitrogen content of the steel. Precipitation of intermetallic phases is more detrimental to tensile ductility than that of Cr_2N.
11. The impact toughness of the studied steels annealed at 750 °C decreased with increasing annealing time. The decrease of impact toughness is controlled by the amount, and especially, by the type of the grain boundary precipitates. The decrease in impact toughness increased with the increasing amount of intergranular precipitates and with increased annealing time. Precipitation of Cr_2N is more detrimental to impact toughness than that of intermetallic phases.
12. The hardness of the studied steels annealed at 750 °C increased with increasing annealing time, due to precipitation of intermetallic phases and Cr_2N.
13. The localized corrosion resistance of the studied steels annealed at 750 °C decreased as the annealing time increased. The decrease in crevice corrosion resistance seems to be less the higher the nitrogen content of the steel is, which is due to the retardation of precipitation of intermetallic phases by nitrogen.
14. The actual mechanisms how nitrogen retards intermetallic phase precipitation remained unclear and needs further studying.

7 REFERENCES

1. Advani, A. H., Murr, L. E., Atteridge, D. G., Chelakara, R. and Bruemmer, S. M., Deformation Effects on Intragranular Carbide Precipitation and Transgranular Chromium Depletion in Type 316 Stainless Steels. Corrosion Vol. 47(1991), No. 12, p. 939 - 947.

2. Azuma, S., Miyuki, H. and Kudo, T., Effect of Alloying Nitrogen on Crevice Corrosion of Austenitic Stainless Steels. ISIJ Int. Vol. 36(1996), No. 7, p. 793-798.

3. Barcik, J., Mechanism of σ-phase Precipitation in Cr-Ni Austenitic Steels. Mat. Sci. Tech. Vol.4(1988), p. 5-15.

4. Berns, H. and Wang, G., High-Nitrogen Hard Alloys by Powder Metallurgy. Proceedings of the 2nd International Conference on High-Nitrogen Steels, Aachen, Germany, October 10-12, 1990, Verlag Stahleisen, Düsseldorf, Germany, (1990), p. 332-337.

5. Betrabet, H. S., Nishimoto, K., Wilde, B. E. and Clark, W. A. T., Electrochemical and Microstructural Investigation of Grain Boundary Precipitation in AISI 304 Stainless Steels Containing Nitrogen. Corrosion Vol. 43(1987), No. 2, p. 77 - 84.

6. Biancaniello, F. S., Ricker, R. E. and Ridder, S. D., Structure and Properties of Gas Atomized HIP-Consolidated High Nitrogen Stainless Steel. Proceedings of the 5th International Conference on Advanced Particulate Materials & Processes, April 7-9, 1997, West Palm Beach, Florida, U.S.A., p. 309 - 316.

7. Bracconi, P. and Gasc, G., Surface Characterization and Reactivity of a Nitrogen Atomized 304L Stainless Steel Powder. Met. Trans. Vol. 25A(1994), p. 509 - 520.

8. Brandis, H., Heimann, W. and Schmidtmann, E., Einfluβ von Stickstoff auf das Ausscheidungsverhalten des Stahles X3CrNiMoNbN 23 17 (Amagnit 3974). TEW-Technische Berichte, Vol. 2(1976A)No. 2, p. 150 - 166.

9. Brandis, H., Heimann, W. and Schmidtmann, E., Einfluβ von Stickstoff un Ausscheidungen auf die Festigkeits- und Zähigkeitseigenschaften des Stahles X3CrNiMoNbN 23 17 (Amagnit 3974). TEW-Technische Berichte, Vol. 2(1976B)No. 2, p. 167 - 171.

10. Briant, C. L., Mulford, R. A. and Hall, E.L., Sensitization of Austenitic Stainless Steels, I. Controlled Purity Alloys. Corrosion Vol. 38(1982), No.9, p. 468 - 477.

11. Bruemmer, S. M., Quantitative Modeling of Sensitization Development in Austenitic Stainless Steel. Corrosion Vol. 46(1990), No. 9, p. 698 - 709.

12. Byrnes, M., Grujicic and Owen, W. S, Nitrogen Strengthening of a Stable Austenitic Stainless Steel. Acta Metall. Vol. 35(1987), p. 1853-1862.

13. Covino, Jr., B.S., Cramer, S. D., Russell, J. H. and Simmons, J. W., Corrosion and Polarization Behavior of Sensitized High-Nitrogen Stainless Steels. Corrosion Vol. 53(1997), No. 7, p. 525 - 536.

14. Defilippi, J. D., Brickner, K.G. and Gilbert, E. M., Ductile-to-Brittle Transition in Austenitic Chromium-Manganese-Nitrogen Stainless Steels. Trans. AIME Vol. 245(1969), p. 2141-2148.

15. Dunning, J.S., Simmons, J.W. and Rawers, J., Advanced Processing Technology for High-Nitrogen Steels. J. Mat. Vol. 3(1994), No. 6, p. 1195 - 1199.

16. Eckenrod, J. J. and Kovach, C. W., Effect of Nitrogen on the Sensitization, Corrosion and Mechanical Properties of 18Cr-8Ni Stainless Steel. ASTM Special. Tech. Pub. 679, ASTM, Philadelphia, (1977), p. 17 - 41.

17. Ezaki, H., Morinaga, M. and Yukawa, N., Prediction of the Occurrence of the σ phase in Fe-Cr-Ni Alloys. Phil. Mag. A. Vol. 53(1986), No. 5, p. 709 - 716.

18. Feichtinger, H., Satir - Kolorz, A. and Zheng, X., Solubility of Nitrogen in Solid and Liquid Iron Alloys with Special Regard to the Melting Range. Proceedings of the International Conference on High-Nitrogen Steels, Lillé, France, May 18-20, 1988, Institute of Metals, London, (1989), p. 75 - 80.

19. Feichtinger, H.K. and Zheng, X., Powder Metallurgy of High Nitrogen Steels. Powder Met. Int. Vol. 22(1990), p. 7 - 13.

20. Feichtinger, H.K., Alternative Methods for the Production of High-Nitrogen Steels, Proceedings of the International Conference on Stainless Steels. Chiba, Japan, 10.-13. 6. 1991, The Iron and Steel Institute of Japan, (1991), p. 1125 - 1132.

21. Ferriss, D.P., Surface Analysis of Steel Powders by ESCA, The Int. J. Powder Met. & Powder Tech. Vol. 19(1983), p. 11 - 19.

22. Foct, J., Rochegude, P. and A. Mastorakis, Mechanical Alloying of H.N.S. Studied by Mössbauer Spectrometry. Proceedings of the 2nd International Conference on High-Nitrogen Steels, Aachen, Germany, October 10-12, 1990, Verlag Stahleisen, Düsseldorf, Germany, (1990), p. 72 - 77.

23. Frisk, K. and Hillert, M., Thermodynamics of the Fe - Cr - Ni - N System. Proceedings of the International Conference on High-Nitrogen Steels, Lillé, France, May 18-20, 1988, Institute of Metals, London, (1989), p. 1 - 9.

24. Frisk, K., A Thermodynamic Analysis of the Cr-Fe-Mo-Ni-N System. Doctoral Thesis, Division of Physical Metallurgy, Royal Institute of Technology, Stockholm, Sweden, 1990, 211 p.

25. Gagnepain, J. C., Charles, J., Coudreuse, L. and Bonnefois, B., A New High Nitrogen Super Austenitic Stainless Steel with Improved Structure Stability and Corrosion Resistance Properties. Proceedings of the International Conference Corrosion 96, NACE International, Houston, TX, 1996, Paper No. 414.

26. Grabke, H. J., The Role of Nitrogen in the Corrosion of Iron and Steels. ISIJ Int. Vol. 36(1996), No. 7, p. 777-786.

27. Grujicic, M., Nilsson, J.-O., Owen, W. S. and Thorvaldsson, T., Basic Deformation Mechanisms in Nitrogen Strengthened Stable Austenitic Stainless Steels. Proceedings of the International Conference on High-Nitrogen Steels, Lillé, France, May 18-20, 1988, Institute of Metals, London, (1989), p. 151 - 158.

28. Hales, R. and Hill, A. C., The Diffusion of Nitrogen in an Austenitic Stainless Steel. Metal Science Vol. 11(1977), p. 241 - 244.

29. Harzenmoser, M., Reed. R. P., Uggowitzer, P. J. and Speidel, M. O., The Influence of Nickel and Nitrogen on the Mechanical Properties of High-Nitrogen Austenitic Steels at Cryogenic Temperatures. Proceedings of the 2nd International Conference on High-Nitrogen Steels, Aachen, Germany, October 10-12, 1990, Verlag Stahleisen, Düsseldorf, Germany, (1990), p. 197 - 202.

30. Hertzman, S. and Jarl, M., A Thermodynamic Analysis of the Fe - Cr - N System, Met. Trans. Vol. 18 A(1987), p. 1745 - 1752.

31. Herzberg, R.W., Deformation and Fracture Mechanics of Engineering Materials. 4th ed., John Wiley & Sons, Inc., New York, NY, 1996, 680 p.

32. Heubner, U., Rockel, M. and Wallis, E., Das Ausscheidungsverhalten von Hochlegierten Austenitischen Stählen mit 6 % Molybdän und sein Einfluβ auf die Korrosionbeständigkeit. Werkstoffe und Korrosion Vol. 40(1989), p. 459 - 466.

33. Hillert, M. and C. Qiu, The Effect of N and Mn on Equilibria in Austenitic Stainless Steels, Illustrated with Computer Calculations. International Conference on Applications of Stainless

Steels '92, Stockholm, 9.-11. 6. 1992, Jernkontoret, The Institute of Metals and ASM International, (1992), p. 13-22.

34. Ilola, R. J., Hänninen, H. E. and Ullakko, K. M., Mechanical Properties of Austenitic High-Nitrogen Cr-Ni and Cr-Mn Steels at Low Temperatures. ISIJ Int. Vol. 36(1996), No. 7, p. 873 - 877.

35. Irvine, K. J., Llewellyn, D. T. and Pickering, F.B., High-Strength Austenitic Stainless Steels. JISI Vol. 199(1961), p. 153 - 175.

36. Jack, K.H., Nitrogen Precipitation - Retrospect and Prospect. Proceedings of the International Conference on High-Nitrogen Steels, Lillé, France, May 18-20, 1988, Institute of Metals, London, (1989), p. 117 - 135.

37. Janik-Czachor, E., Lunarska, E. and Szklarska-Smialowska, Z., Effect of Nitrogen Content in a 18Cr-5Ni-10Mn Stainless Steel on the Pitting Susceptibility in Chloride Solutions. Corrosion Vol. 31(1975), p. 394 - 398.

38. Jargelius, R. and Wallin, T., The Effect of Nitrogen Alloying on the Pitting and Crevice Corrosion Resistance of CrNi and CrNiMo Stainless Steels. Proceedings of the 10^{th} Scandinavian Corrosion Congress, Stockholm, June 2 - 4, 1986, Swedish Corrosion Institute, 1986, p. 161 - 164.

39. Jargelius-Petterson, R.F.A, Ekman, T., Hertzman, S., Holm, T. and Linder, J., Nitrogen Uptake by an Austenitic Stainless Steel on Annealing in N_2-H_2 Atmospheres. Mat. Sci. Tech. Vol. 9(1993B), p. 1123 - 1132.

40. Jargelius-Petterson, R.F.A., Precipitation in a Nitrogen Alloyed Stainless Steel at 850 °C. Scripta Met. Mater. Vol. 28(1993A), No.11, p. 1399 - 1403.

41. Jargelius-Petterson, R.F.A., Phase Transformations in a Manganese-Alloyed Austenitic Stainless Steel. Scripta Met. Mater. Vol. 30(1994), No. 9, p. 1233 - 1238.

42. Jargelius-Petterson, R.F.A., Localised Corrosion of Stainless Steels: Ranking, Alloying and Microstructure Effects. Scan. J. Metall. Vol. 24(1995), p. 188 - 193.

43. Jargelius-Petterson, R.F.A., Sensitization Behaviour and Corrosion Resistance of Austenitic Stainless Steels Alloyed with Nitrogen and Manganese. ISIJ Int. Vol. 36(1996), No. 7, p. 818-824.

44. Jargelius-Petterson, R.F.A., The Influence of N, Mo and Mn on the Microstructure and Corrosion Resistance of Austenitic Stainless Steels. Doctoral Thesis, Division of Corrosion Science, Royal Institute of Technology, Stockholm, Sweden, 1998, 85 p.

45. Jarl, M., A Thermodynamic Analysis of the Interaction Between Nitrogen and Other Alloying Elements in Ferrite and Austenite. Scand. J. Met. Vol. 7(1978), p. 93 - 101.

46. Johansson, A., Arnberg, L., Gustafsson, P. and Savage, S., Nitrogen Alloyed Stainless Steels Produced by Nitridation of Powder. Met. Powder Rep. Vol. 5(1991), p. 64 - 68.

47. Jonsson, J. Y., Wegrelius, L., Heino, S., Liljas, M. and Östberg, R., The Influence of Tungsten (W) on Properties in High Nitrogen Stainless Steels. To be published in the Proceedings of the 5th International Conference on High Nitrogen Steels, Espoo, Finland - Stockholm, Sweden, May 24 - 28, 1998, Trans Tech Publications, Zürich, Switzerland, 1999.

48. Kearns, J. R. and Deverell, H. E., The Use of Nitrogen to Improve the Corrosion Resistance of FeCrNiMo Alloys for the Chemical Process Industries. Mater. Perform. Vol. 26(1987), No. 6, p. 18 - 28.

49. Kikuchi, M., Kajihara, M. and K. Frisk, Solubility of Nitrogen in Austenitic Stainless Steels, Proceedings of the International Conference on High-Nitrogen Steels. Lillé, France, May 18-20, 1988, Institute of Metals, London, 1989, p. 63 - 74.

50. Kikuchi, M., Kajihara, M. and Choi, S. K., Cellular Precipitation Involving both Substitutional and Interstitial Solutes: Cellular Precipitation of Cr_2N in Cr-Ni Austenitic Steels. Mater. Sci. Vol. A146(1991), p. 131 - 150.

51. Kunii, D., Levenspiel, O., Fluidization Engineering. John Wiley & Sons, Inc., New York, 1969.

52. Kunze, H. D., Diffusion des Stickstoffs in Flüssigen Eisenreichen Mehrstofflegierungen. Arch. Eisenhüttenwes. Vol. 44(1973), No. 3, p. 173 - 179.

53. Lall, C., Fundamentals of High Temperature Sintering: Application to Stainless Steels and Soft Magnetic Alloys. Int. J. Powder Met. Vol. 27(1991), No. 4, p. 315 - 329.

54. Latanision, R. M. and Ruff, A. W., Jr., The Temperature Dependence of Stacking Fault Energy in Fe - Cr - Ni Alloys. Met. Trans. Vol. 2(1971), p. 505 - 509.

55. Ledbbetter, H. M. and Austin, M. W., Effects of Carbon and Nitrogen on the Elastic Constants of AISI Type 304 Stainless Steels. Mat. Sci. Eng. Vol. 70(1985), p. 143 - 149.

56. Levey, P. R. and van Bennekom, A., A Mechanistic Study of the Effects of Nitrogen on the Corrosion Properties of Stainless Steels. Corrosion Vol. 51(1995), No. 12, p. 911-921.

57. Liska, M., Vodárek, V., Sobotková, M. and Sobotka, J., Precipitation Behaviour and Creep Rupture Properties of CrNi(Mo)N Austenitic Stainless Steels. Proceedings of the 2nd

International Conference on High-Nitrogen Steels, Aachen, Germany, October 10-12, 1990, Verlag Stahleisen, Düsseldorf, Germany, (1990), p. 78 - 83.

58. Lu, Y. C., Luo, J. L. and Ives, M. B., Effect of Nitriding on the Anodic Behavior of Iron and Its Signifigance in Pitting Corrosion of Iron-Based Alloys. Corrosion Vol. 47(1991), p. 835 - 839.

59. Marshall, P., Austenitic Stainless Steels, Microstructure and Mechanical Properties. Elsevier Applied Science Publishers Ltd, Essex, England, 1984, 431 p.

60. Maziaz, P. J., Precipitation Response of Austenitic Stainless Steel to Simulated Fusion Irradiation. Proceedings of the Symposium ´´The Metal Science of Stainless Steels´´, 107th AIME Annual Meeting, Denver, March, 1987, Met. Soc. AIME, (1987), p. 160 - 180.

61. Mielityinen-Tiitto, Kirsti, Precipitation of Cr_2N in Some Nitrogen-Alloyed Austenitic Stainless Steels. Doctor´s thesis, Acta Polytechnica Scandinavica, Chemistry Including Metallurgy Series No. 141, Helsinki 1979, Finnish Academy of Technology, 67 p.

62. Minami, Y., Kimura, M. and Ihara, Y., Microstructural Changes in Austenitic Stainless Steels during Long Term Aging. Mat. Sci. Tech. Vol. 2(1986), p. 795 - 806.

63. Morinaga, M., Yukawa, N., Ezaki, H. and Adachi, H., Solid Solubilities in Transition-Metal-Based f.c.c. Alloys. Phil. Mag. A. Vol. 51(1985), No. 2, p. 223 - 252.

64. Mozhi, T. A., Clark, W. A. T., Nishimoto, W. B., Johnson, W. B. and Macdonald, D. D., The Effect of Nitrogen on Sensitization of AISI 304 Stainless Steel. Corrosion Vol. 41(1985), No. 10, p. 555 - 559.

65. Müllner, P., Solenthaler, C., Uggowitzer, P. and Speidel, M.O., On the Effect of Nitrogen on the Dislocation Structure of Austenitic Stainless Steel. Mater. Sci. Eng. Vol. A164(1993), p. 164 - 169.

66. Newman, R. C. and Sharabi, T., The Effect of Alloyed Nitrogen or Dissolved Nitrate Ions on the Anodic Behaviour of Austenitic Stainless Steel in Hydrochloric Acid. Corrosion Sci. Vol. 27(1987), p. 827 - 838.

67. Norström, L. A., The Influence of Nitrogen and Grain Size on Yield Strength in Type AISI 316L Austenitic Stainless Steel. Metal Sci. Vol.11(1977), No. 6, p. 208 - 212.

68. Nyborg, L. and Olefjord, I., Surface Analysis of PM Martensitic Steel Before and After Consolidation; Part 1: Surface Analysis of Powder. Powder Met. Vol. 31(1988), No. 1, p. 33-39.

69. Nyborg, L., Tunberg, T., Wang, P.X. and Olefjord, I., Surface Analysis of Water-atomized Austenitic Stainless Steel Powder. Proceedings of the PM´90, PM into the 1990 ´s, International Conference on Powder Metallurgy, Vol. 3, London, UK, July 2-6, (1990), p. 199-203.

70. Olefjord, I. and Nyborg, L., Surface Analysis of Gas Atomized Ferritic Steel Powder. Powder Met. Vol. 28(1985), No. 4, p. 237-243.

71. Orita, K., Ikeda, Y., Iwadate, T. and Ishizaka, J., Development and Production of 18Mn-18Cr Nonmagnetic Retaining Ring with High Yield Strength. ISIJ Int. Vol. 30(1990), No. 8, p. 587 - 593.

72. Paulus, N., Magdowski, R. and Speidel, M.O., Cold Worked High Nitrogen Superaustenitics. Proceedings of the 3rd International Conference on High-Nitrogen Steels, Kiev, Ukraine, September 14-16, 1993, Institute for Metal Physics, Ukraine, (1993), p. 394-400.

73. Perrot, P. and Foct, J., Discussion on the Thermodynamical Bases Used in High-Nitrogen Steel Making. Proceedings of the 2nd International Conference on High-Nitrogen Steels, Aachen, Germany, October 10-12, 1990, Verlag Stahleisen, Düsseldorf, Germany, (1990), p. 32 - 37.

74. Presser, R. and Silcock, J. M., Aging Behaviour of 18Mn-18Cr High Nitrogen Austenitic Steel for End Rings. Metal Sci. Vol.17(1983), No. 5, p. 241 - 247.

75. Purtscher, P. T., Krauss, G. and Matlock, D. K., Temperature-Induced Transition in Ductile Fracture Appearance of a Nitrogen-Strengthened Austenitic Stainless Steel. Met. Trans. Vol.24A(1993), No. 11, p. 2521 - 2529.

76. Rawers, J. and Grujicic, Effects of Metal Composition and Temperature on the Yield Strength of Nitrogen Strengthened Stainless Steels. Mat Sci. & Eng. Vol A207(1996), p. 188 - 194.

77. Rawers, J., Dunning, J. and Reed, R., Nitride Formation in HIP-melted Metals. Proceedings of the 2nd International Conference on High-Nitrogen Steels, Aachen, Germany, October 10-12, 1990, Verlag Stahleisen, Düsseldorf, Germany, (1990), p. 63 -66.

78. Rawers, J., Dunning, J., Asai, G. and Reed, R., Characterization of Stainless Steels Melted under High Nitrogen Pressure. Met. Trans. Vol. 23A(1992), p. 2061 - 2068.

79. Rawers, J.C. and Doan, R.C., Mechanical Processing of Iron Powders in Reactive and Nonreactive Gas Atmospheres. Met. Trans. Vol. 25A(1994A), p. 381 - 388.

80. Rawers, J.C., Frisk, K. and Govier, D., Nitrogen in Pressure-Diffused Powder Iron Alloys, Mater. Sci. Eng. Vol. A177(1994B), p. 243 - 251.

81. Rayaprolu, D. B. and Hendry, A., High Nitrogen Stainless Steel Wire. Mat. Sci. Tech. Vol. 4(1988), p. 136 - 145.

82. Rayaprolu, D. B. and Hendry, A., Cellular Precipitation in a Nitrogen Alloyed Stainless Steel. Mat. Sci. Tech. Vol. 5(1989), p. 328 - 332.

83. Rechsteiner, A. A., Metallkundliche und Metallurgische Grundlagen zur Entwicklung Stickstoffreicher, Zäher, Hochfester Austenitischer Stähle. Diss. ETH Nr. 10647, Doctoral Thesis, Swiss Technical University, Zürich, Switzerland, 1994, 141 p.

84. Reed, R. P. and Simon, N. J., Nitrogen Strengthening of Austenitic Stainless Steels at Low Temperatures, Proceedings of the International Conference on High-Nitrogen Steels. Lillé, France, May 18-20, 1988, Institute of Metals, London, (1989), p. 180 - 188.

85. Reynoldson, R.W., Heat Treatment in Fluidized Bed Furnaces. ASM International, Materials Park, Ohio, 1993.

86. Rhodes, G. O. and Conway, J. J., High-Nitrogen Austenitic Stainless Steels with High Strength and Corrosion Resistance. J. Mater. Vol. 4(1996), p. 28 - 31.

87. Rhodes, G. O., Habel, U., Eckenrod, J. J. and Conway, J. J., Development, Properties and Applications of High Strength Corrosion Resistant High-Nitrogen Austenitic Stainless Steels Produced by HIP P/M. Proceedings of the 5th International Conference on Advanced Particulate Materials & Processes, April 7-9, 1997, West Palm Beach, Florida, U.S.A., p. 295 - 308.

88. Rhodes, G. O. and Eisen, W. B., High Nitrogen Corrosion Resistant Austenitic Stainless Steels Produced by HIP P/M Processing. To be published in the Proceedings of the 5th International Conference on High Nitrogen Steels, Espoo, Finland - Stockholm, Sweden, May 24 - 28, 1998, Trans Tech Publications, Zürich, Switzerland, 1999.

89. Romu, J. J., Tervo, J. J., Hänninen, H. E. and Liimatainen, J., Wear Resistance of High Nitrogen Austenitic Stainless Steels Manufactured by Molten and Powder Metallurgy Routes. Proceedings of the 3rd International Conference on High-Nitrogen Steels, Kiev, Ukraine, September 14-16, 1993, Institute for Metal Physics, Ukraine, (1993), p. 372 - 378.

90. Romu, J. J., Manufacturing of P/M High Nitrogen Stainless Steels. Licentiate´s Thesis. Helsinki University of Technology, 1994, 177 p.

91. Romu, J. J., Tervo, J. J., Hänninen, H. E. and Liimatainen, J., Development of Properties of P/M Austenitic Stainless Steels by Nitrogen Infusion. ISIJ Int. Vol.36(1996), No. 7, p. 938 - 346.

92. Romu, J. J., Tervo, J. J., Hänninen, H. E., Corrosion and Mechanical Properties of Nitrogen Alloyed PM HIP Stainless Steels. Proceedings of the Joint Nordic Conference in Powder Technology. Helsinki, November 26-27, 1997, p. 58.

93. Sandström, R. and Bergqvist, H., Temperature Dependence of Tensile Properties and Strengthening of Nitrogen Alloyed Austenitic Stainless Steels. Scand. J. Metall. Vol. 6(1977), p. 156 - 169.

94. Schramm, R. E. and Reed, R. P., Stacking Fault Energies of Seven Commercial Austenitic Stainless Steels. Met. Trans. Vol. 6A(1975), p. 1345-1351.

95. Sedriks, A. J., Effects of Alloy Composition and Microstructure on the Passivity of Stainless Steels. Corrrosion, Vol. 42(1986), No. 7, p. 376 - 389.

96. Simmons, J. W., Mechanical Properties of Isothermally Aged High-Nitrogen Stainless Steel. Met. Trans. Vol. 26A(1995A), p. 2085-2101.

97. Simmons, J. W., Influence of Nitride (Cr_2N) Precipitation on the Plastic Flow Behavior of High-Nitrogen Austenitic Stainless Steel. Scripta Metall. Mater. Vol. 32(1995B), No. 2, p. 265-270.

98. Simmons, J. W., Overview: High-Nitrogen Alloying of Stainless Steels. Mat. Sci. & Eng. Vol. A207(1996A), p. 159 - 169.

99. Simmons, J. W., Covino, Jr., B. S., Hawk, J. A. and Dunning, J. S., Effect of Nitride (Cr_2N) Precipitation on the Mechanical, Corrosion and Wear Properties of Austenitic Stainless Steels. ISIJ Int. Vol. 36(1996B), No. 7, p. 846 - 854.

100. Simmons, J. W., Kemp, W. E. and Dunning, J. S., The P/M Processing of High-Nitrogen Stainless Steels. J. Mater. Vol. 4(1996C), p. 20 - 23.

101. Simmons, J.W., Atteridge, D. G. and Rawers, J. C., Sensitization of High-Nitrogen Austenitic Stainless Steels by Dichromium Nitride Precipitation. Corrosion Vol. 50(1994), No. 7, p. 491-501.

102. Soussan, A., Degaillax, S. and Magnin, T., Work-Hardening Behavior of Nitrogen-Alloyed Austenitic Stainless Steels. Mater. Sci. Eng. Vol. A142(1991), p. 169 - 176.

103. Speidel, M.O., Properties and Applications of High - Nitrogen Steels. Proceedings of the International Conference on High-Nitrogen Steels, Lillé, France, May 18-20, 1988, Institute of Metals, London, (1989), p. 92 - 96.

104. Stawström, C. and Hillert, M., An Improved Depleted-Zone Theory of Intergranular Corrosion of 18-8 Stainless Steel. J. Iron Steel Inst. Vol. 97(1969), No. 1, p. 77 - 85.

105. Stoltz, R. E. and Vander Sande, J. B.. The Effect of Nitrogen on Stacking Fault Energy of Fe - Ni - Cr - Mn Steels. Met. Trans. Vol. 11A(1980), p. 1033 - 1037.

106. Swann, R. P., Dislocation Substructure vs. Transgranular Stress Corrosion Susceptibility of Single Phase Alloys. Corrosion Vol. 19(1963), p. 102t - 112t.

107. Taillard, R., Vanderschaeve, F. Foct, J., Mechanical Behaviour of Aged and Not Prestrained High Nitrogen Austenitic Stainless Steels. To be published in the Proceedings of the 5th International Conference on High Nitrogen Steels, Espoo, Finland - Stockholm, Sweden, May 24 - 28, 1998, Trans Tech Publications, Zürich, Switzerland, 1999.

108. Tervo, J. J., Properties of P/M High Nitrogen Austenitic Stainless Steels. Licentiate´s Thesis, Helsinki University of Technology, 1994, 249 p.

109. Tervo, J. J., Romu, J. J., Hämäläinen, E. A., Hänninen, H. E. and Liimatainen, J., Properties of P/M High Nitrogen Austenitic and Duplex Stainless Steels. Proceedings of the 5th International Conference on Advanced Particulate Materials & Processes, April 7-9, 1997, West Palm Beach, Florida, U.S.A., p. 317 - 330.

110. Tervo, J. J., Wear Properties of High Nitrogen Austenitic Stainless Steels. Doctor´s thesis, Acta Polytechnica Scandinavica, Mechanical Engineering Series No. 128, Espoo 1998, Finnish Academy of Technology, 88 p.

111. Thier, H., Bäumel, A. and Schmidtmann, E., Einfluß von Stickstoff auf das Ausscheidungsverhalten des Stahles X 5 CrNiMo 17 13. Archiv für das Eisenhüttenwesen Vol.40(1969), No. 4, p. 333 - 339.

112. Tobler, R. L. and Meyn, D., Cleavage-Like Fracture along Slip Planes in Fe-18Cr-3Ni-13Mn-0,37N Austenitic Stainless Steel at Liquid Helium Temperature. Met. Trans.Vol. 19A(1988), No. 6, p. 1626 - 1631.

113. Tomota, Y. and Endo, S., Cleavage-Like Fracture at Low Temperatures in an 18Mn-18Cr-0,5N Austenitic Steel. ISIJ Int. Vol. 30(1990), No. 8, p. 656 - 662.

114. Truman, J. E., Effects of Nitrogen Alloying on Corrosion Behaviour of High Alloy Steels. Proceedings of the International Conference on High-Nitrogen Steels, Lillé, France, May 18-20, 1988, Institute of Metals, London, (1989), p. 225 - 239.

115. Uggowitzer, P. J. and Speidel, M. O., Ultrahigh-strength Austenitic Steels. Proceedings of the 2nd International Conference on High-Nitrogen Steels, Aachen, Germany, October 10-12, 1990, Verlag Stahleisen, Düsseldorf, Germany, (1990), p. 156-160.

116. Uggowitzer, P. J. and Harzenmoser, M., Strengthening of Austenitic Stainless Steels by Nitrogen. Proceedings of the 2nd International Conference on High-Nitrogen Steels, Aachen, Germany, October 10-12, 1990, Verlag Stahleisen, Düsseldorf, Germany, (1990), p. 174-179.

117. Uggowitzer, P. J., Magdowski, R. and Speidel, M. O., Nickel Free High Nitrogen Austenitic Steels. ISIJ Intl. Vol. 36(1996), No. 7, p. 901 - 908.

118. Uggowitzer, P.J., Paulus, N. and Speidel, M.O., Ductile-to-Brittle Transition in Nitrogen Alloyed Austenitic Stainless Steels. International Conference on Applications of Stainless Steels '92, Stockholm, 9.-11. 6. 1992, Jernkontoret, The Institute of Metals and ASM International, (1992), p. 62-71.

119. Uggowitzer, P.J., Magdowski, R. and Speidel, M.O., High Nitrogen Austenitic Stainless Steels - Properties and New Developments. Proceedings of the International Conference Innovation Stainless Steels, Florence, Italy, 11-14 October, 1993, Associazione Italiana di Metallurgia, (1993), p. 2.359-2.372.

120. Virta, J. and Hannula, S.-P., Nitrogen Alloying of Steel Powder Using Ammonia Gas in the Fluidised Bed. To be published in the Proceedings of the 5th International Conference on High Nitrogen Steels, Espoo, Finland - Stockholm, Sweden, May 24 - 28, 1998, Trans Tech Publications, Zürich, Switzerland, 1999.

121. Wada, S. and Ohta, Y., Effects of Alloying Elements on Properties of Ultrahigh Nitrogen Containing Stainless Steel - Development of 30Cr - 10Ni - 10Mn - 2Mo - 1.1N - Fe Alloy. Nippon Stain. Tech. Rep., Vol. 24(1989), p. 13 - 30.

122. Wallis, E., Influence of the Molybdenum Content of High-Alloy Stainless Steels and the Precipitation of Intermetallic Phases on Pitting Resistance in Chloride-Containing Media. Wekstoffe und Korrosion Vol.41(1990), p. 155 - 162.

123. Werner, E., Solid Solution and Grain Size Hardening of Nitrogen-Alloyed Austenitic Steels. Mater. Sci. Eng. A. Vol. 101(1988), p. 93 - 98.

124. Werther, J., Influence of the Bed Diameter of the Hydrodynamics of Gas Fluidized Bed, AIChe Symposium Series. Vol. 70(1974), No. 141, p. 53 - 62.

125. Wiegand, H. and Doruk, M., Einfluβ von Kohlenstoff und Molybdän auf die Auscheidungsvorgänge, besonders auf die Bildung intermetallischer Phasen in austenitischen Chrom-Nickel-Stählen. Archiv für das Eisenhüttenwesen, Vol. 33(1962), No. 8, p. 559 - 566.

126. Wilson, E.G., Development of Powder Routes for TiN Dispersion Strengthened Stainless Steels. Proceedings of the International Conference on High-Nitrogen Steels, Lillé, France, May 18-20, 1988, Institute of Metals, London, (1989), p. 305-309.

127. Zheng, X., Feichtinger, H.K. and Speidel, M.O., Investigation of the Nitriding Process of Stainless Steel Powder, Proceedings of the 2nd International Conference on High-Nitrogen Steels, Aachen, Germany, October 10-12, 1990, Verlag Stahleisen, Düsseldorf, Germany, (1990), p. 320 - 325.

128. Zheng, X., Nitrogen Solubility in Iron-Base Alloys and Powder Metallurgy of High-Nitrogen Steels. Thesis for Doctor of Technical Sciences, Swiss Federal Institute of Technology, Zürich, Switzerland, May 1991, 111 p.

129. Zheng, X., Rechsteiner, A., Uggowitzer, P. and Speidel, M.O., New Metallurgical Processing Routes for Newly Developed Martensitic and Duplex Steels. Proceedings of the 3rd International Conference on High-Nitrogen Steels, Kiev, Ukraine, September 14-16, 1993, Institute for Metal Physics, Ukraine, (1993), p. 426 - 431.

APPENDIX A.

Thermodynamic analysis for calculation of nitrogen solubility in iron-base alloys.

Dissolution of nitrogen in alloyed steels can be described by the reaction:

$$\tfrac{1}{2}\, N_2(g) = [N](s) \qquad (A1)$$

Dissolution is considered to take place in two steps: first, nitrogen molecules split into atoms at the steel surface, and subsequently atomic nitrogen enters the interstitial sites of the steel. The equilibrium constant for reaction (A1) is as follows:

$$K_N = \frac{a_N}{\sqrt{p_{N_2}}} = \frac{f_N[wt-\%N]}{\sqrt{p_{N_2}}} \qquad (A2)$$

where a_N is the activity of nitrogen dissolved in steels, p_{N_2} is the partial pressure of nitrogen and is related to the nitrogen activity in the gas phase, f_N is the activity coefficient, and wt-% N is the weight percent of nitrogen in steel. The reaction is considered to take place in 1 atm pressure of nitrogen gas. The activity coefficient f_N is a proportionality factor, and it describes the relation between the chemical activity, and the concentration of dissolved nitrogen. Usually, when determining nitrogen solubility in iron-base alloys, an infinitely dilute solution of nitrogen in pure iron is considered as the reference state. Based on that, the activity coefficient of nitrogen in pure iron is unity. After the reference state is determined, it is possible to evaluate how alloying elements affect nitrogen solubility, i.e., how they change the activity coefficient f_N. At a given temperature and pressure, and since nitrogen solubility follows Sievert´s law, i.e., the amount of nitrogen dissolved in the metal is proportional to the square root of nitrogen partial pressure, the changes of the activity coefficient caused by alloying elements can be evaluated as follows:

$$f_N = \left(\frac{[wt-\%N]_{Fe}}{[wt-\%N]_{Fe-j}} \right)_{T,P} \qquad (A3)$$

where j is an alloying element. The activity of interstitial elements in iron is usually described by Wagner´s interpretation. Using Taylor series expansion, the logarithm of activity coefficient and additionally the fact that nitrogen activity in pure iron is unity, it is possible to determine the activity coefficients of nitrogen in different iron-base alloys using the following equation (Zheng, 1991):

$$\log f_N = \sum_j e_N^j (\%j)^2 + \sum_j r_N^j (\%j)^2 + \sum_{j,k} r_N^{jk} (\%j\%k) + \ldots \quad \text{(A4)}$$

where k also refers to alloying elements, e_N^j, r_N^j and r_N^{jk} are interaction parameters, and %j and %k are different alloying element contents in wt-%. Interaction parameters describe how different alloying elements affect nitrogen solubility in iron-base alloys through the logarithm of the activity coefficient f_N. With these interaction parameters, which in most cases depend on temperature, the thermodynamic properties of different iron-base alloys can be evaluated.

The nitrogen solubility in the liquid phase of multicomponent alloys can be calculated with the interaction parameter method, which is based on Equation (A4), and the activity coefficient of nitrogen can be evaluated by adding the effect of each element. Temperature dependent interaction parameters for different alloying elements are described in Appendix B. Nitrogen solubility in iron-base multicomponent alloys can be calculated in a wide range of pressures, temperatures and alloying element concentrations with the following equation (Zheng, 1991):

$$\log(\text{wt}-\%\text{N}) = -\frac{293}{T} - 1{,}16 - \frac{3757}{T-0{,}81}\sum_j e_{N,2073K}^j (\%j) - \frac{1}{2}\left(\frac{5132}{T} - 1{,}48\right)\sum_j r_{N,2073K}^j (\%j)^2 - \frac{1}{6}\left(\frac{8424}{T} - 3{,}06\right)\sum_j q_{N,2073K}^j (\%j)^3 + \frac{1}{2}\log p_{N_2} \quad \text{(A5)}$$

where $e_{N,2073K}^j$, $r_{N,2073K}^j$ and $q_{N,2073K}^j$ are interaction parameters at 2073 K, %j is each alloying element content in wt -%, and p_{N_2} is the partial pressure of nitrogen.

Calculations of nitrogen solubilities in the austenite phase for multicomponent alloys can also be performed with the interaction method (Zheng, 1991). The nitrogen activity coefficient can be calculated with the help of Equation (A4), in which the combined effect of each alloying element on the nitrogen activity is obtained by using the interaction parameters. The temperature dependent interaction parameters of different alloying elements for nitrogen solubility in the austenite phase are given in Appendix B. Combining the values obtained by using Equation (A4) with the results in pure iron, it is possible to determine the nitrogen solubility in the austenite phase as follows (Zheng, 1991):

$$\log(\text{wt}-\%\text{N}) = \left(\frac{441{,}5}{T} - 1{,}922\right) - \log f_N + \frac{1}{2}\log p_{N_2} \quad \text{(A6)}$$

APPENDIX B.

Interaction parameters of alloying elements for nitrogen solubility in the austenite phase.

Table B1. Interaction parameters of alloying elements for nitrogen solubility in the austenite phase (Zheng, 1991).

$$e_N^{Cr} = -\frac{320.6}{T} + 0.1127 \qquad r_N^{Cr} = \frac{6.41}{T} - 0.0028$$

$$e_N^{Ni} = \frac{16.0}{T} + 0.00288 \qquad r_N^{Ni} = 1.887 \times 10^{-4}$$

$$e_N^{Mn} = -\frac{135.5}{T} + 0.03567 \qquad r_N^{Mn} = \frac{2.789}{T} - 0.001245$$

$$r_N^{CrNi} = \frac{7.0}{T} - 0.005$$

$$r_N^{CrMn} = \frac{7.23}{T} - 0.00165 \qquad r_N^{CrCrMn} = -1.06 \times 10^{-4}$$

$$e_N^{Mo} = -0.05$$

$$e_N^{V} = -\frac{1540}{T} + 0.79$$

$$e_N^{Co} = -\frac{9}{T} + 0.0215$$

$$e_N^{C} = 0.12$$

$$e_N^{Si} = 0.052$$

$$e_N^{P} = 0.050$$

APPENDIX C.

The data and formulas needed for the calculation of the maximum temperature of Cr_2N precipitation.

The thermodynamic data for Cr_2N formation is:

$$G^0_{Cr_2N} = -106{,}14 + 0{,}051\ T \tag{C1}$$

$$\log a_{Cr} = \log X_{Cr} + (1 - X_{Cr})^2 \frac{455}{T} \tag{C2}$$

In Equation (C2), X_{Cr} is the mole fraction of chromium in the alloy. This precipitation procedure is based, like all precipitation procedures, on the decrease of the free energy of the system. With the parameters in Equations (C1) and (C2), it is possible to calculate the equilibrium nitrogen content at the precipitate interface by thermodynamic analysis.

It is important to determine the equilibrium nitrogen content in the austenite phase corresponding to the beginning of Cr_2N precipitation. The equilibrium nitrogen activity at the precipitate interface can be evaluated as follows (Zheng, 1991) :

$$a_N = \frac{1}{a_{Cr}^2} \exp\left(\frac{G^0_{Cr_2N}}{RT}\right) \tag{C3}$$

The evaluation can be done with Equations (C1) and (C2), where Cr is considered as pure metallic chromium, N as nitrogen gas (N_2) at 1 atm, and Cr_2N as a stoichiometric phase without other elements. Additionally, in Equation (C2) the mixture of chromium and iron is simplified to be a regular solution. The relation between nitrogen activity and its content should be also considered. The nitrogen activity is proportional to the nitrogen content in austenite, i.e.:

$$a_N = f_N'[\text{wt-\%N}] \tag{C4}$$

where f_N' is the nitrogen activity coefficient in the austenite phase and a_N is the nitrogen activity corresponding to the reference state at 1 atm. Now, f_N' can be evaluated through the isobaric nitrogen solubility in alloys:

$$a_N = \sqrt{p_{N_2}} = 1 = f_N'[\text{wt-\%N}]_\gamma^{P = 1\ atm} \tag{C5}$$

$$f_N' = \frac{1}{[\text{wt-\% N}]_\gamma^{P=1\text{ atm}}} \tag{C6}$$

The nitrogen solubility in the austenite phase at 1 atm can be evaluated with Equation (B2), and with the interaction parameters in Table B1 in Appendix B. Finally, the equilibrium nitrogen content for the beginning of the Cr_2N formation can be calculated by substituting Equations (C5) and (C6) into Equation (C4):

$$[\text{wt}-\%\text{N}] = \frac{[\text{wt}-\%\text{N}]_\gamma^{P=1\text{atm}}}{a_{Cr}^2} \exp\left(\frac{G^0_{Cr_2N}}{RT}\right) \tag{C7}$$

The calculated nitrogen content depends on the temperature and the chromium content. The influence of alloying elements is introduced by changes in the nitrogen solubility $[\text{wt}-\%\text{N}]_\gamma^{P=1\text{ atm}}$. It can also be noted, that chromium addition affects the activity of chromium.

APPENDIX D.

Optical microscopy of SMO 0,5N1 and SMO 0,7N steels isothermally annealed at 750 °C.

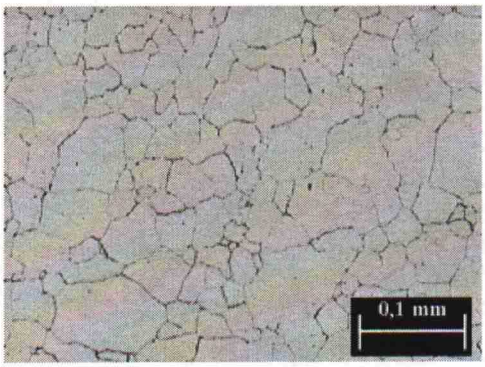

a) SMO 0,5N1: 750 °C/1 h.

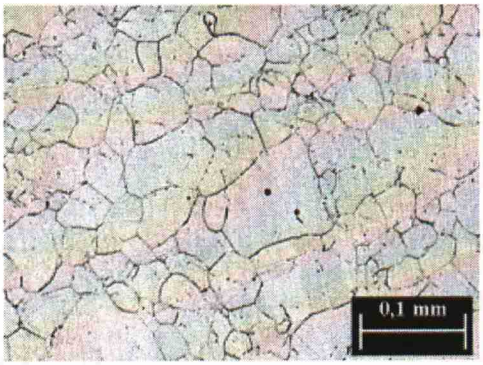

b) SMO 0,7N: 750 °C/1 h.

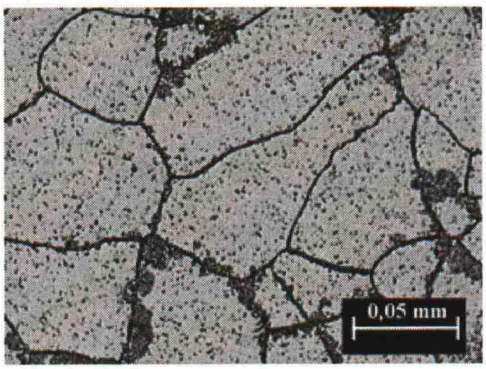

a) SMO 0,5N1: 750 °C/10 h.

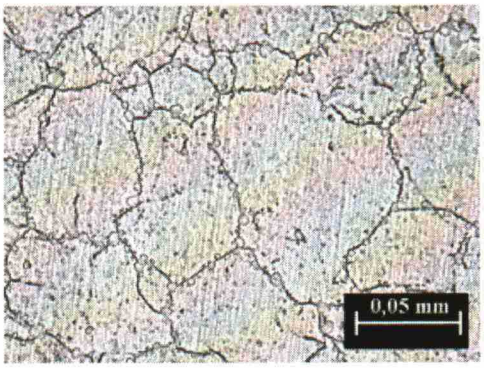

b) SMO 0,7N: 750 °C/10 h.

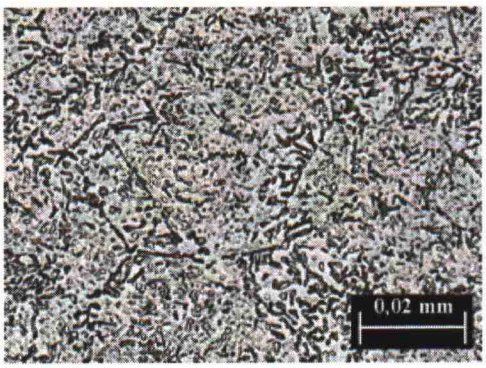

a) SMO 0,5N1: 750 °C/72h.

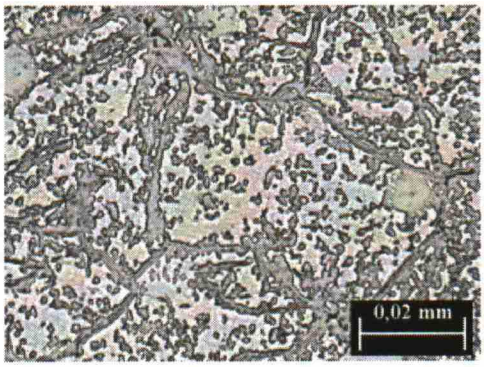

b) SMO 0,7N: 750 °C/72 h.

APPENDIX E.

Dilatometric curves (dL/lo and dL/dt) during heating a) and cooling b) for SMO 0,5N1.

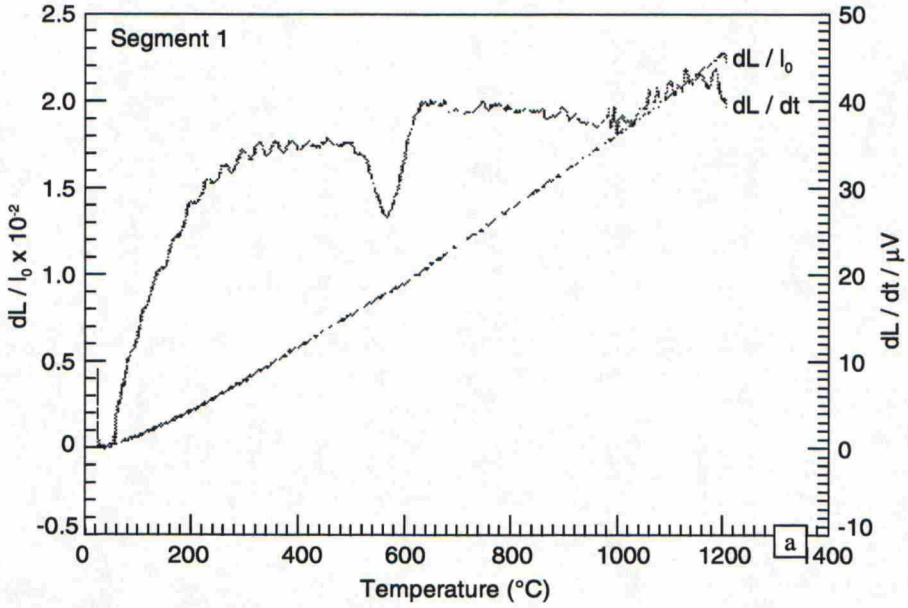

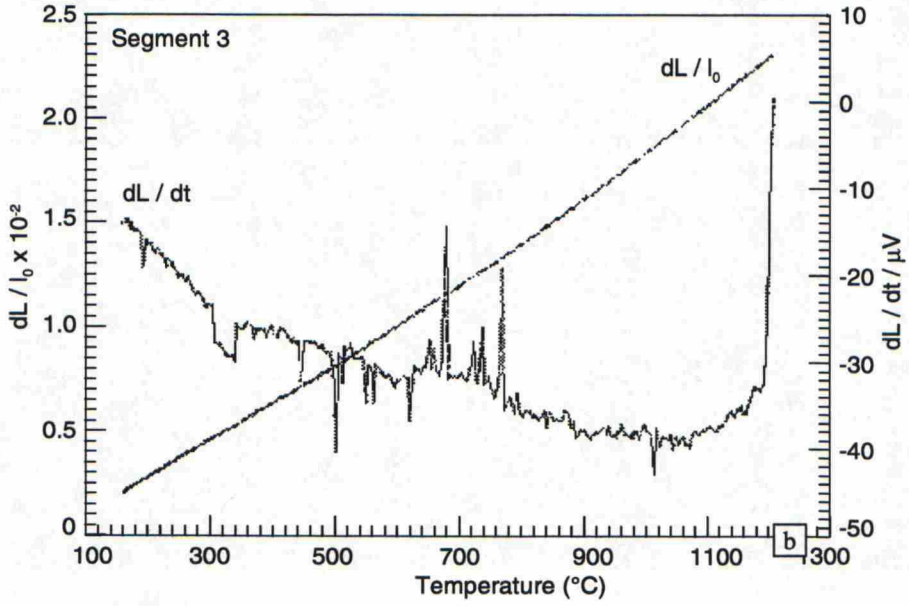

APPENDIX F.

Fracture surfaces of tensile samples of the studied solution annealed and isothermally at 750 °C annealed steels.

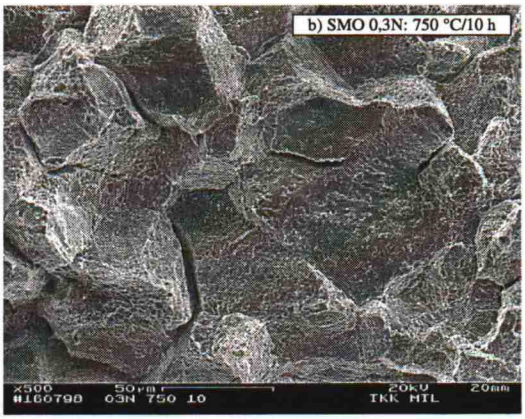

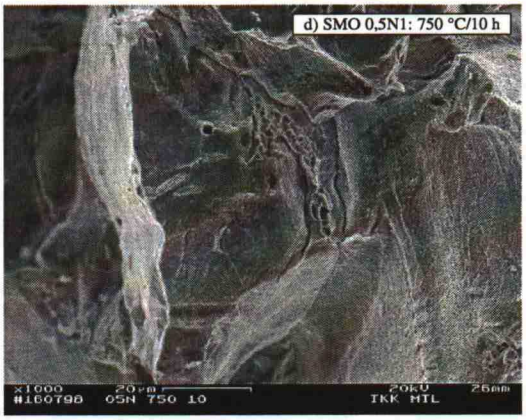

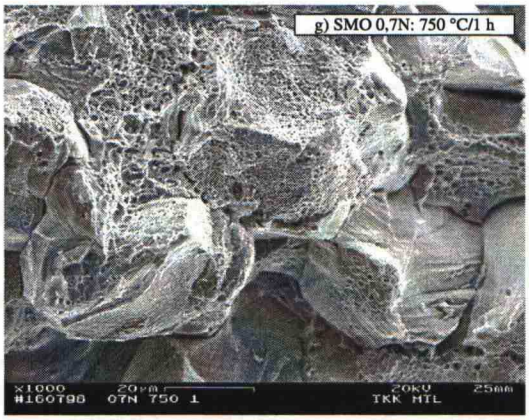
g) SMO 0,7N: 750 °C/1 h
x1000 20µm 20kV 25mm
#160798 07N 750 1 TKK MIL

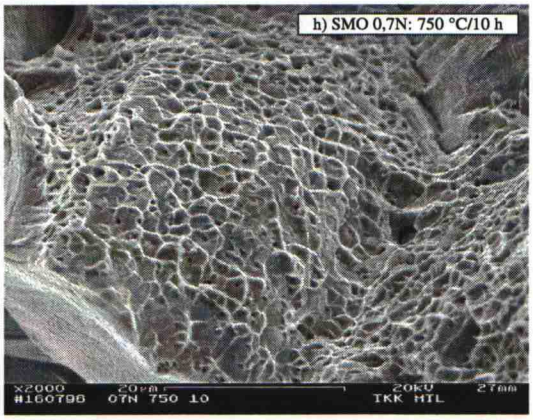
h) SMO 0,7N: 750 °C/10 h
x2000 20µm 20kV 21mm
#160798 07N 750 10 TKK MIL

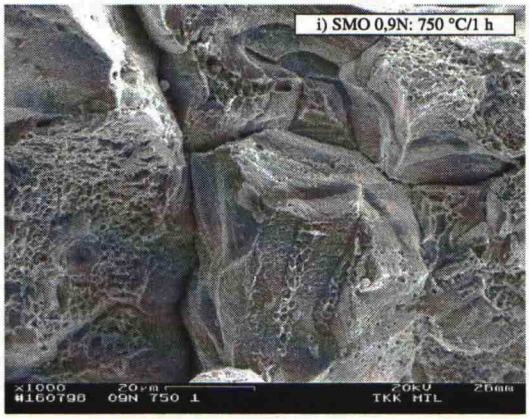
i) SMO 0,9N: 750 °C/1 h
x1000 20µm 20kV 25mm
#160798 09N 750 1 TKK MIL

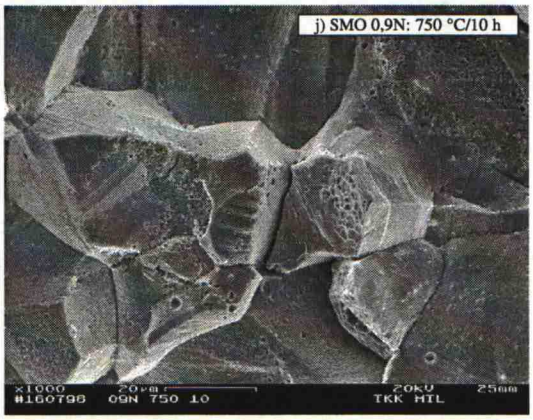
j) SMO 0,9N: 750 °C/10 h
x1000 20µm 20kV 25mm
#160798 09N 750 10 TKK MIL


k) SMO 0,9N: 750 °C/72 h
x500 50µm 20kV 25mm
#160798 09N 750 72 TKK MIL

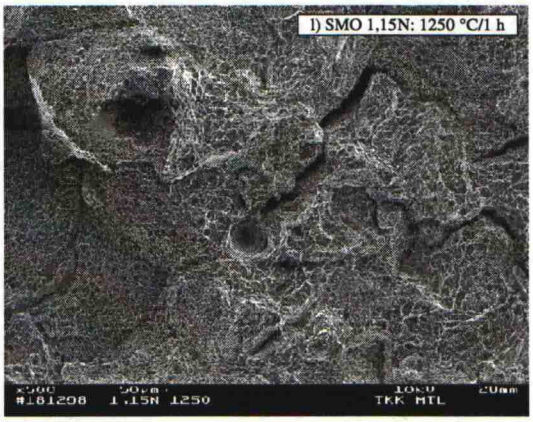
l) SMO 1,15N: 1250 °C/1 h
#181208 1.15N 1250 TKK MIL

APPENDIX G

Fracture surfaces of impact samples of the studied solution annealed and isothermally at 750 °C annealed steels.

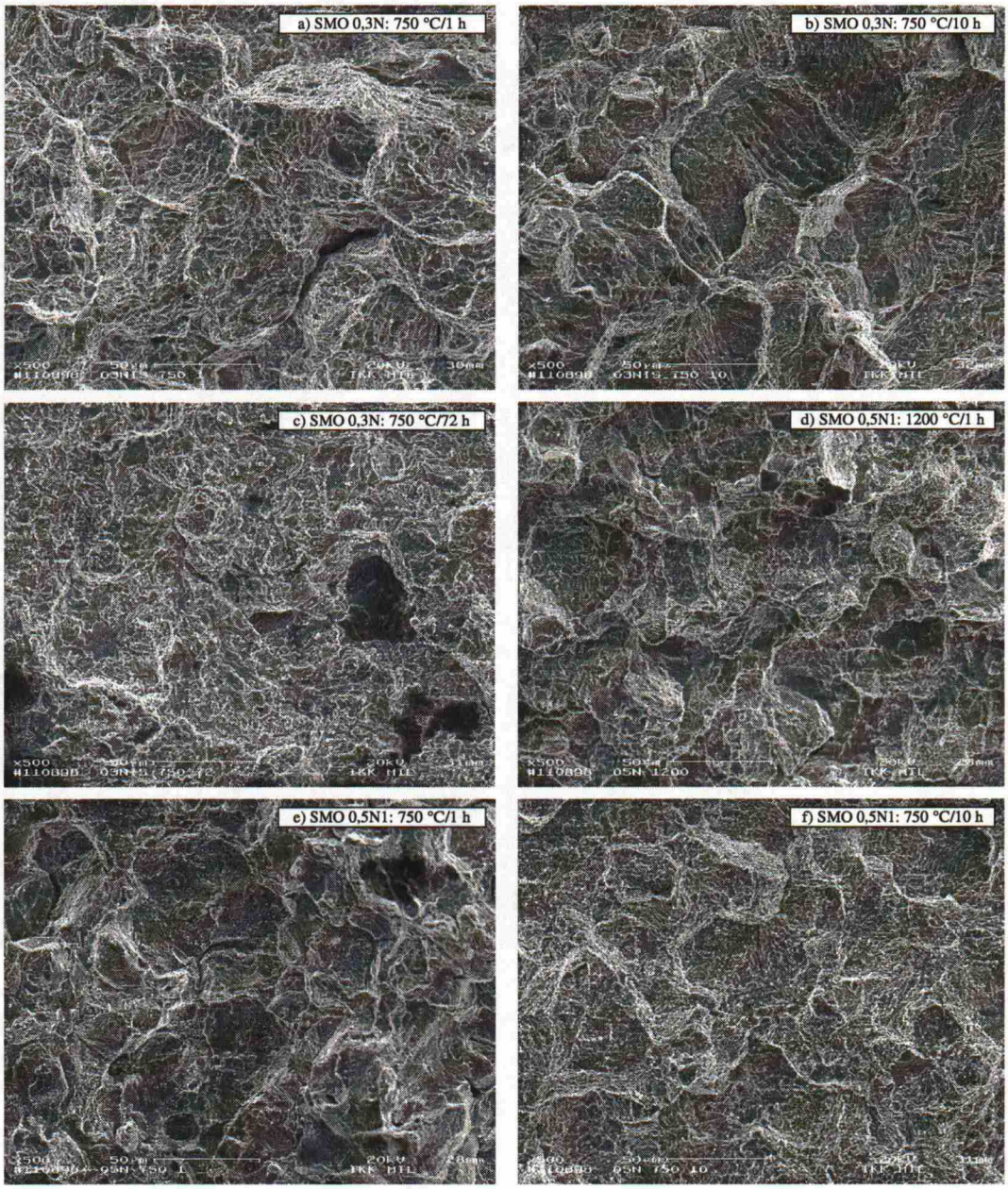


g) SMO 0,7N: 750 °C/1 h

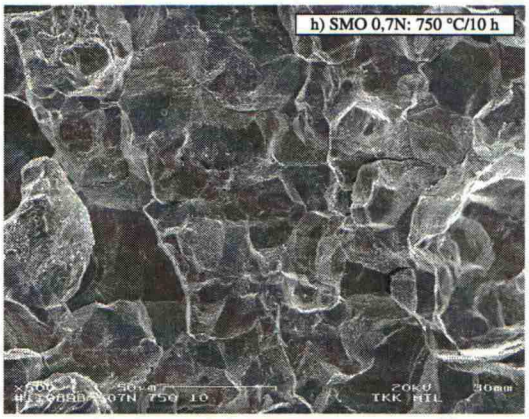
h) SMO 0,7N: 750 °C/10 h

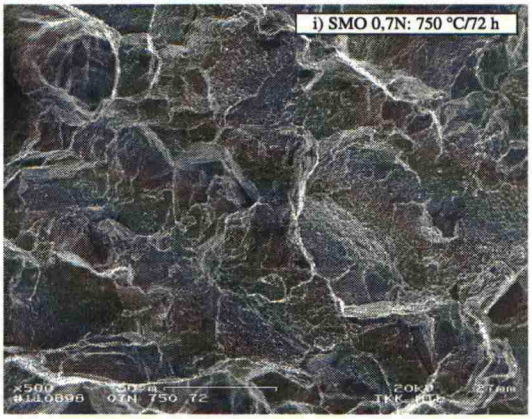
i) SMO 0,7N: 750 °C/72 h

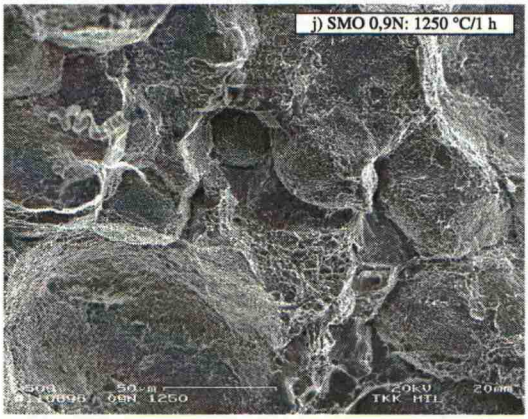
j) SMO 0,9N: 1250 °C/1 h

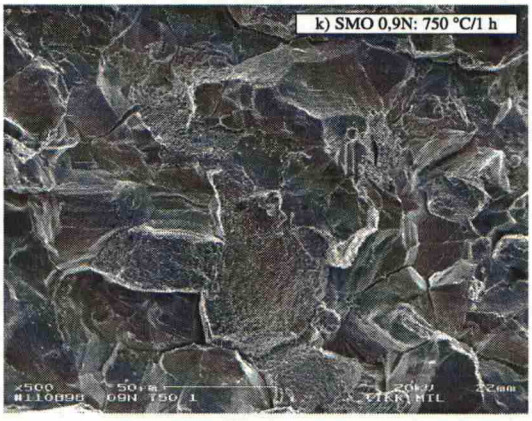
k) SMO 0,9N: 750 °C/1 h


l) SMO 0,9N: 750 °C/10 h

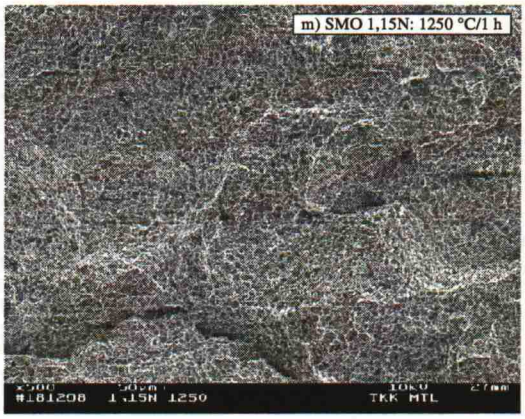
m) SMO 1,15N: 1250 °C/1 h
#181208 1,15N 1250
TKK MTL

INSTRUCTIONS TO AUTHORS

Acta Polytechnica Scandinavica (APS) publishes original accounts of research in English, French, and German. Three copies of papers submitted for publication in APS should be sent to:

The Editor/Acta Polytechnica Scandinavica
The Finnish Academy of Technology
Tekniikantie 12
FIN-02150 ESPOO
FINLAND

Please indicate the APS subseries in which you wish your paper to be published.

Papers accepted for publication in APS must be submitted in camera ready format. A booklet with detailed instructions to authors is provided on request. Papers will be printed within a month after receipt of the final camera ready manuscript.

Page Charge

A page charge is normally applied to cover the cost of printing of work done outside Finland. A cheque or money order drawn on a Finnish bank to cover the page charge and cost of additional copies must be included with the final camera ready manuscript.

The page charge is 2000 FIM + 270 FIM per four manuscript pages (less than 64 pages), and 2500 FIM + 240 FIM per four manuscript pages (more than 64 pages).

Additional Copies

Authors receive 25 copies free of charge. Additional copies may be ordered at 330 FIM + 45 FIM/4 pp. per 100 copies.

ACTA POLYTECHNICA SCANDINAVICA

Mechanical Engineering Series

Me 128 TERVO, J., Wear Properties of High Nitrogen Austenitic Stainless Steels. Espoo 1998, 88 pp. ISBN 952-5148-46-7.

Me 129 LINJAMA, M., The Modeling and Actuator Space Control of Flexible Hydraulic Cranes. Espoo 1998, 115 pp. ISBN 952-5148-54-8.

Me 130 EL HAJ ASSAD, M., Performance Characteristics of Thermal Cycles and Energy Conversion Systems. Espoo 1998, 35 pp. ISBN 952-5148-55-6.

Me 131 JACOBSON, T., Computational Fluid Dynamics Aided Combustion Analysis. Espoo 1998, 201 pp. ISBN 952-5148-61-0.

Me 132 KOHOPÄÄ, J., Effects of Post-Irradiation Thermal Annealing on Radiation Embrittlement Behaviour of Cr-Mo-V Alloyed Weld Metals. Espoo 1998, 112 pp. ISBN 952-5148-64-5.

Me 133 KALSKE, S., Added Resistance and Unsteady Bow Wave Field of a Ship in Short Waves. Espoo 1998, 96 pp. ISBN 952-5148-67-X.

Me 134 NIEMI, E., Engineering Cost Functions in Make-to-Order Production with Applications. Espoo 1998, 139 pp. ISBN 952-5148-81-5.

Me 135 ÅSTRÖM, T., Monitoring the Level of Magnetization in AC-Yokes by Utilizing the Twin Induction Method. Espoo 1999, 128 pp. ISBN 952-5148-85-8.

Me 136 ILOLA, R., Effects of Temperature on the Mechanical Properties of Austenitic High Nitrogen Steels. Espoo 1999, 100 pp. ISBN 952-5148-95-5.

Me 137 IOANNIDES, E. et al., An Analytical Formulation for the Life of Rolling Bearings. Espoo 1999, 82 pp. ISBN 951-666-503-9.

Me 138 PILLAI, B., Adaptation of Neural Network and Fuzzy Logic for the Wet-End-Control and Process Management of Paper or Board Machines – A Tool-Making Approach. Espoo 1999, 155 pp. ISBN 951-666-511-X.

Me 139 KAJASTE, J., Of the Capability of Component Models to Predict the Response of a Fluid Power System with a Long Pipeline and Accumulator. Espoo 1999, 116 pp. ISBN 951-666-517-9.

Me 140 SMUK, S., Application of Internal Friction Method for Studying Point Defect Behavior in Engineering Materials. Espoo 1999, 100 pp. ISBN 951-666-518-7.

ISBN 951-666-524-1
ISSN 0001-687X

Libella Painopalvelu Oy